Outdoor Performance Analysis and Prediction of Photovoltaic Modules Using Machine Learning Algorithm

By

Md. Kamrul Islam
16121105
Md. Mehedi Hasan Shawon
16221056
Sumaiya Akter
16321012
Sabbir Ahmed
16321003

A thesis submitted to the Department of Electrical and Electronic Engineering in partial fulfillment of the requirements for the degree of
Bachelor of Science in Electrical & Electronic Engineering

Department of Electrical and Electronic Engineering
Brac University
June 2020

Declaration

It is hereby declared that

1. The thesis submitted is our own original work while completing degree at Brac University.
2. The thesis does not contain material previously published or written by a third party, except where this is appropriately cited through full and accurate referencing.
3. The thesis does not contain material which has been accepted, or submitted, for any other degree or diploma at a university or other institution.
4. We have acknowledged all main sources of help.

Student's Full Name & Signature:

Md. Kamrul Islam 16121105	**Md. Mehedi Hasan Shawon** 16221056
Sumaiya Akter 16321012	**Sabbir Ahmed** 16321003

Approval

The thesis titled “Outdoor Performance Analysis and Prediction of Photovoltaic Modules Using Machine Learning Algorithm” submitted by

1. Md. Kamrul Islam (16121105)
2. Md. Mehedi Hasan Shawon (16221056)
3. Sumaiya Akter (16321012)
4. Sabbir Ahmed (16321003)

of Spring, 2020 has been accepted as satisfactory in partial fulfillment of the requirement for the degree of Bachelor of Science in Electrical & Electronic Engineering on 27th June, 2020.

Examining Committee:

Supervisor:
(Member)

_____

Dr. Md. Mosaddequr Rahman
Professor, Dept. of EEE
BRAC University

Program Coordinator:
(Member)

_____

Dr. Abu S.M. Mohsin
Assistant Professor, Dept. of EEE
BRAC University

Departmental Head:
(Chair)

_____

Dr. Shahidul Islam Khan
Professor and Chairperson, Dept. of EEE
BRAC University

Abstract

The objective of this study is to inspect the performance of the photovoltaic (PV) modules in different environmental conditions and to apply a machine learning algorithm for prediction analysis. Photovoltaic modules are very sensitive to weather conditions such as cloudy, rainy, sunny days. Hence, weather parameters, for example, Irradiance, temperature, humidity, air-pressure have an impact on PV modules performance. Two Mono-Silicon PV modules have been set up on a seven-storied building in Gabtoli, Dhaka to collect the environmental data. Among two PV modules, one module is cleaned regularly and the other module is not cleaned to observe the dust effect on PV modules performance. A weather station is designed using Raspberry Pi 3B+ modules where different sensors are used to collect both modules short circuit current as well as temperature, humidity, wind speed and air-pressure data. The data of the PV modules and the environmental parameters are being collected from the end of October 2019. Data from November 2019 to February 2020, are used to analyze the performance of these PV modules. Furthermore, a theoretical calculation is done to calculate the solar irradiance (Ideal and Experimental), PV modules power output and energy output. Moreover, one of the segments of machine learning that is neural network which is used to train the model based on the collected data so that a fruitful prediction can be done. An algorithm named Multi-Layer Perceptron (MLP) using Artificial Neural Network has been developed which can provide us with the PV modules energy output of a particular day or time based on the training dataset. The accuracy of the output depends on the training dataset but most importantly it depends on the correct parameters which have been shown in this study.

Keywords: Short Circuit Current; Temperature; Wind Speed; Humidity; Solar Irradiance; Cumulative Electrical Energy

Dedication

This thesis is dedicated to our beloved parents who raised us to be the persons we are today, who were always there for us whenever we needed them, and who constantly support us with their love and kindness. Also, this thesis is specially dedicated to the memory of Md. Nurul Islam, father of Md. Kamrul Islam, who had passed away during the Coronavirus pandemic. With his help, it became possible for us to collect enough data for our thesis work. We all are forever grateful to him.

Acknowledgement

All thanks to Almighty Allah, who made it possible for us to complete our thesis work in time without any significant obstacle. We want to thank and show our heartiest gratitude to our honorable supervisor Dr. Md. Mosaddequr Rahman Professor of BRAC University, for his incomparable guidelines, as well as his continuous support and motivation throughout the thesis work. We are immensely grateful for his dedicated involvement at every step, professionalism and precious guidelines which paved the pathway to the completion of this thesis work.

Table of Contents

List of Tables

List of Figures

List of Acronyms

ANN	Artificial Neural Network
MLP	Multi-Layer Perceptron
Isc	Short Circuit Current

Chapter 1

Introduction

1.1 Introduction

The sun provides us all the energy that anyone could need to meet the entire world's energy demand, and not at all like non-renewable energy source which is destined to run out at any point shortly. Despite being a sustainable power source, the main constraint is to convert sunlight-based vitality into electrical vitality in a productive and savvy way. At the point when one utilizes solar energy, no ozone depleting substance outflows are discharged into the air. Electricity from solar energy is a fundamental energy source in the transition to clean vitality creation. As an inexhaustible CO2 free power source, the ecological effect of solar energy is significantly lesser than other available power generation techniques. The effect is predominantly identified with the production and supply of the exceptional materials and metals that are required to deliver solar panels. Nowadays, photovoltaic (PV) module is one of the fastest developing sustainable power source innovation with an underlying condition of less carbon emission and flexible maintenance. At present, 90% individuals of Bangladesh have access to electricity with per capita energy generation at around 464kwh, according to the utilization of sustainable power source with a vision to satisfy the increasing need for power. Around 62 off-network rooftop solar projects with a generation capacity of 14.36 MW and 50 on-grid projects with a generation capacity of 26.45 MW have been finished and run by public and private sectors till October 2019. In Bangladesh, the leading export sector is RMG which expects to reach $50bn in trades by 2021. This industry to a great extent relies upon petroleum derivatives like flammable gas and diesel. Emission of ozone depleting substance because of the garments sector is around 38% of GHG and is the highest outflow of greenhouse gases amongst the other industries in Bangladesh. To forestall this, rooftop solar PV can be the

correct alternative to decrease some level of the employments of petroleum derivatives. As indicated by the Ministry of Power Energy and Mineral Resources. To meet the increasing energy demand in Bangladesh, the Government has just propelled "500 MW Solar Power Mission" to promote the administration's Power System Master Plan (PSMP), Bangladesh can produce 635 MW (17.3%) from the solar rooftop, and the annual generation will be 860GWh which will decrease around 576,200 tons of CO2 emission.

In a nutshell, the best idea for the world is to change over more to solar based energy as it is ecofriendly. It is high time, the concerned authority of Bangladesh should make a move to urge the private financial specialists to put resources into residential, commercial and industrial structures to enhance the renewable power generation. In the light of this vision, solar PV manufacturers ought to get investment advantages from the legislature. In conclusion, to give a sound future to the people to come and furthermore to ensure the livings, solar power energy is the most proficient method of generating power.

1.2 Literature Review

The world is moving towards sustainable energy source where solar energy is the most reliable source to meet the escalating energy demand. Solar energy is effectively available and significantly eco-friendly with minimum carbon emission. Moreover, numerous researcher and students are working with greater enthusiasm due to the increasing demand for energy and the reliability of solar energy. Therefore, different tasks are being explored both theoretically and physically. Besides, a huge amount of research papers and books have been published in several renowned conferences and journals. By going barely any books for understanding the core concept of how solar modules function as well as how it acts with ecological parameters, additionally the research papers and books identified with the subject of intrigue, provides

information about past work and results. Lots of theoretical analysis along with practical investigation has been done to achieve the purpose of the research topic.

"Design of a Solar Powered LED Street Light: Effect of Panel's Mounting Angle and Traffic Sensing" was presented in the 2013 IEEE Conference on Sustainable Utilization and Development in Engineering and Technology. This paper discusses the cumulative energy outputs of panels Wh/m^2/day varying different seasons for three different mounting angles (θ = 0°, 23.1° & 46.5°). During the summer period, the solar photovoltaic module delivers the highest energy output exceeding 1000 W/m^2 but during winter energy output is low. The solution to this problem resolves through changing the mounting angle of the solar module.

"Modeling Effect of Dust Particles on Performance Parameters of the Solar PV Module" written by three Indian researchers named Paresh G. Kale, Kaushal Kishor Singh and Chintu Seth. In the paper, the author discusses the effect of dust properties on the power output of the PV module. The output power decreases quantitatively with the dust accumulation on the surface of the PV module.

2015 International Conference on Circuit, Power and Computing Technologies a paper presented name "ENVIRONMENTAL EFFECT ASSESSMENT ON PERFORMANCE OF SOLAR PV PANEL". The following research portrays that the output power and efficiency of the solar panel are affected by various environmental factors like dust, color, irradiance, shading etc.

A conference paper named "Forecast of Solar Energy Production – A Deep Learning Approach" which was presented in 2018 IEEE International Conference on Big Knowledge. Solar production is impacted by various environmental parameters like sun position, weather condition and the characteristic of PV panels etc but on a cloudy day because of cloud movement becomes the main factor in solar energy production. This paper focuses on using

several deep convolutional neural networks utilizing the weather forecast data exploring various temporal and capturing the cloud movement pattern and its effect on solar energy generation. The error rate was 21% in a persistent model, and using the SVR model it was 15.1% but using the convolutional neural networks error decrease to 11.8%.

“The Performance Analysis of Single and Dual Axis Sun Tracking System: A Comparative Study” a thesis group from BRAC University department of Electrical & Electronic Engineering studied both the dual and single-axis sun tracking system to claim which one would be beneficial. The result shows that there are no significant differences between dual and single-axis sun tracking system, the differences between dual and single axis with and without the cloud effect are 3.96% & 3.44% which has a variance of 0.52%.

1.3 Aim & Objective

The primary aim of this research is to examine the climate parameters impact on solar modules, conjointly to examine the dust impact on the solar modules output energy. In addition, there is a vision to foresee the yield of solar photovoltaic modules depending on the weather parameters by utilizing the Artificial Neural Network approach. Temperature, wind speed, humidity, air pressure and solar surface irradiance are considered as the environmental parameters, where the short circuit current is the solar modules output parameter. Temperature, humidity, wind speed and air pressure data have been collected by different sensors integrated into a combined system, known as a weather station. On the other hand, the solar module surface irradiance is measured through theoretical calculation. The real-time data of each sensor has been collected from November 2019 to February 2020 effectively. The Artificial Neural Network models are trained with the extracted data of each sensor and test the predicted output depending on only the input weather parameters. Thus, the future energy from the solar panels is predicted in advance.

1.4 Thesis Organization

The book is organized as follows. Chapter 1 gives a general presentation followed by the foundation and the targets of the work. Chapter 2 shows the theoretical foundation of the following thesis topic. Chapter 3 presents the hardware set up as well as the description of the software used. Chapter 4 provides the theoretical analysis for both clean and dusty solar panels over the four months datasets. Chapter 5 and Chapter 6 shows the prediction analysis of the short circuit current and energy for both the solar panels. In the end, Chapter 7 provides the conclusion of the work and offers future research work proposals.

Chapter 2

Theoretical Background

2.1 Introduction

The world is almost at the verge of shifting the extraction of energy from non-renewable resources into renewable resources. In light of this venture, solar energy amongst all renewable resources is easily extractable with higher efficiency. The following thesis work is entitled as, "Outdoor Performance Analysis and Prediction of Photovoltaic Modules Using Machine Learning Algorithm", which requires a clear understanding of the theoretical fundamentals of the solar module. So, this chapter is focused on the theoretical overview of the solar panel considering the effect of various weather parameters on the energy output. Initially, the working mechanism of a solar module is discussed briefly along with the explanation of affiliated parameters such as short circuit current (I_{sc}), open circuit voltage (V_{oc}), ideality factor, fill factor, power, energy. These aforementioned parameters are analogous with the solar cell from the IV characteristics curve. Later on, it is described how the expected energy output from a solar module varies radically due to the change of patterns in the weather parameters such as humidity, wind speed, air pressure and temperature. In addition, the vital role of solar irradiance (W/m^2) on the solar module's output power is illustrated.

2.2 Solar Panel

2.2.1 *What is Solar Panel?*

Sun is the source of solar energy. Solar panels are also identified as Photovoltaic panels in short PV panels. Solar panels convert the sunlight into electricity which is used to supply power to electrical loads. A PV module is an assembly of photovoltaic cells mounted in a system for establishment. Photo-voltaic cells use sunlight as a source of energy and create direct current

electricity. An assortment of PV modules is known as a PV Panel and an arrangement of Panels is an Array. Arrays of photovoltaic framework supply solar power to electrical equipment.

Assembly of many solar cells made up Photovoltaic (PV) solar panels. Solar panels are made of solar cells. These cells are semiconductors material which is made of silicon, and therefore solar cells are nothing but p-n junctions, solar panel. Multiple cells connected in series-parallel to boost the current and voltage form solar panel. As like a battery solar cells have two-layer positive layer and a negative layer which create an electric field. At the time when the sunlight hit the solar panel surface, the cells absorb the photon from the sunlight energy so generate electric current. This energy generated from the photons by hitting the surface of the solar panel release the electrons from their atomic orbits which released in the electric field created by the solar cells as a result free electron are pulled out in the directional current.

There are three types of solar panels which are monocrystalline, polycrystalline and thin-film. Each of the three types of the panel has some advantage and disadvantage but for our experiment, we have chosen monocrystalline due to its high efficiency.

Table 2.1: This Table contains the Advantages and Disadvantages of the Monocrystalline, Polycrystalline and Thin-film Solar Panel:

Solar panel type	Advantages	Disadvantages
Monocrystalline	• High efficiency • Exquisite	• Higher price
Polycrystalline	• Low price	• Lower efficiency
Thin-film	• Portable and flexible • Low weight • Exquisite	• Lowest efficiency

2.2.2 *How Do Solar Panels Work?*

At the point sunlight hit the solar panel, photons from the sunlight hit a solar cell where electrons gain enough energy and loose from their atoms. By creating an electrical circuit attaching the positive and negative sides of the cell with conductors then they generate electricity when electrons flow through such a circuit. A solar panel is the assembly of multiple cells and a solar array is made by wiring together multiple panels or modules. By adding more panels, we can generate more and more energy. Solar panels generate DC (Direct Current). DC define that electrons flow in one direction around a circuit. For example, a battery powering a light bulb. In this case, the electrons move from the negative side of the battery through the lamp and then return to the positive side of the battery.

2.2.3 *Mechanism of Solar Panel*

For a better comprehension of the mechanism of solar panels, understanding the semiconductors and p-n junction is very important. For this purpose, this segment is divided into 3 parts, they are semiconductors, p-n junction and working mechanism of the solar panels. The first segment is about a concise discussion of the semiconductor material. Solar cells are made of semiconductors materials, like silicon. There is material which allows the electricity to flow through them easily, they are the conductor. Other materials such as plastics and wood, they are called insulators because they don’t let electricity to flow from them. On the other hand, semiconductor materials inherit properties which lies between the electrical conductivity property of the conductor and insulator type materials. Semiconductor materials do not allow electricity to flow through them but under certain circumstances, they can allow electricity to flow. In the materials, the electrons in the atoms are organized in layers which are known as band or shells. By moving the electrons from the valance band to conductor band electricity can be generated. From the figure, it is seen that there is a bandgap which needs to be crossed by the electrons to generate electricity. As the two bands are overlapping in the conductor

materials, it is easy to produce electricity from them. On the other side, there is a gap between the valence band and conduction band in the semiconductor materials and also in the insulator materials. The bandgap energy of the insulator is much higher than the semiconductor materials so it is very difficult to overcome this huge bandgap energy so electricity does not flow through them. But by providing adequate energy in the semiconductor materials this bandgap can be a break so the valence electrons can be released by energizing them with heat or light. As a result, they will become the free electrons and providing the higher energy than energy bandgap they can be promoted to the conduction band. For semiconductor like silicon, the energy band gap is 1.11 eV.

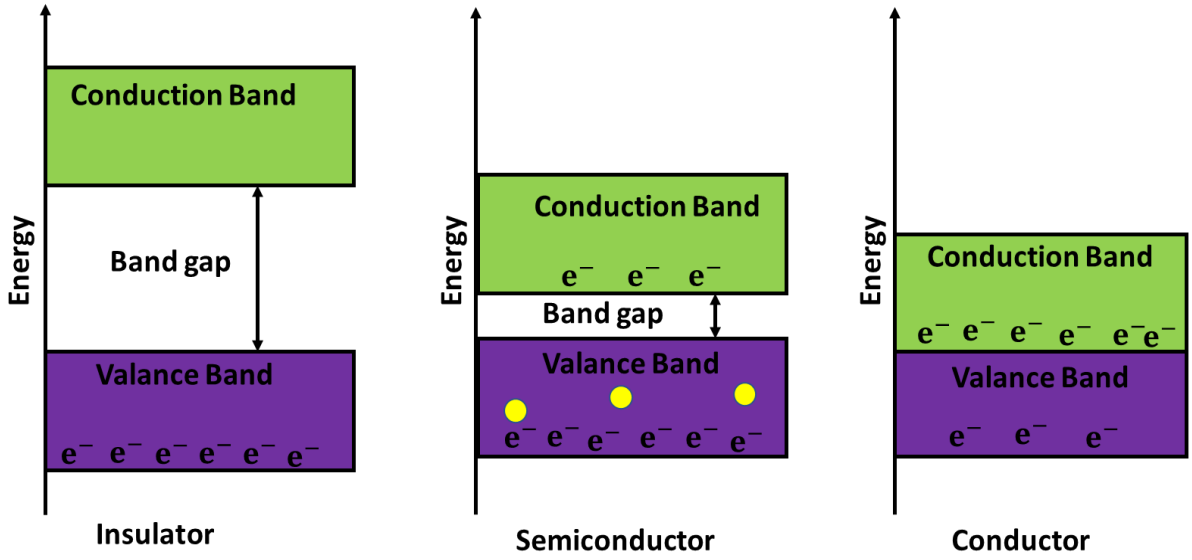

Figure 2.1: Insulators, Semiconductors, and Conductors materials

The second segment briefly discuss the PN junction. A solar cell is two distinct types of silicon that have been doped to let electricity flow through them in a particular way. The lower layer is the p-type or positive type silicon which is doped such a way so that they have few electrons. The upper layer is the n-type layer or negative type silicon which has been doped opposite of the p-type layer, as a result, they many electrons. PN junction can be created by placing a layer of n-type silicon on a layer of p-type silicon which will create a barrier at the junction of the

two materials. In the PN junction, no current will flow as the electrons cannot cross the barrier. But when they are exposed to light, the photons of the light energized the atoms of the silicon. This energy pushes the electrons of the p-type (lower layer) to cross the barrier to jump to the n-type (upper layer) and flow out around the circuit. By exposing into the light more electrons will jump up and more current will flows.

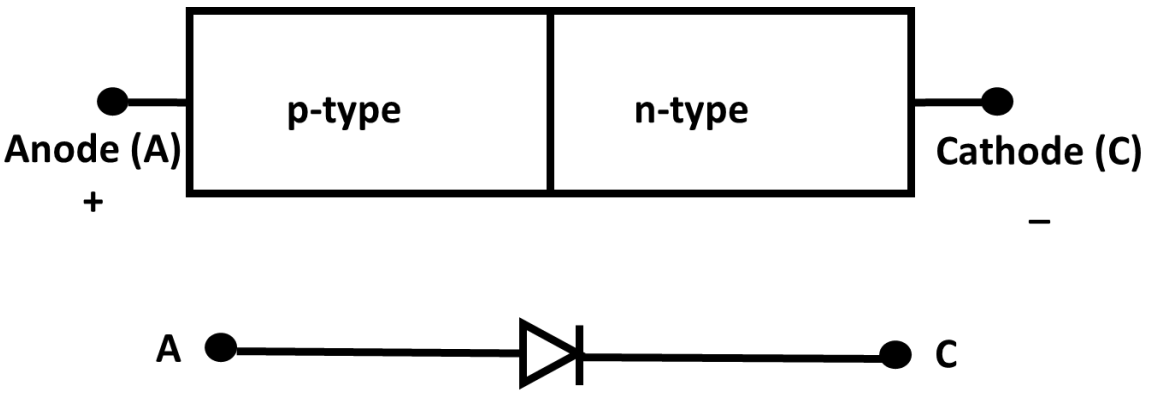

Figure 2.2: PN Junction

The last segment is about the working mechanism of the solar panel. Earlier the discussion was about the materials of the solar cell which is the semiconductor materials such as silicon and about PN junction working principle. The working mechanism of the solar panel with the knowledge of the PN junction is very simple to understand. The solar panel is made of solar cells. When exposed into sunlight this cell which is nothing but PN junction catch the sunlight energy (photons). Through the photoelectric effect, electrons that absorb photons will jump through the bandgap energy, from the valence band to the conduction band and flow out around the circuit which will generate electricity. So, the more sunlight we get the more electrons will jump up from the valence to the conduction band and more current will flow. Lastly, the current depends on the illumination and area but the voltage depends on the built-in the field between the P side and the N side. Solar cell mechanism is shown in figure 2.3 [10].

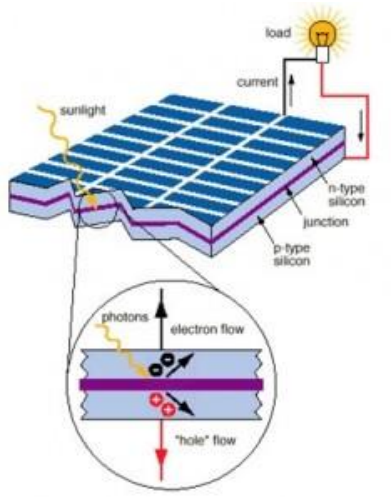

Figure 2.3: Solar Cell Mechanism

2.2.4 *Solar Cell Characteristics*

To master the solar cell characteristics, we need to comprehend the single diode model by followed by the IV characteristics of the solar cell and lastly the associated parameters. We can divide this topic into three-part which includes single diode model, IV characteristic and the parameters of solar cell.

Single diode model:

The I-V characteristic curve of a cell, module or array as a continuous function for a given set of operating conditions which can be shown by equivalent circuit models. One basic equivalent circuit model in common use is the Single Diode model. A practical solar cell equivalent circuit is shown below:

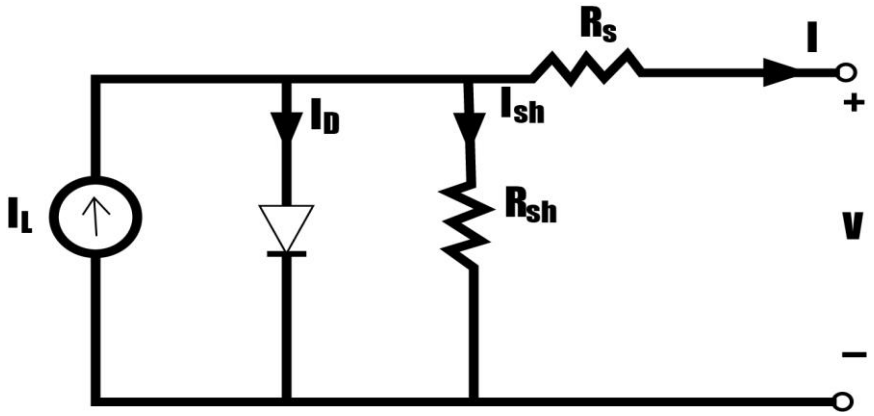

Figure 2.4: Single Diode Model

In the above figure, a constant current source I_L representing the light induced current generated in the cell is parallel with the PN junction diode. R_S represents series resistance and R_{sh} represent shunt resistances of the cell. The output current (I) of the PV module can be expressed as

$$I = I_L - I_D - I_{sh} = I_L - I_s\left(e^{\frac{q\left(\frac{V}{N_S}+IR_S\right)}{nkT}} - 1\right) - \frac{\frac{V}{N_S}+IR_S}{R_{sh}} \qquad (2.1)$$

Typically R_{sh} is less important than R_s in overall device behavior. The series resistance R_s can significantly deteriorate the solar cell performance where R_s=0 is the best solar cell case. It is apparent that the available maximum output power decreases with the series resistance which therefore reduces the cell efficiency. When R_s is larger it limits the short circuit current. Similarly, low shunt resistance values (due to defects on the materials) also reduce the efficiency.

IV Characteristics:

Solar cell IV characteristics curve is the superposition of the IV curves of the solar cell diode in presence of the light. But in the equation, there is a presence of dark current, this is the leakage or dark current in the absence of the light. The equation is given below

$$I = I_0 \left[e^{\left(\frac{qV}{nkT}\right)} - 1 \right] - I_L \qquad (2.2)$$

Here,

I_0 is the dark saturation current

q is the electronic charge

V is the applied voltage

n is the ideality factor

k is the Boltzman's constant

T is the temperature

I_L is the light generated current

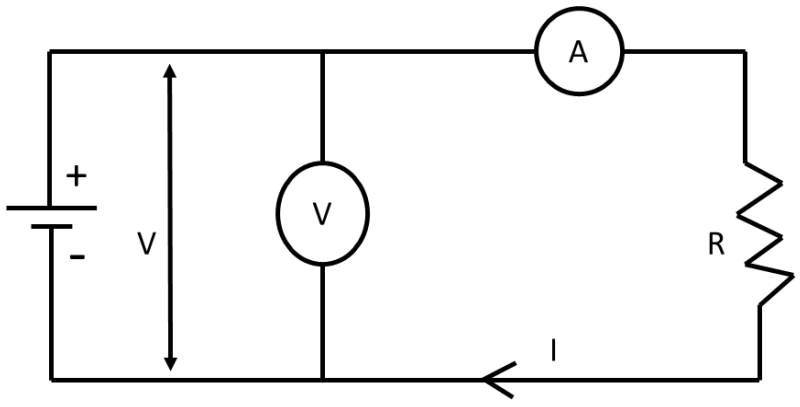

Figure 2.5: Circuit for IV characteristics of the solar cell

From the above circuit of the IV characteristics of the solar cell various parameters can be determined such as short circuit current (I_{sc}), open circuit voltage (V_{oc}), the fill factor (FF), and the efficiency etc. The rating of the solar cell depends on this cell parameters.

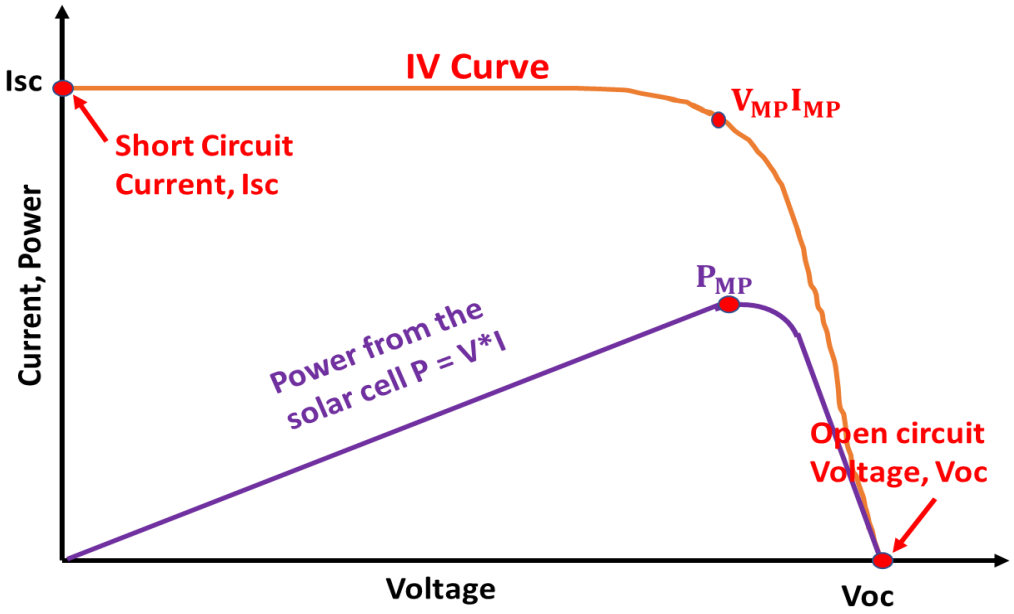

Figure 2.6: IV Characteristics curve of the Solar panel

The parameters of the Solar cell:

Short circuit current:

Short circuit current is expressed as I_{sc}. The short circuit current is the current when the voltage across the solar cell is zero, due to the generation and collection of the light generated carriers. At that time the solar cell is short circuited and this is the largest amount of current that can be drawn from the solar cell.

Ideality Factor:

The ideality factor is denoted by n and it is one of the diodes I-V characteristics parameters. It indicates the recombination mechanisms ruling inside the diode. Therefore, the ideality factor

of a diode is a measure of how closely the diode follows the ideal diode equation. For ideal case ideality factor n=1 but in nonideal case, it is more than 1. The equation of the ideality factor is given below;

$$n = \frac{(V_{oc1} - V_{oc2}) * q}{k * T * N_s * ln\left(\frac{I_{sc1}}{I_{sc2}}\right)} \quad (2.3)$$

Here;

q is the charge of an electron

k is the Boltzmann's constant

N_s is the number of cells connected in series in the panel

V_{oc1} & V_{oc2} is the open-circuit voltage at the same temperature with different solar irradiance

I_{sc1} & I_{sc2} is the short circuit current at the same temperature with different solar irradiance

For our experiment, we measure the open-circuit voltage and short circuit current almost the same temperature but with different solar irradiance then we calculated the ideality factor using the above equation. For our solar module, the ideality factor is 1.35.

Reverse Saturation Current:

A measure of the leakage of carriers across the p-n junction in reverse bias is known as reverse saturation current. This leakage is a result of carrier recombination in the neutral regions on either side of the junction. The reverse saturation current denoted as I_0 and ideality factor denoted as n of a p-n junction solar cell are an indication of the quality of the cell. The equation of the reverse saturation current is given below;

$$I_0 = \frac{I_{SC}}{e^{\left(\frac{V_{OC} * q}{n * k * T * N_S}\right)}} \quad (2.4)$$

Here;

q is the charge of an electron

k is the Boltzmann's constant

n is the ideality factor

Ns is the number of cells connected in series in the panel

T is the temperature in kelvin

I_{sc} is the short circuit current

V_{oc} is the open circuit current

For our experiment, we have selected the time at 12:35 pm where Isc and Voc of the solar module as well as the temperature using a temperature sensor is measured experimentally. The temperature recorded was 46°. Using the above equation, reverse saturation current is 1.13×10^(-7) according to the calculation. In the following experiment, a large number of data is being recorded daily which makes it laborious to calculate reverse saturation current to each of the data. As a result, another equation is applied to calculate the other reverse saturation current for each short circuit current. The equation is given below;

$$I_{02}=I_0*\left(\frac{T_2}{T_1}\right)^3 *e^{\frac{Eg}{k}\left(\frac{1}{T_1}-\frac{1}{T_2}\right)} \quad (2.5)$$

Here;

E_g is the energy bandgap of silicon

k is the Boltzmann's constant

T_1 is the temperature at I_0 calculation

I_0 is the reverse saturation current experimentally

T_2 is the temperature at I_{02} calculation

Open circuit voltage:

At zero current, voltage is maximum which is called the open-circuit voltage (V_{oc}) of a solar cell. Hence, it can be stated that the open-circuit voltage is the maximum voltage from a solar module and occurs when the net current is zero.

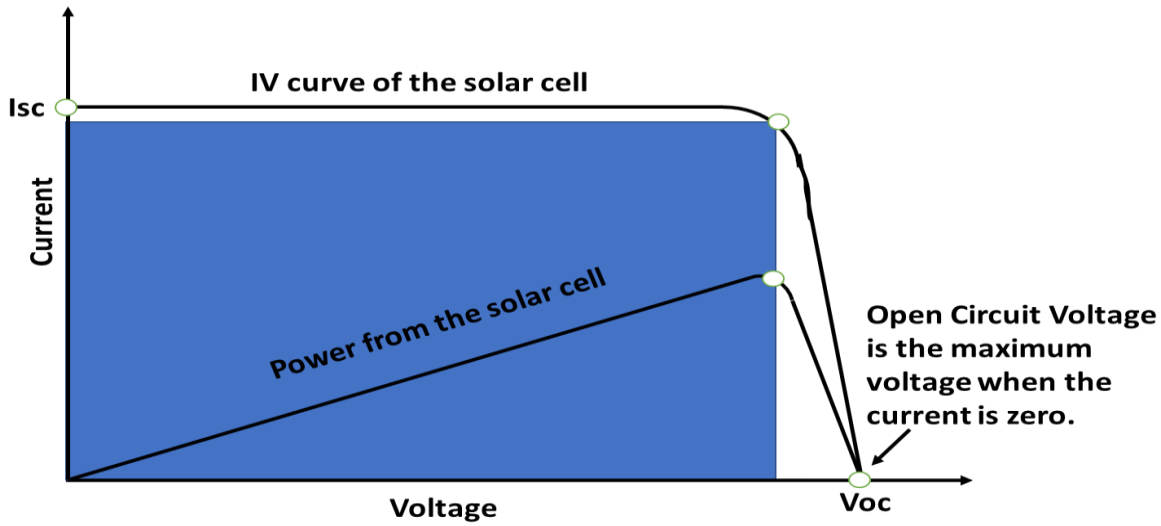

Figure 2.7: IV curve of a solar module showing the open-circuit voltage

The equation of the open-circuit voltage is given below;

$$V_{oc} = \frac{n*k*T*N_s}{q} ln\left(\frac{I_{sc}}{I_{02}}\right) \quad (2.6)$$

Here,

q is the charge of an electron

k is the Boltzmann's constant

n is the ideality factor

Ns is the number of cells connected in series in the panel

T is the temperature in kelvin

I_{sc} is the short circuit current

I_{02} is the reverse saturation current

From the given equation, the notion that open-circuit voltage goes up linearly with temperature is clear. However, as the reverse saturation current increases rapidly with temperature due to changes in the intrinsic carrier concentration the following notion does not sustain. Therefore, change in open circuit voltage does not rely on temperature solely but also on the solar irradiance.

Fill Factor:

The power of the solar module is zero at both operating points of the short circuit current and open-circuit voltage but the maximum current and voltage is obtained at that time from the solar module. Fill factor is the ratio between the maximum power from the solar module to the product of the open-circuit voltage and short circuit current. Fill factor is denoted by FF and it can be easily calculated through IV characteristic curve.

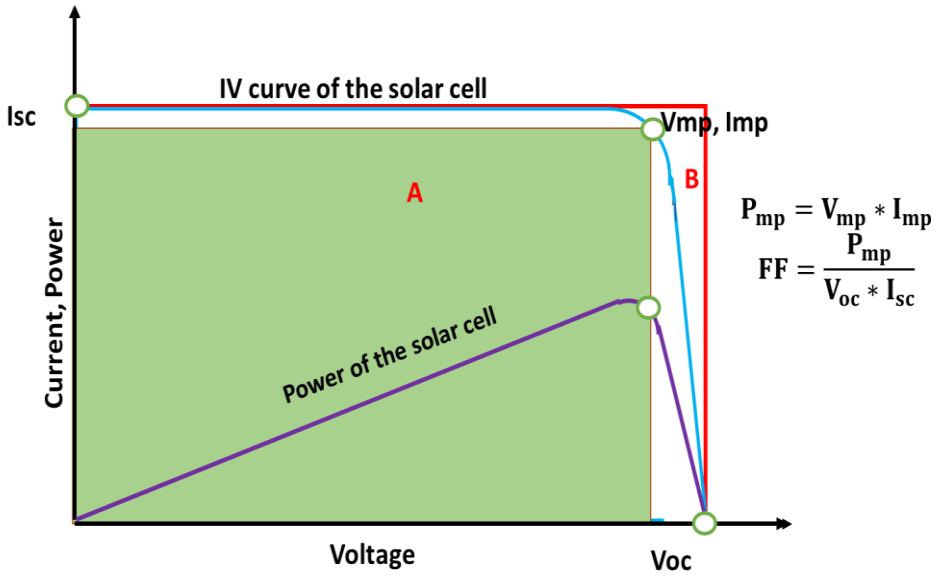

Figure 2.8: IV characteristic curve of a solar module

The maximum power can be calculated by the large rectangular area under the IV characteristic curve. The point where the rectangular region cuts the IV characteristic curve is the maximum voltage (V_{mp}) and maximum current (I_{mp}) that the solar module can provide. The equation for maximum power is given below;

$$P_{mp} = V_{mp} * I_{mp} \tag{2.7}$$

The equation of the fill factor is given below;

$$FF = \frac{P_{mp}}{V_{oc} * I_{sc}} \tag{2.8}$$

In this experiment, the Fill factor is 0.65 and the solar module specification Fill factor is 0.62. Therefore, the calculated fill factor is close to the solar module fill factor. Using this fill factor, the solar module maximum power is intended.

Maximum Power:

Maximum power is defined as the product between the maximum voltage and the maximum current of the solar module. The maximum power is 20W for the solar module used in this experiment. Since, the hardware setup is planted in outdoor, the IV characteristic curve cannot be obtained experimentally on a daily basis. For this reason, fill factor is used to calculate the maximum power output of the solar module. The equation of the maximum power is given below;

$$P_{mp} = V_{oc} * I_{sc} * FF \tag{2.9}$$

Using the above equation, maximum power is calculated for each data retrieved from the sensors daily. Moreover, the error between the calculated maximum power obtained from fill factor corresponding to the maximum power from the IV characteristics curve is very low; hence negligible. The unit of Power is W/m^2 for this respective experiment.

Energy:

Energy can be defined simply as the ability to do work which comes in different forms, for example heat (thermal), light (radiant), nuclear, chemical, electrical energy etc. Solar panel uses the sun as a source of energy which converted into electricity. This electricity produces the energy to run a load like a bulb. The incident solar irradiance (W/m^2) is integrated using the trapezoidal method of integration with respect to Time (hour) in order to compute the incident cumulative light energy (Wh/m^2). Unit of the cumulative incident sunlight energy is Wh/m^2, as energy is calculated for each day.

Efficiency:

The efficiency is the most commonly used parameter to compare the performance of the one solar cell to another. Efficiency is defined as the ratio of energy output from the solar cell to the input energy from the sun. In addition, to reflecting the performance of the solar cell itself, the efficiency depends on the spectrum and intensity of the incident sunlight and the temperature of the solar cell.

2.3 Effect of various weather parameters on the performance on PV solar module:

An Earth-wide temperature boosts commonly termed as global warming is a caution that we ought to depend on the renewable energy source, for example, solar energy. So, to extract solar energy, sunlight is the main component of generating energy and considering the situation of global environment solar energy is the most efficient source. However, there are various weather parameters which influence the performance of the solar module. The parameters that affect the solar module mostly are solar Irradiance, the ambient temperature, the surface temperature of the module, the wind speed, the humidity, the air pressure, Dust, height etc.

Among all these parameters, Solar-Irradiance and Temperature are the main components that affect the solar module most.

2.3.1 *Effect of Temperature*

Solar cells are semiconductor device that is sensitive to changes in temperature. The bandgap of a semiconductor reduces by increasing the temperature, thereby affecting most of the semiconductor material parameters. The energy of the electrons in the material increases by decreasing the bandgap of a semiconductor relative to the increasing temperature. Therefore, lower energy is needed to break the bond. In the bond model of a semiconductor bandgap, reduction in the bond energy also reduces the bandgap. Thus, increasing the temperature decrease the bandgap of a semiconductor. In the solar module, there are two parameters the short circuit current and the open-circuit voltage and the parameters that mostly affected by increasing the temperature is the open circuit voltage. The following curve reflects the effect of increasing temperature on the open-circuit voltage.

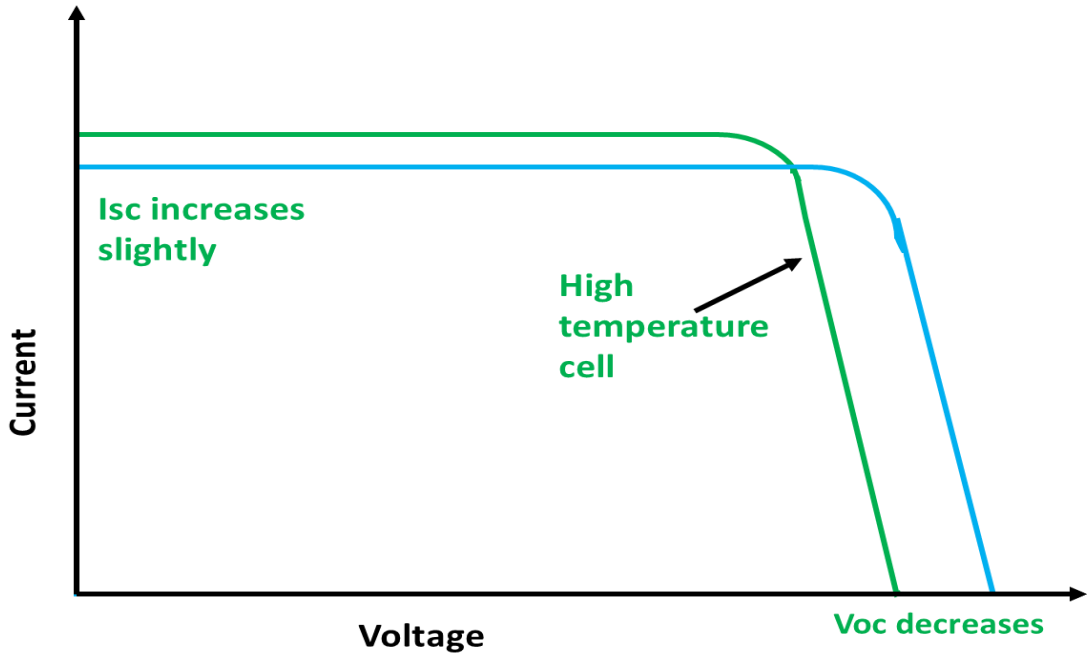

Figure 2.9: The effect of temperature on the IV characteristics of a solar cell

With temperature, the open-circuit voltage reduces because of the temperature dependency of the reverse saturation current I_0. The equation of I_0 can be expressed in terms of n_i^2

$$I_0 = qA\frac{Dn_i^2}{LN_D} \tag{2.10}$$

Here,

q is the electronic charge

A is the area

D is the diffusivity of the minority carrier for silicon

L is the minority carrier diffusion length

N_D is the doping

n_i is the intrinsic carrier concentration for silicon

In the above I_0 equation, there are few parameters that depend on temperature but the intrinsic carrier concentration mainly effects with temperature. The intrinsic carrier concentration in the above equation is directly proportional to the square. If the temperature increases, n_i increases in direct proportional with the square. Moreover, the intrinsic carrier concentration relies on the bandgap energy. If the band gap energy is lower than the intrinsic carrier concentration is higher. Therefore, increasing temperature also increase the intrinsic carrier concentration.

$$n_i^2 = BT^3 exp\left(-\frac{E_{G0}}{kT}\right) \tag{2.11}$$

Here,

T is the temperature

E_{G0} is the energy band gap of silicon

K is the Boltzmann's constant

B is a constant

Nearly at room temperature, I_0 approximately doubles for every 10℃ increase in temperature. In the open-circuit voltage there is the impact of I_0. The equation of V_{oc} is given below,

$$V_{oc} = \frac{kT}{q}\, ln\,(\frac{I_{SC}}{I_0}) \tag{2.12}$$

We can write,

$$\frac{dV_{oc}}{dT} = -\frac{V_{GO}-V_{oc}+\frac{kT}{q}}{T} \approx -2.2mV\ per\ ℃\ for\ si \tag{2.13}$$

From calculations it is observed that the relation between voltage and temperature is inversely proportional for silicon cell and (dVoc/dT) is approximately equal to -2.2mV per℃, therefore power relationship is about 0.4 % for the increase of every 1℃.

2.3.2 *Effect of Relative Humidity*

Humidity is defined as the amount of wetness or water vapor in the air. Water vapor, the gaseous state of water, is generally invisible to the human eye. Humidity indicates the likelihood for precipitation, dew, or fog to be present. The humidity level is high when there is a lot of water vapor in the air that means it is time for rain. The average summer humidity is 76% and the winter it is 74%. There are three distinct methods to measure humidity and they are absolute humidity, relative humidity and specific humidity.

Absolute humidity: Absolute humidity defines as the total mass of water vapor present in a given volume of air. Temperature does not count for calculating absolute humidity. Absolute humidity in the atmosphere ranges from near zero to roughly 30 grams per cubic meter when the air is saturated at 30 °C (86 °F). The equation for absolute humidity is given below;

$$AH = \frac{m_{H_2O}}{V_{net}} \tag{2.14}$$

Here,

m_{H_2O} is the mass of the water vapor

V_{net} is the volume of the air.

Relative humidity: Relative humidity is the ratio of the partial pressure of the water vapor in the mixture to the equilibrium vapor pressure of water over a flat surface of pure water at a given temperature. The relative humidity is expressed as a percentage (%) which means the air-water mixture is more humid for a higher percentage. The equation for relative humidity is given below;

$$\varphi=\frac{p_{H_2O}}{p^*_{H_2O}} \tag{2.15}$$

Here,

p_{H_2O} is the partial pressure of water vapor

$p^*_{H_2O}$ is the equilibrium vapor pressure of water

Specific humidity: Specific humidity is defined as the ratio of the mass of water vapor to the total mass of the air parcel. The amount of water vapor needs to reach saturation while decreasing the temperature, it will reach the point of saturation without adding or losing water mass.

The method of measuring humidity applied in this experiment is relative humidity. Humidity has also impact on the solar module as the relative humidity decrease it results in higher output

short circuit current but lowers open-circuit voltage. If the relative humidity is low which means there is low water vapor in the air as a result higher solar flux that increases the short circuit current. So, it can be stated that for better efficiency of the solar module it is better to have low relative humidity.

2.3.3 *Effect of Wind Speed*

Wind speed is a fundamental atmospheric rate or quality caused by air moving from high to low pressure due to changes in temperature. Wind direction is almost parallel to isobars due to earth's rotation. Wind speed affects weather forecasting, aviation and maritime operations, construction projects, growth and metabolism rate of many plant species, and has countless other implications. Already wind speed was estimated utilizing the more seasoned Beaufort scale which depends on individuals' perception yet these days an anemometer is utilized to quantify the wind speed.

Wind speed has less impact on solar module performance. Usually, the solar module is installed with an angle that is the latitude angle of the area. Numerous examinations show that when wind streams and contacts the slanted solar panel surface it makes an inconsistent pressure on its two surfaces. Therefore, in the direction of the wind flow the solar module surface experience the drag force and on the other side, it experiences the lift force which in the direction perpendicular to wind flow. As a result, it produces torque. It is unethical to state that the wind velocity has direct implications on the efficiency of solar modules, however, it has a major role to play in PV generation. Whenever, the wind does not provide any extra oomph to the sunlight rays while powering panels, the effect of wind then works as a boost in solar efficiency. If the surface of a solar panel is too hot, the efficiency decreases due to the science behind the generation of electricity. Then again, on account of a cooler solar panel, its effectiveness improves. On the other hand, in the case of a cooler solar panel, its efficiency improves. In short, the effect of wind

on solar cell performance can be explained as; cooler panels allow more energy to get through like an electric current than hot panels do.

At the point when the wind streams, the temperature of solar cell drops. The wind cools the solar modules bringing about delivering less vibration of the electrons so the electrons can convey more energy while moving to the upper state. Solar modules cooled by 1 degree Celsius are 0.05% progressively productive. This rate adds up over time.

2.4 Solar Radiation

2.4.1 *Solar Radiance*

Solar irradiance (W/m^2) is the measurement of the sunlight energy on the earth surface. It is the sunlight in the form of electromagnetic radiation as reported in the wavelength range of the measuring instrument. Performing mathematical calculations such as integrating the solar irradiance over a given time period, results in radiant energy(J/m^2) that is the energy of the sunlight emitted into the surrounding environment. The integrated solar irradiance is called solar irradiation, solar exposure, solar insolation. The measurement of solar irradiance on the earth surface depends on the tilt of the measuring surface, the height of the sun above the horizon and the atmospheric conditions.

Solar radiation comes in many forms, such as visible light, radio waves, heat (infrared), x-rays, and ultraviolet rays. Besides, measuring the spectral irradiance is important, since, different wavelengths of the sunlight are absorbed in different parts of our atmosphere. The visible and infrared radiation that reaches the surface gives us warm feelings. Ultraviolet light creates the ozone layer and higher still ultraviolet light creates the thermosphere, which is ionized by light at the short wavelengths of the extreme ultraviolet (EUV). Because radio communications are

affected by the created ions, changes in the solar EUV output are a primary Space Weather concern.

Solar irradiance is used as a parameter in the following experiment where the theory of solar irradiance is implemented in the vision to calculate solar energy. The theory is based on features like zenith angle, solar altitude angle, latitude angle, declination angle, hour angle. A brief description of all these features and their respective figures are given below.

2.4.2 *Declination Angle*

Declination angle varies with the season due to the tilt of the earth on its axis of rotation and the rotation of the earth around the sun; denoted by δ. The declination angle would always be 0° if the earth were not tilted on its axis of rotation. The earth is tilted by 23.45°C and the declination angle varies plus or minus this amount. When the earth rotates around the sun declination angle changes. Only at the spring and fall equinoxes is the declination angle equal to 0°.

$$\delta = 23.45° \; sin\left[\frac{360(n-80)}{365}\right] \tag{2.16}$$

Here, n is the particular day of the year

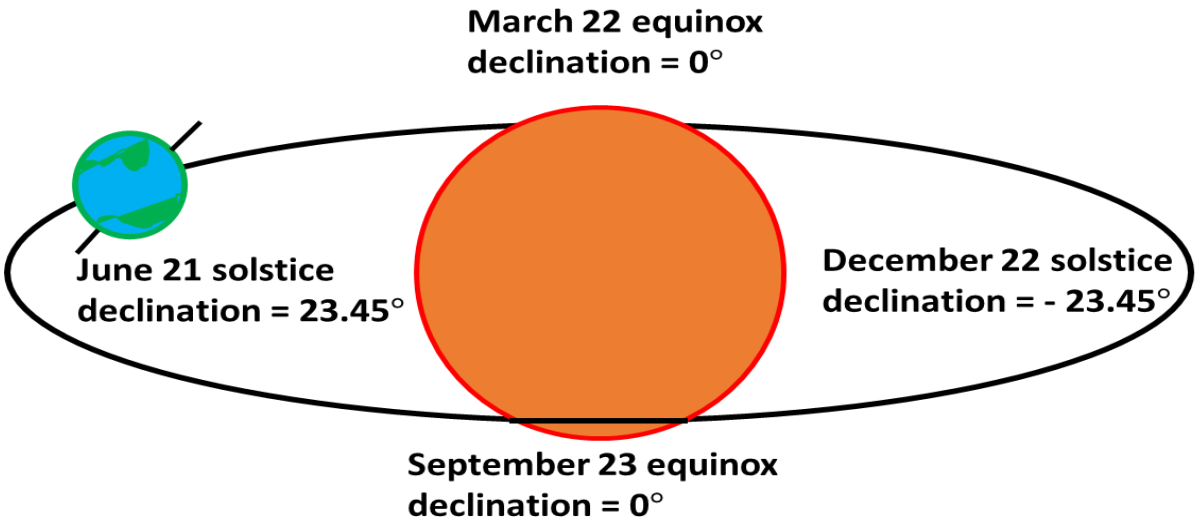

Figure 2.10: The rotation of the earth around the sun

2.4.3 *Latitude Angle*

The position or location of any place on the earth's surface can be determined and described by the latitude or longitude coordinate system. It is shown in figure 2.11 [14].

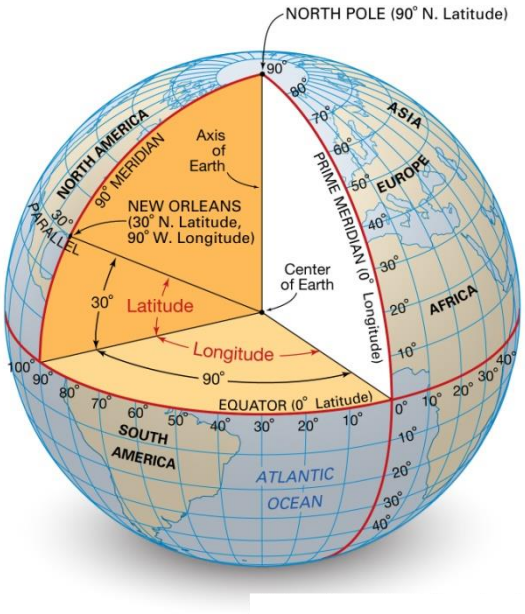

Figure 2.11: The latitude and longitude of any place are based on the sizes of the two angles that originate at the center of the earth

A measurement on a globe or map of location north or south of the equator is defined as latitude. There are different kinds of latitude like geocentric, astronomical and geographic but the difference between them is minor. Commonly geocentric latitude is used. Given in degrees, minutes, and seconds, the geocentric latitude is the arc subtended by an angle at Earth's center and measured in a north-south plane poleward from the Equator. Thus, a point at 30°15′20″ N subtends an angle of 30°15′20″at the center of the globe; similarly, the arc between the Equator and either geographic pole is 90° (one-fourth the circumference of the Earth, or $^1/_4 \times 360°$), and thus the greatest possible latitudes are 90° N and 90° S. Furthermore, to indicate different latitudinal positions on maps or globes, equidistant circles are plotted and drawn parallel to the Equator and each other; they are known as parallels or parallels of latitude.

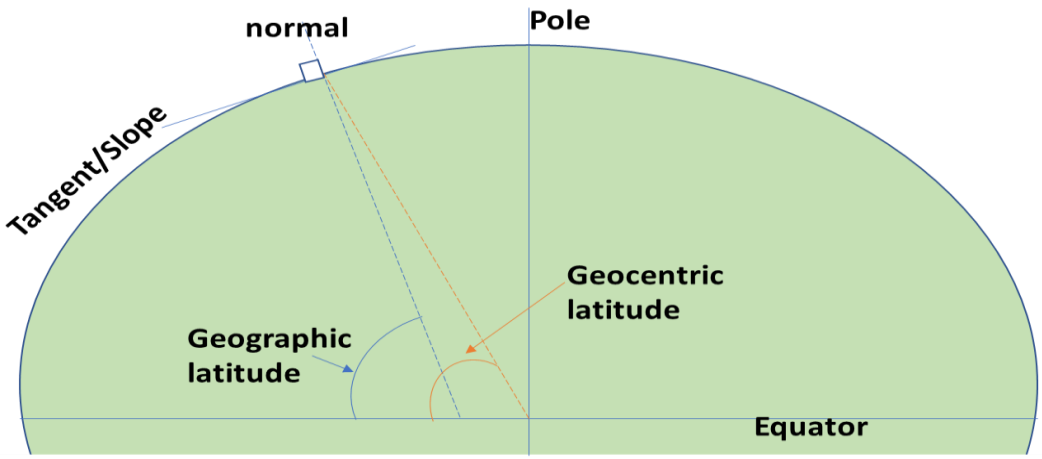

Figure 2.12: Geocentric latitude and geographic latitude

The hardware setup of this experiment is installed at Gabtoli, Dhaka, Bangladesh. The respective latitude angle is φ=23.777176°.

2.4.4 *Solar Altitude Angle*

The angle between the sun's ray and a horizontal plane is known as the solar altitude angle. It is related to the solar zenith angle, denoted as θ_Z, which is the angle between the sun's ray and the vertical. Solar altitude refers to the angle of the sun relative to the earth's horizon and is measured in degree. The solar altitude value varies with the passing time of the day, the time of the year and also the latitude on earth. The regions near the earth's poles have lower solar altitude than the regions close to the equator. The equation of the solar altitude angle is given below;

$$\alpha=\sin^{-1}(\sin\delta*\sin\varphi+\cos\delta*\cos\varphi*\cos\omega) \quad (2.17)$$

Here,

δ is the declination angle

φ is the latitude angle

ω is the hour angle

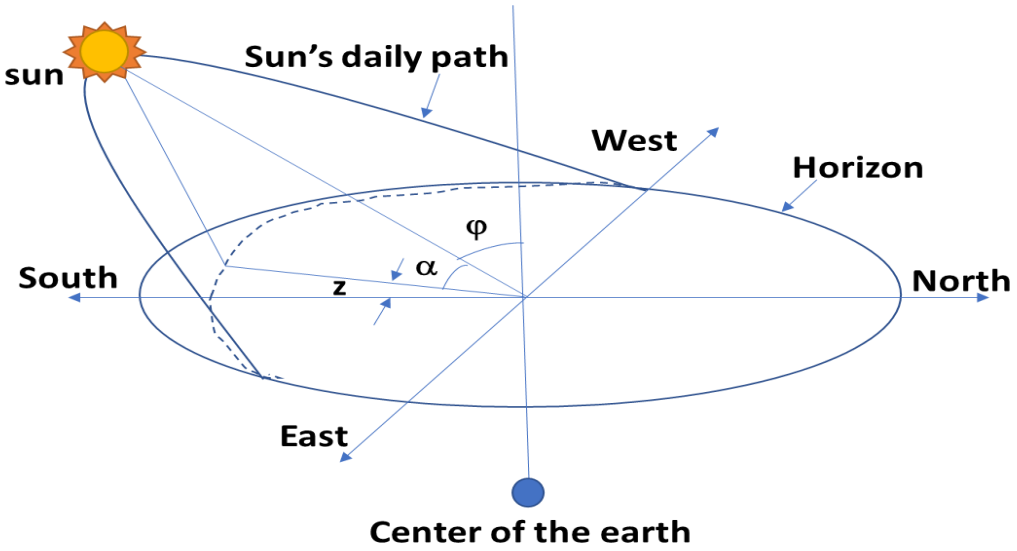

Figure 2.13: Solar Altitude Angle

2.4.5 *Zenith Angle*

The angle between the sun and the vertical is called the zenith angle and denoted as θ_Z. The zenith angle is similar to the elevation angle or solar altitude angle but it is measured from the vertical perspective rather than horizontal perspective. The equation of the zenith angle is given below;

$$\theta_Z = 90° - \alpha \tag{2.18}$$

Here;

α is the solar altitude angle

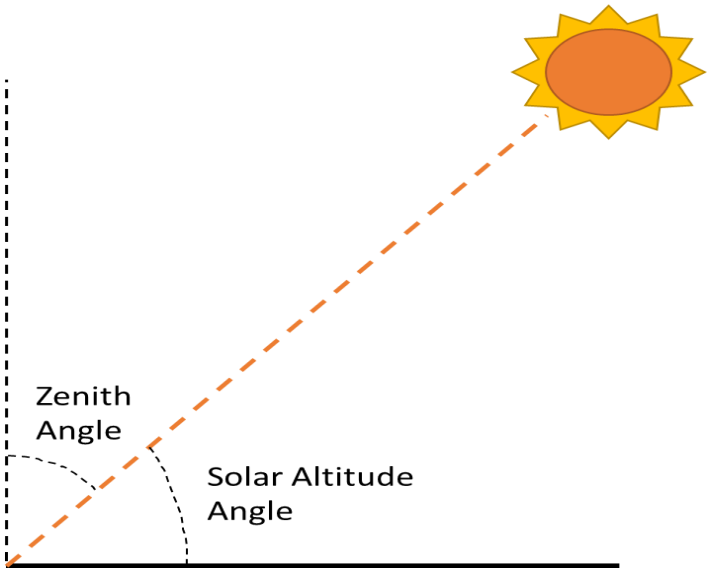

Figure 2.14: Zenith Angle and Solar Altitude Angle

2.4.6 *Sunrise Angle*

The angle when the upper limb of the sun appears on the horizon in the morning is called the sunrise angle; denoted by ω_s and measured in degree. The equation of the sunrise angle is given below;

$$\omega_s=\cos^{-1}(-\tan\varphi*\tan\delta) \quad (2.19)$$

Here,

φ is the latitude angle

δ is the declination angle

2.4.7 *Sunrise and Sunset Time*

By calculating the sunrise and sunset time for a particular day, the total hours of sunlight available for that particular day is measurable. This can be easily done by subtracting the sunrise time from the sunset time then the output will be the total hours(t) of sunlight available time. The equation for the sunrise and sunset time is given below;

$$S_r=12-\left(\frac{1}{15}\right)*(\cos^{-1}(-\tan\delta*\tan\varphi)) \quad (2.20)$$

$$S_s=12+\left(\frac{1}{15}\right)*(\cos^{-1}(-\tan\delta*\tan\varphi)) \quad (2.21)$$

$$t= S_S-S_r \quad (2.22)$$

Here,

φ is the latitude angle

δ is the declination angle

2.4.8 *Hour Angle*

The hour angle is defined as a point on the earth's surface. It is the angle through which the earth would turn to bring the meridian of the point directly under the sun. As the earth is rotating so the angular displacement represents the time. Therefore, by observing the sun from the earth we can measure the solar hour angle by an expression of time, expressed in angular measurement which is in degree from the solar noon. At solar noon, the hour angle is 0.00 degree and the time before the solar noon is expressed as negative degrees. The local time after the solar noon is expressed as positive degrees. For example, at 10:30 am local apparent time, the hour angle is -22.5° . The equation for the hour angle is given below;

$$\omega=\omega_s-15(t-t_{sr}) \quad (2.23)$$

Here;

t is the local apparent time

t_{sr} is the sunrise time

2.4.9 *Air Mass*

An air mass is a large volume of air in the atmosphere that is mostly uniform in temperature and moisture. Air masses can extend thousands of kilometers in any direction and can reach from ground level to the stratosphere 16 kilometers into the atmosphere. As for simplicity, a measurement of how much atmosphere the sun's rays have to pass through on their way to the surface of the earth is known as air mass. The solar energy extracted is less than expected because the particles in the atmosphere absorb and scatter light rays. The equation of the air mass is given below;

$$AM=\frac{1}{cos\theta_z} = \csc\alpha = \sec\theta_z \quad (2.24)$$

2.4.10 *Solar Irradiance Calculation*

The following experiment is based on two solar modules whose positions are fixed. So, dual-axis solar irradiance is calculated first. The results from the calculation is used to measure the solar irradiance of fixed axis solar module. The equation of dual-axis and fixed axis solar module are given below;

Dual Axis:

$$I=I_0*(0.7)^{AM^{0.078}} \quad (2.25)$$

Here,

I_0 is the solar irradiance in space outside the atmosphere which is 1376 W/m^2

AM is the air mass

Fixed Axis:

$$G=I*\cos\delta*\cos\theta_z \quad (2.26)$$

Here;

I is the dual axis solar irradiance

δ is the declination angle

θ_z is the zenith angle

2.5 Chapter Summary

The chapter as entitled, “Theoretical Background” discussed the basic fundamentals of a solar module. Initially, it started with a glimpse of the construction of a solar module along with the working principle. The effect of temperature on p-n junction is explained which implicates that the bandgap energy between the distinct energy bands decides the electrical conductivity property of different materials. Afterwards, theoretical parameters associated with the solar module working principle is elaborated that implicates a point in the IV characteristics graph where the module has its highest Voltage and Current denoted as maximum power point. Alongside the theoretical parameters affecting the module’s output, weather parameters also have a visible effect on the output power of solar module. So, the hardware setup used in this experiment updates the reading of weather parameters such as humidity, temperature, air pressure and windspeed dynamically with respect to time. The weather parameters and their effects are discussed in this chapter. Moreover, some basic angles are defined for the theoretical calculation of the incident solar irradiance (W/m^2) on the solar module used in this experiment. The results are further integrated to measure the cumulative light energy (Wh/m^2).

Chapter 3

Experimental Setup

3.1 Introduction

The main focus of this chapter is to elaborately discuss how the Hardware Setup was built and configured. In short, the hardware setup was built using several environmental factors measuring sensors, current sensors, microcontrollers and some software. The sensors that were used are Temperature sensors, Humidity sensor, Current sensors, Anemometer (the wind speed measuring sensor) and Barometric Pressure Sensor. All these sensors were interfaced using Arduino Uno and Raspberry Pi 3 B+ microcontrollers. The data of each sensor was collected and saved with respect to the built-in real-time clock of Raspberry Pi 3 B+, so that the effect of the weather change can be tracked over time. As the Raspberry Pi 3 B+ has internet connectivity, these data can be directly uploaded to any online storage using Putty and Tight VNC Server which are Remotely Accessible Tools for Raspberry Pi 3 B+. The data has been collected since October 2019 and the data collection target is at least until November 2020.

This chapter is mainly divided into two parts i.e. Hardware Implementation and Software Implementation. Hardware Implementation is divided into three sub-sections - Data Collection System, Sensor Brief Description & Connection Diagrams Explanation. In these sub-sections, how the system is working and collecting sensor data, each sensor's description and performance and how the sensors are connected with the microcontrollers are discussed respectively. Software Implementation is divided into three sub-sections – Data Extraction System, Software Brief Description and Flow Chart for Each Sensor Interface. In these sub-sections, the data extraction process, used software tools for data collection are discussed and flow charts of all the sensor interfacings are shown.

3.2 Hardware Implementation

In this section, The Weather data collection system using Raspberry Pi 3 B+ & Arduino UNO is explained with detailed block diagram and connection diagram of each circuit. Also, a brief description and performance of each sensor are shown in this section.

3.2.1 *Data Collection System*

The hardware setup is divided into two parts to reduce the pressure on microcontrollers. In one part of the system one Raspberry Pi 3 B+ is dedicated to collect the data of a DS18B20 temperature sensor, a BMP180 Barometric Pressure sensor and an anemometer. In another part of the system another Raspberry Pi 3 B+ is dedicated to collect the data of two INA219 Current Sensor, a DHT11 Humidity sensor and a temperature sensor. How both parts of the system are working is shown with help of block diagrams in Figure 3.1 and Figure 3.2.

In Part – 1 (Figure 3.1), a temperature sensor is connected to Raspberry Pi through 1-Wire bus communication system. The sensor sends its digital data to the Raspberry Pi through its output pin which is received by the GPIO pin of the Raspberry Pi. The BMP180 Barometric Pressure sensor communicates with the Raspberry Pi through I^2C Communication. The sensor sends its data through its SCL and SDA pinouts, which is received by the Raspberry Pi's SCL and SDA pins. In this part of the system an anemometer is sending its analog data to the Raspberry Pi through Serial Communication which was previously collected by an Arduino UNO microcontroller. After the collection of all the data, the built-in real-time clock has been used to save the data in the Raspberry Pi's storage and to track the data's corresponding date and time.

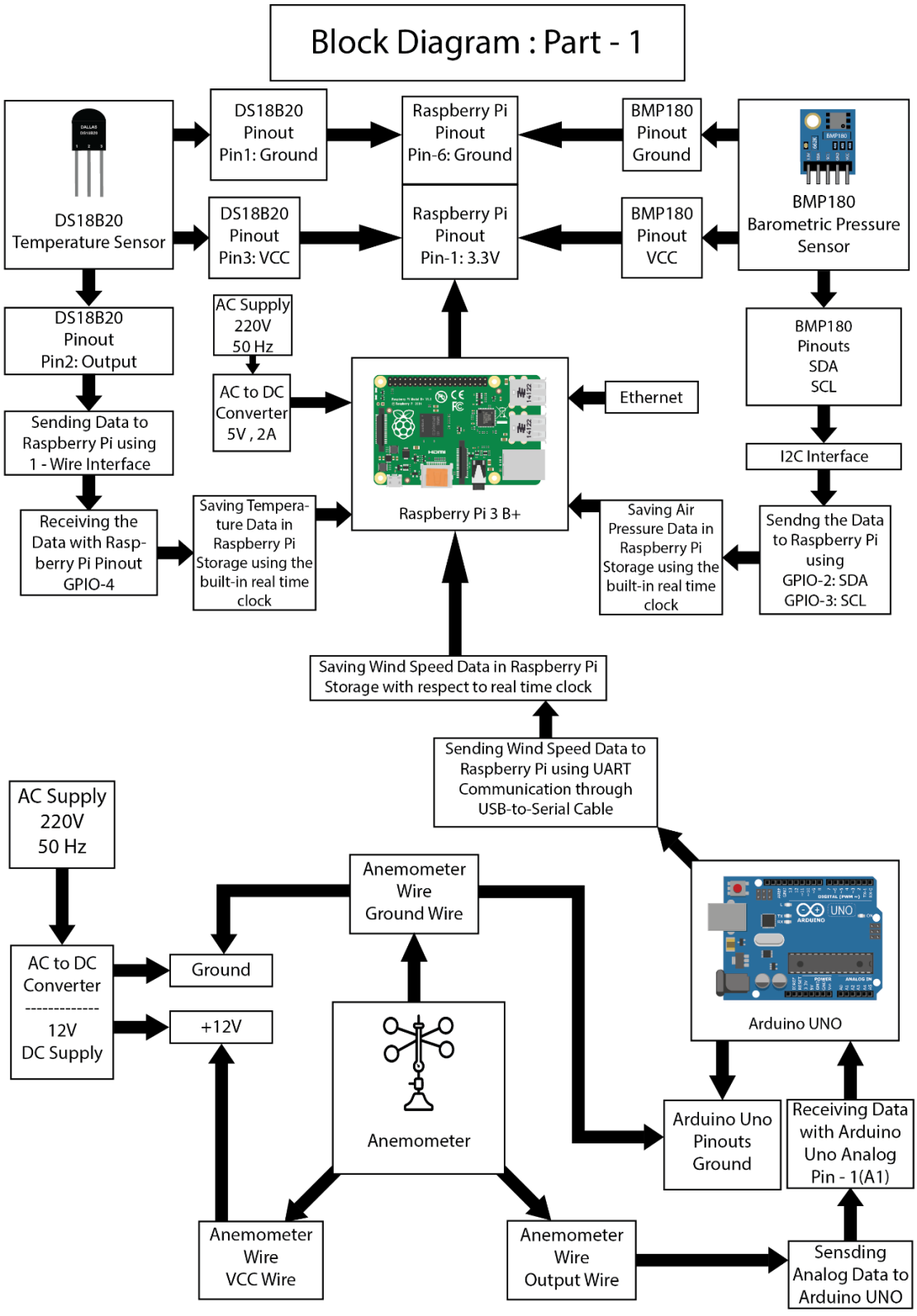

Figure 3.1: Block Diagram of the System (Part – 1), containing an Arduino UNO, a Raspberry Pi 3 B+, a DS18B20 Temperature sensor, an Anemometer and a BMP180 Barometric Pressure sensor.

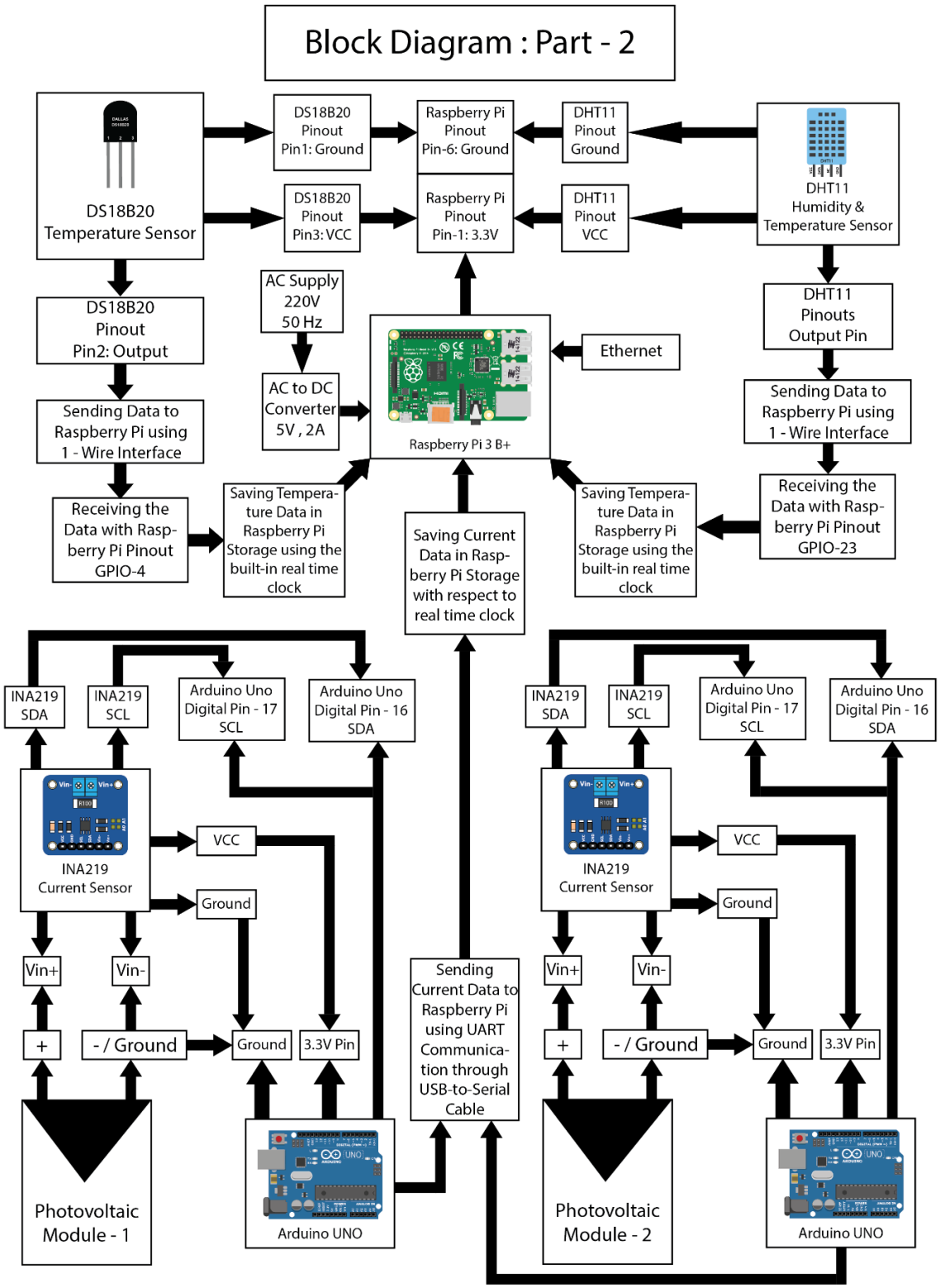

Figure 3.2: Block Diagram of the System (Part – 2), containing two PV Modules, two INA219 Current sensors, two Arduino UNO, one Raspberry Pi 3 B+, one DS18B20 Temperature sensor and one DHT11 Humidity sensor.

In Part – 2 (Figure 3.2) of the system a Raspberry Pi 3 B+ is collecting the short circuit current data of two separate solar modules using two separately connected INA219 current sensor through I^2C communication. For each INA219 sensor, the data is firstly collected by an Arduino UNO microcontroller, then the data gets transmitted to the Raspberry Pi 3 B+ through Serial communication system using a USB-to-Serial Cable. A DHT11 Humidity sensor and a DS18B20 temperature sensor are also connected with Raspberry Pi 3 B+ directly through 1-Wire bus communication. They transmit their output data through the output pinouts, which are connected to the GPIO pin of the Raspberry Pi 3 B+ that supports 1-wire bus communication. After the collection of all the data, the built-in real-time clock has been used to save the data in the Raspberry Pi's storage and to track the data's corresponding date and time.

3.2.2 *Sensor Description and Performance*

Anemometer

The three-cup type wind speed sensor (Figure 3.3) is an instrument which can determine the wind speed. It is made out of a shell, the wind cups and circuit module.

Figure 3.3: Anemometer

The sensor shell and wind cups are made of such materials that are made of aluminum alloy, where the special mold precision casting technology is being used. The tolerance size is so

little. The surface accuracy is very high, and the interior circuit has been protected with the metal body. The quality of the sensor is very high. It is weather resistance, corrosion resistance and waterproof. The cable's plug is a military plug. It has a decent anti-corrosive painting and can prevent erosion performance. So, it is guaranteed that the instrument can be utilized for a long time.

Equation:

$$V = 6 * U \tag{3.1}$$

The sensor gives two types of output -

i. Voltage Output

ii. Current Output

It depends on the pinout combination used by the user.

Anemometer Performance Test:

Before using the sensor in the experimental setup of the thesis project, the sensor was tested by comparing its experimental readings with the readings given in the sensor Datasheet.

Some curves were plotted by analyzing the data collected from the Table 3.3. In Figure 3.4 the voltage vs wind speed curve and in Figure 3.5 the percentage difference between experimental voltage & datasheet voltage vs wind speed curve are plotted.

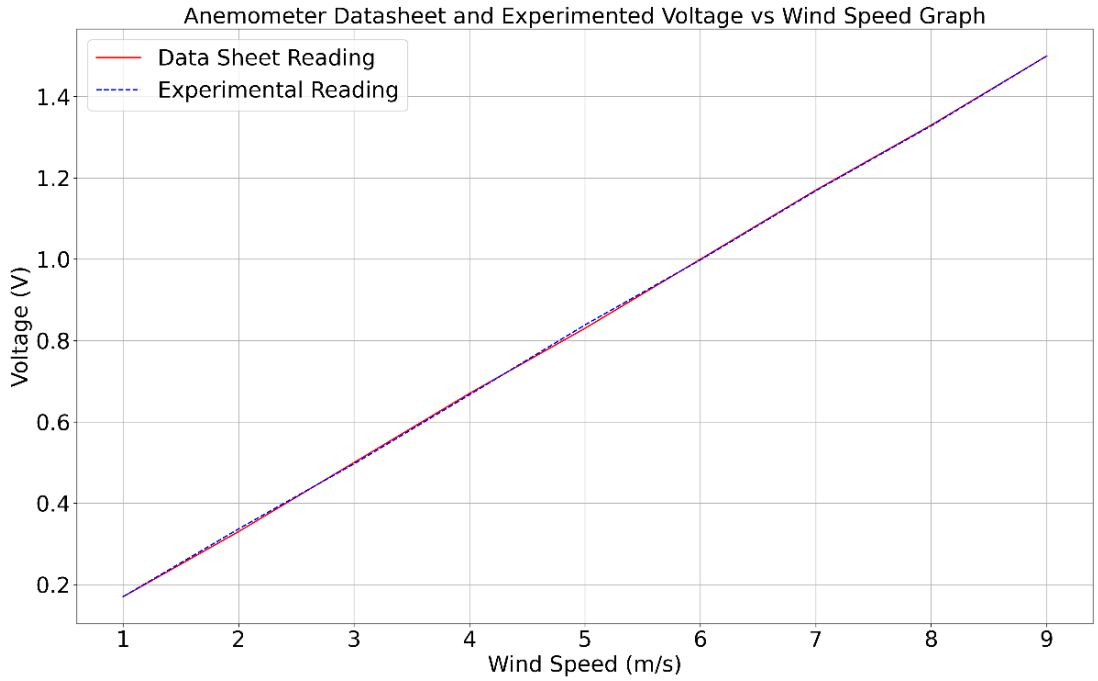

Figure 3.4: Anemometer Datasheet & Experimental Voltage vs Wind Speed Curve

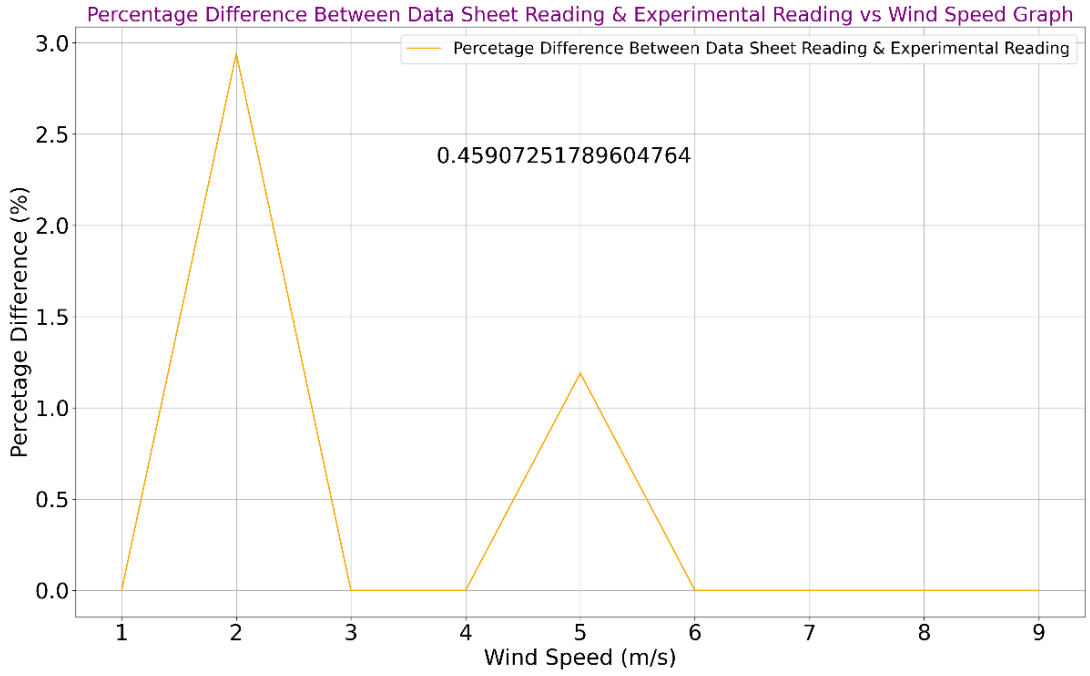

Figure 3.5: Percentage Difference between Datasheet & Experimental Data

INA219 Current Sensor

The INA219 Sensor (Figure 3.6) is a digital current sensing amplifier, which is compatible with the I^2C interface. It can provide digital voltage, current & power readings.

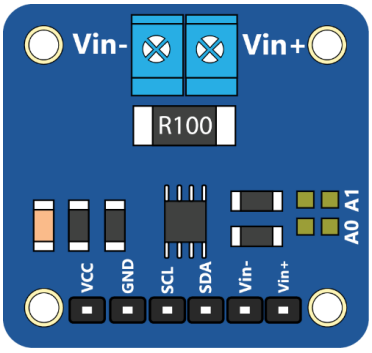

Figure 3.6: INA219 Current Sensor

Even though the sensor is powered with 3V to 5V DC, it can handle high side current measuring up to +26VDC, because the INA219 chip is smarter. The sensor is great for tracking battery life of photovoltaic modules as it reports back that high side voltage. A precision amplifier measures the voltage across the 0.1 Ω, 1% sense resistor. INA219 current sensor can measure up to ±3.2 Amps as the amplifier's maximum input difference is ±320mV.

INA219 Current Sensor Performance Test:

The short circuit current data of the Photovoltaic Module was collected using both INA219 Current Sensor & Multimeter at the same time. The PV Module, INA219 Current Sensor & Multimeter all three devices were connected in a series combination, which allows the same current flow throughout the whole circuit. The measured short circuit current is of 1st April, 2020. The data were manually measured for 30 minutes using a multimeter. The data were collected from 1:43 PM to 2:13 PM. In the Figure 3.7, it can be observed that the value of short circuit current data collected by the INA219 sensor is less than the value of the data collected by using multimeter.

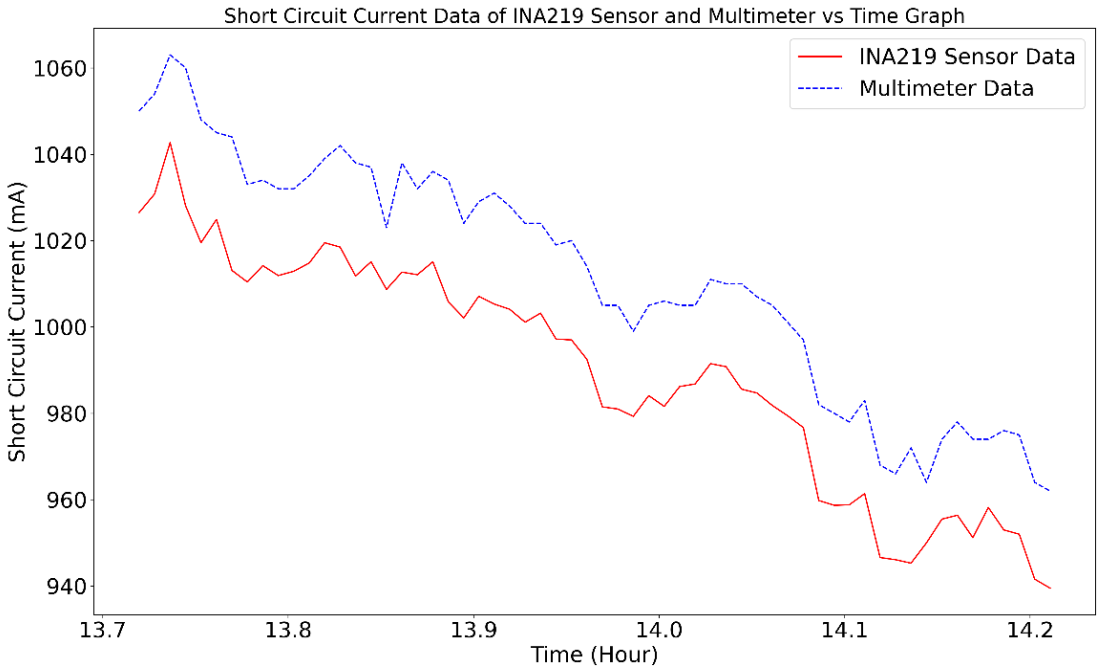

Figure 3.7: Short Circuit Current of INA219 Sensor and Multimeter vs Time Curve

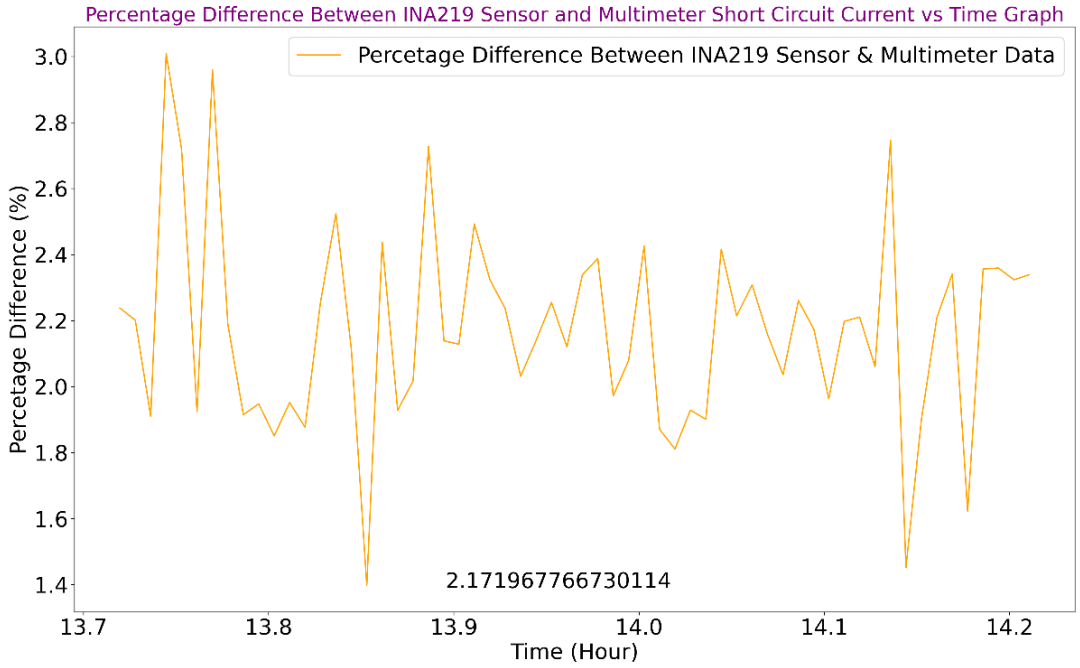

Figure 3.8: Percentage Difference between INA219 & Multimeter Short Circuit Current

The short circuit current data were plotted with respect to time, to find out the percentage difference between the digitally collected (using INA219) data and manually collected (using Multimeter) data in Figure 3.8. The average percentage difference is 2.17%.

DHT11 Humidity Sensor

Humidity sensor also known as Hygrometer is used to measure the humidity of air. Humidity is the measure of the water vapor present in a gas. The humidity measurement is associated with two parameters, absolute humidity and relative humidity. Humidity as a weather parameter has effect on the performance of Photovoltaic Module.

DHT11 (Figure 3.9) is a low-cost digital sensor, which can be used for measuring temperature & humidity. This sensor can be easily interfaced with any microcontroller like Arduino UNO & Raspberry PI. It is available as a sensor and as a module. It is a relative humidity sensor. To measure the surrounding air temperature and humidity, this sensor uses a thermistor and a capacitive humidity sensor.

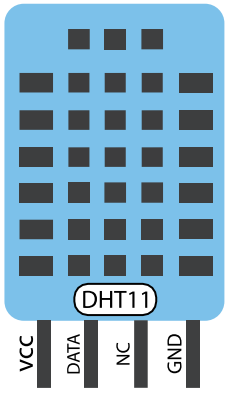

Figure 3.9: DHT11 Humidity Sensor

Data and Graph:

To test the performance of the DHT11 Humidity Sensor, the humidity data of 10th November 2019 & 27th November 2019 were taken, which were respectively a rainy day & a sunny day. Multiplying each Humidity value by 100 gives us the Humidity in percentage. The data was taken from 6 AM to 6 PM (Local Time) with 15 minutes gap in between. With these data a

graph was plotted (Figure 3.10), which shows how differently the DHT11 Humidity sensor performs because of the change in weather.

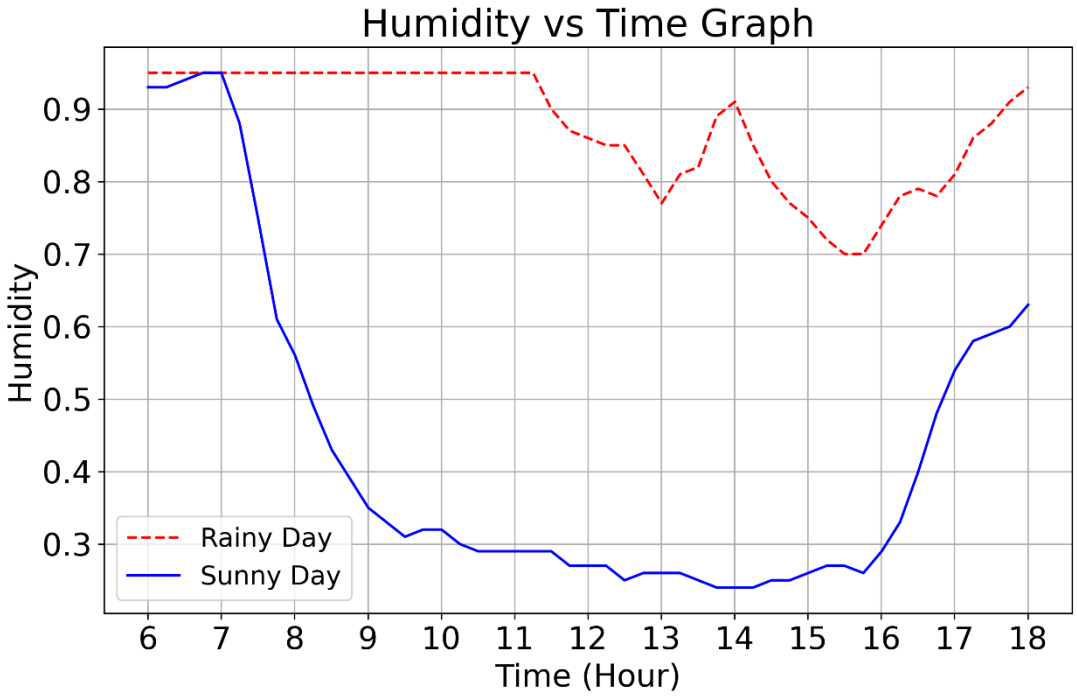

Figure 3.10: Humidity vs Time curve of a Sunny and a rainy Day

In the Figure 3.10, we can see that the humidity is lot higher in the rainy day than the sunny day. And from 6 AM to 7 AM the humidity is almost the same, which is because of the sun light. As the sun rises, the humidity continued to get higher in the sunny day, while the humidity did not rise in the same way for the rainy day. Because, the rate of water vapor was much higher in the atmosphere and the sun was cover by clouds.

DS18B20 Temperature Sensor

The DS18B20 temperature sensor (Figure 3.11) gives 9-bit to 12-bit Celsius temperature measurements. This sensor requires only one data line to communicate with a microprocessor as the sensor by definition communicates over a 1-wire bus. DS18B20 has revolutionized the

digital world because of its 1 wire protocol. The sensors have an accuracy of ±0.5ºC, over the range of -10ºC to +85ºC.

In the same data bus, multiple sensors can be connected. Each sensor has a unique serial number to identify itself. The sensor has two operating modes, which are normal mode and parasite mode. A 3-wire connection is needed in normal mode. In parasite mode, only two wires – data wire and ground wire are required, while the sensor derives its power from the data line.

Figure 3.11: DS18B20 Temperature Sensor

1-Wire Bus System:

This system uses a single bus master to control one or more slave devices. The DS18B20 temperature sensor is always a slave. When there is only one slave the system is referred to as a “single-drop” system & the system is called “multi-drop” system, if there are multiple slaves on the bus. All the data and commands are transmitted least significant bit first over the 1-Wire bus.

Data and Graph:

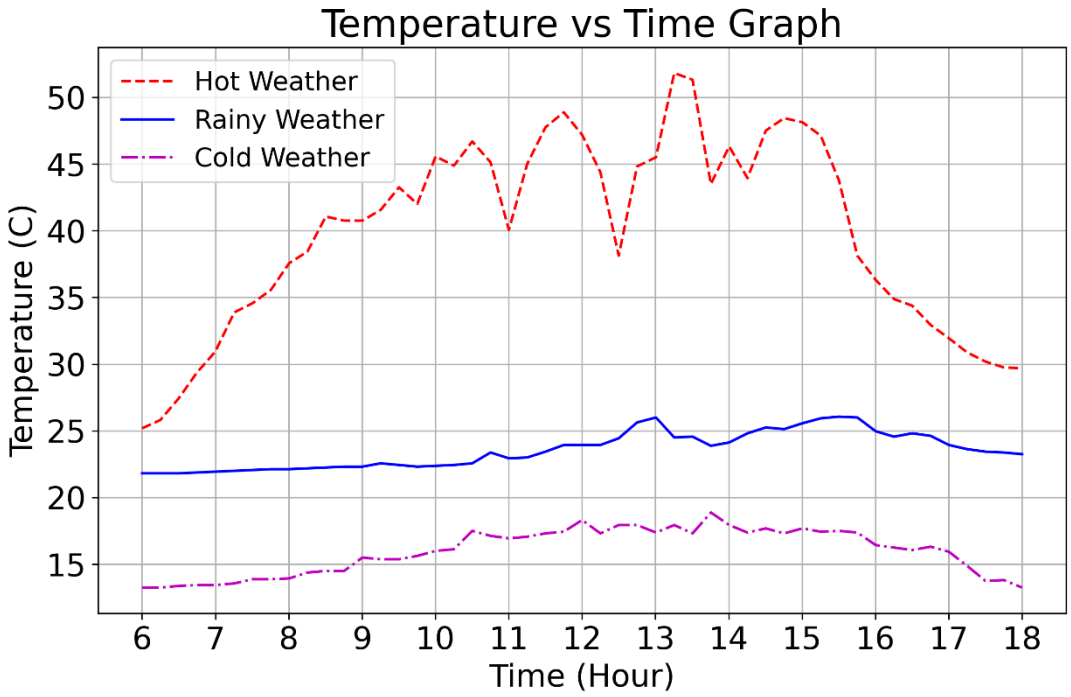

Figure 3.12: Difference in Temperature due to Weather Change

To test the performance of the DS18B20 Temperature sensor, the temperature data of 18th October 2019, 10th November 2019 & 11th January 2020 were taken, which were respectively a Hot Weather day, a Rainy Weather day & a Cold Weather day. We took the data from 6 AM to 6 PM (Local Time) with 15 minutes gap in between each data. With the extracted data from the sensor we plotted some curves (Figure 3.12), which shows how differently the DS18B20 Temperature sensor performs because of the change in weather.

BMP180 Barometric Pressure Sensor

The BMP180 (Figure 3.13) is a digital barometric pressure sensor. It can also measure temperature and altitude. The sensor can be easily interfaced with any microcontroller and requires 1.8V to 3.6V power supply. In advance resolution mode, BMP180 can measure pressure range from 300hPa to 1100hPa with an accuracy of up to 0.02hPa (0.17m). This sensor

is an improved version of the BMP085 sensor. For high accuracy, linearity and stability for a longer period of time, the BMP180 sensor uses the piezo-resistive technology. The sensor has four to five pinouts – 3.3V, SDA (Serial Data), SCL (Serial Clock), Ground and VCC.

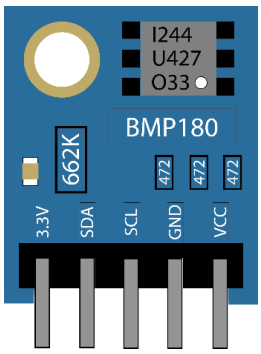

Figure 3.13: BMP180 Barometric Pressure Sensor

3.2.3 *Hardware Setup*

In the hardware setup, two circuits were built with two Raspberry Pi 3 B+ boards, three Arduino UNO boards, two INA219 Current Sensors, two DS18B20 Temperature Sensors, one Anemometer, one DHT11 Humidity Sensor and one BMP180 Barometric Pressure Sensor. Two circuits were built to lessen the pressure on the microcontrollers, as the microcontrollers were set to the data for at least one year.

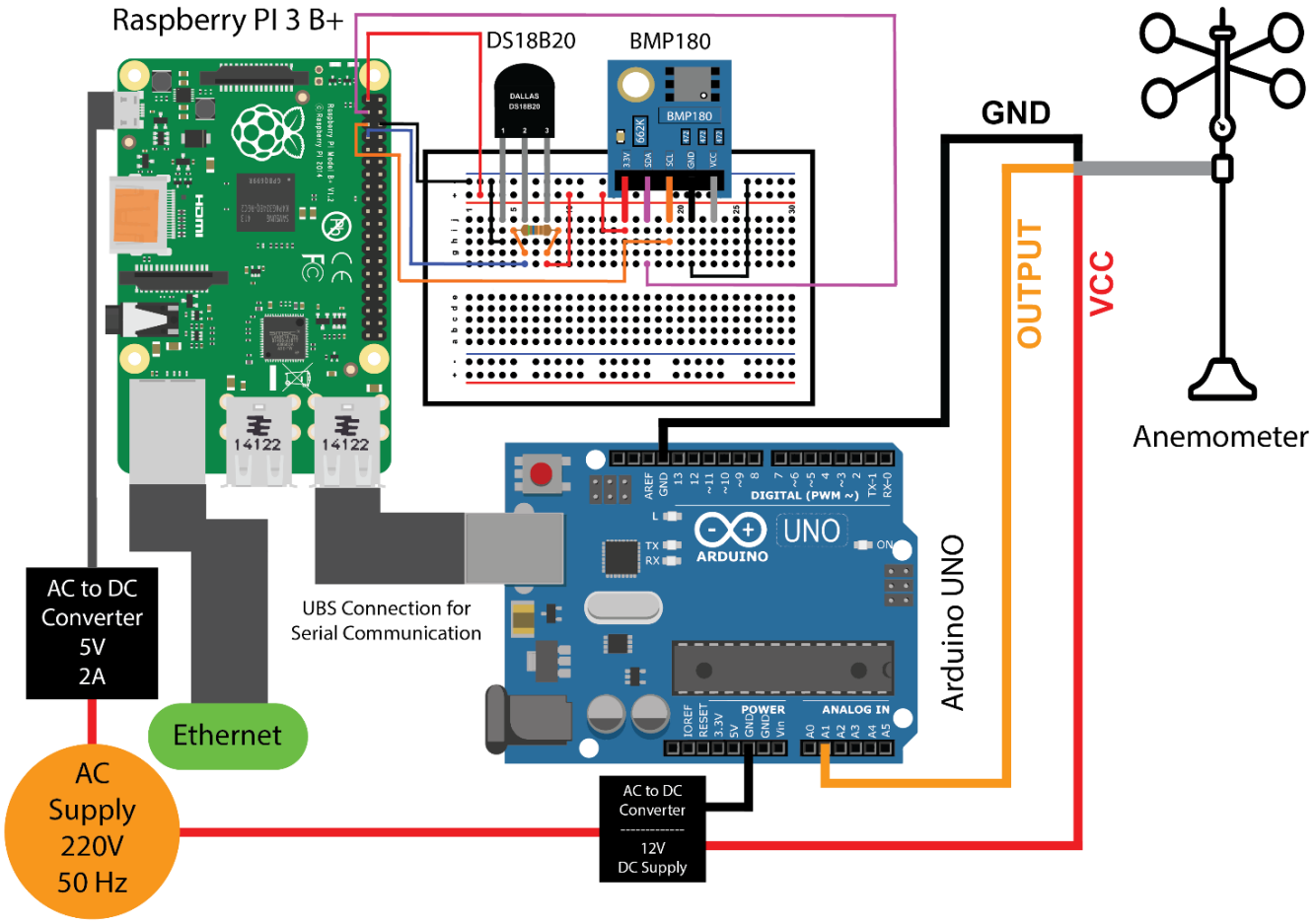

Figure 3.14: Connection Diagram of Circuit – 1 of the system, containing an Arduino UNO, a Raspberry Pi 3 B+, a DS18B20 Temperature sensor, an Anemometer and a BMP180 Barometric Pressure sensor.

The Circuit – 1 shown in the Figure 3.14 contains one Raspberry Pi 3 B+, one Arduino UNO, one DS18B20, the BMP180 Barometric Pressure sensor and the Anemometer.

Explanation of Circuit – 1:

Firstly, a DS18B20 temperature sensor is connected to the Raspberry Pi 3 B+ through 1 – Wire Interface. Its output pin is connected to the GPIO – 4 pin of the raspberry pi 3 B+. The ground and V_{CC} pins of the sensor are connected to the Pin – 6 and Pin – 1 respectively on the raspberry pi 3 B+ board.

Secondly, The BMP180 Barometric Pressure sensor in connected to the Raspberry Pi 3 B+ through I^2C Interface. The sensor's Ground & V_{CC} Pin are respectively connected to the

Raspberry Pi's Pin – 6 and Pin – 1, which are respectively 3.3V supply and Ground. The SDA Serial Data) & SCL (Serial Clock) pins of the BMP180 goes to the GPIO – 2 and GPIO – 3 pins on the raspberry pi board, which also work as SDA and SCL pins.

Finally, the Anemometer sensor is connected directly to the Arduino UNO. Its Voltage output pin is connected to the A1 (Analog Pin) on the Arduino UNO board, while the sensor is powered up by an external 12V AC-DC converter. The Adapter positive end goes to the V_{CC} of the Anemometer and the sensor's ground is connected with adapter's negative end and Arduino UNO's ground pin. After collecting the data sent by the Anemometer, The Arduino UNO transmits the data through Serial interface using an USB cable. For serial interfacing, Serial Interface option must be enabled in Raspberry Pi 3 B+'s Configuration.

After gathering each sensor data, the Raspberry Pi 3 B+ saves the data in a data logger with the help of a built-in Realtime clock. To keep the Realtime clock always updated, internet connection is essential. For this, an ethernet cable is connected to the Raspberry Pi 3 B+. From the 220V, 50Hz AC supply another 5V, 2.5A converter is being used to power up the Raspberry Pi 3B+. The Arduino UNO is powered up by the Raspberry Pi 3 B+ through the USB cable.

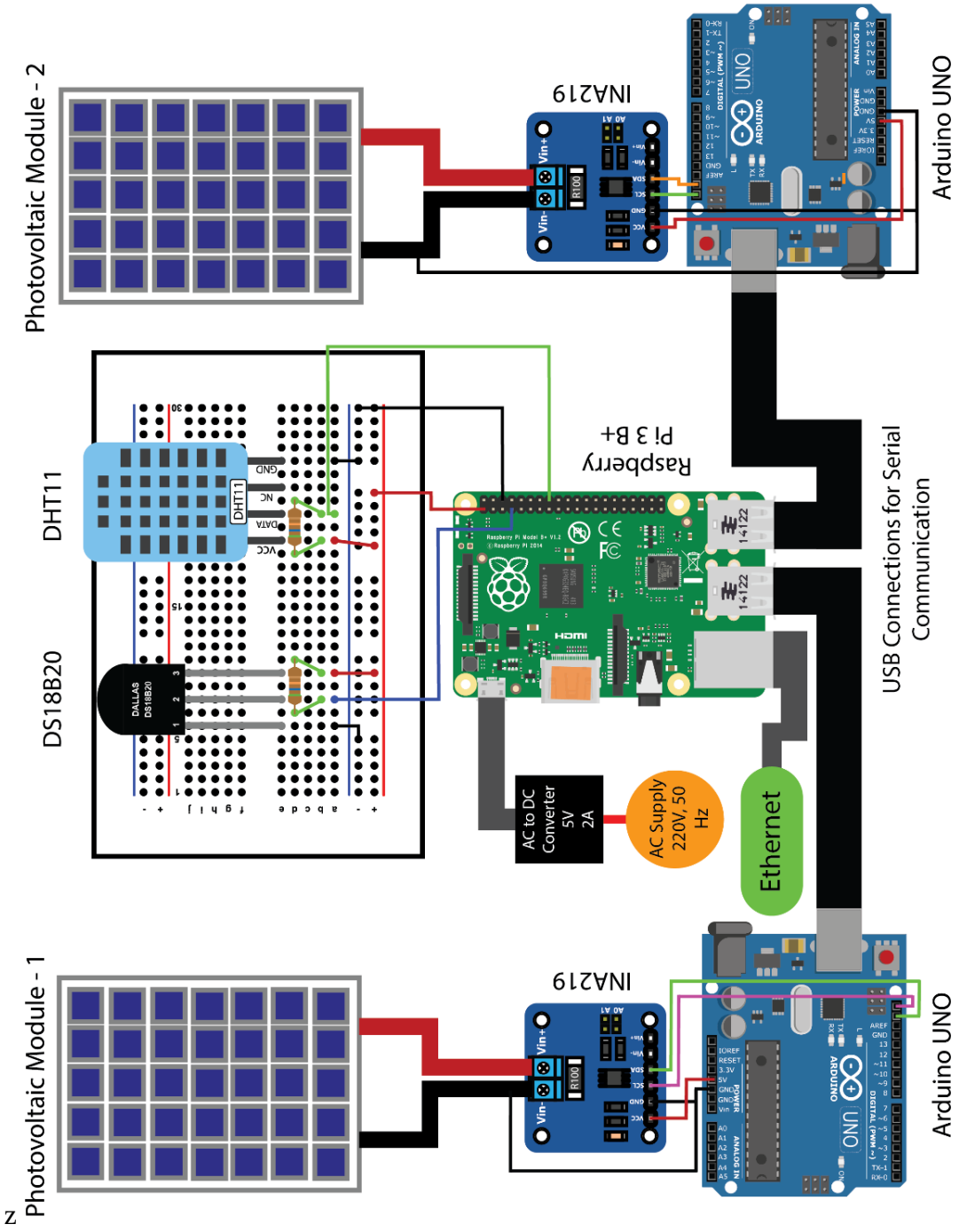

Figure 3.15: Connection Diagram of Circuit – 2 of the system, containing two PV Modules, two INA219 Current sensors, two Arduino UNO, one Raspberry Pi 3 B+, one DS18B20 Temperature sensor and one DHT11 Humidity sensor.

The Circuit – 2 shown in the Figure 3.15 contains one Raspberry Pi 3 B+, two Arduino UNOs, two Photovoltaic Modules, two INA219 Current sensors, one DS18B20 temperature sensor and one DHT11 Humidity sensor.

Explanation of Circuit – 2:

Firstly, Both INA219 Current sensors are connected with the Arduino UNO and Photovoltaic Module in the same way. They are connected with the microcontrollers through I^2C Interface or also known as 2 – Wire Interface. The V_{CC} Pin of the sensor in connected to the 5V supply of Arduino UNO. The sensor's ground is connected with the negative end of the Photovoltaic Module which is also connected with the Vin- pin on the sensor and the ground of Arduino UNO. Vin+ Pin on the INA219 sensor is connected with the Photovoltaic Module's positive end. The SDA and SCL pins of the sensor goes to the SDA and SCL pins on the Arduino UNO board, which are located as unnamed pins near the AREF pin on the Arduino UNO board. After collecting the data sent by the INA219 Current sensor, the Arduino UNO transmits the data to the Raspberry Pi 3 B+ with the help of Serial Communication through an USB cable.

Secondly, The DHT11 Humidity sensor is connected with the Raspberry Pi 3 B+ with 1 – Wire Interface. The V_{CC} and ground pins are connected with the Raspberry Pi 3 B+'s 3.3V and ground pins, which are respectively Pin – 1 and Pin – 6 on the Raspberry Pi Board. The Data Pin of the sensor goes to the GPIO – 23 pins on the Raspberry Pi 3 B+.

The DS18B20 Temperature sensor is connected with the Raspberry Pi 3 B+ in the same way mentioned in the Figure – 3.14.

After gathering each sensor data, the Raspberry Pi 3 B+ saves the data in a data logger with the help of a built-in Realtime clock. To keep the Realtime clock always updated internet connection is essential. For this, an ethernet cable is connected to the Raspberry Pi 3 B+. From the 220V, 50Hz AC supply another 5V, 2.5A converter is being used to power up the Raspberry Pi 3B+. The both Arduino UNO boards are powered up by the Raspberry Pi 3 B+ through the USB cable.

3.3 Software Implementation

In this section, the data extraction system is explained using different software tools. Also, the brief description for all the software that were used are given in this section.

3.3.1 *Data Extraction System*

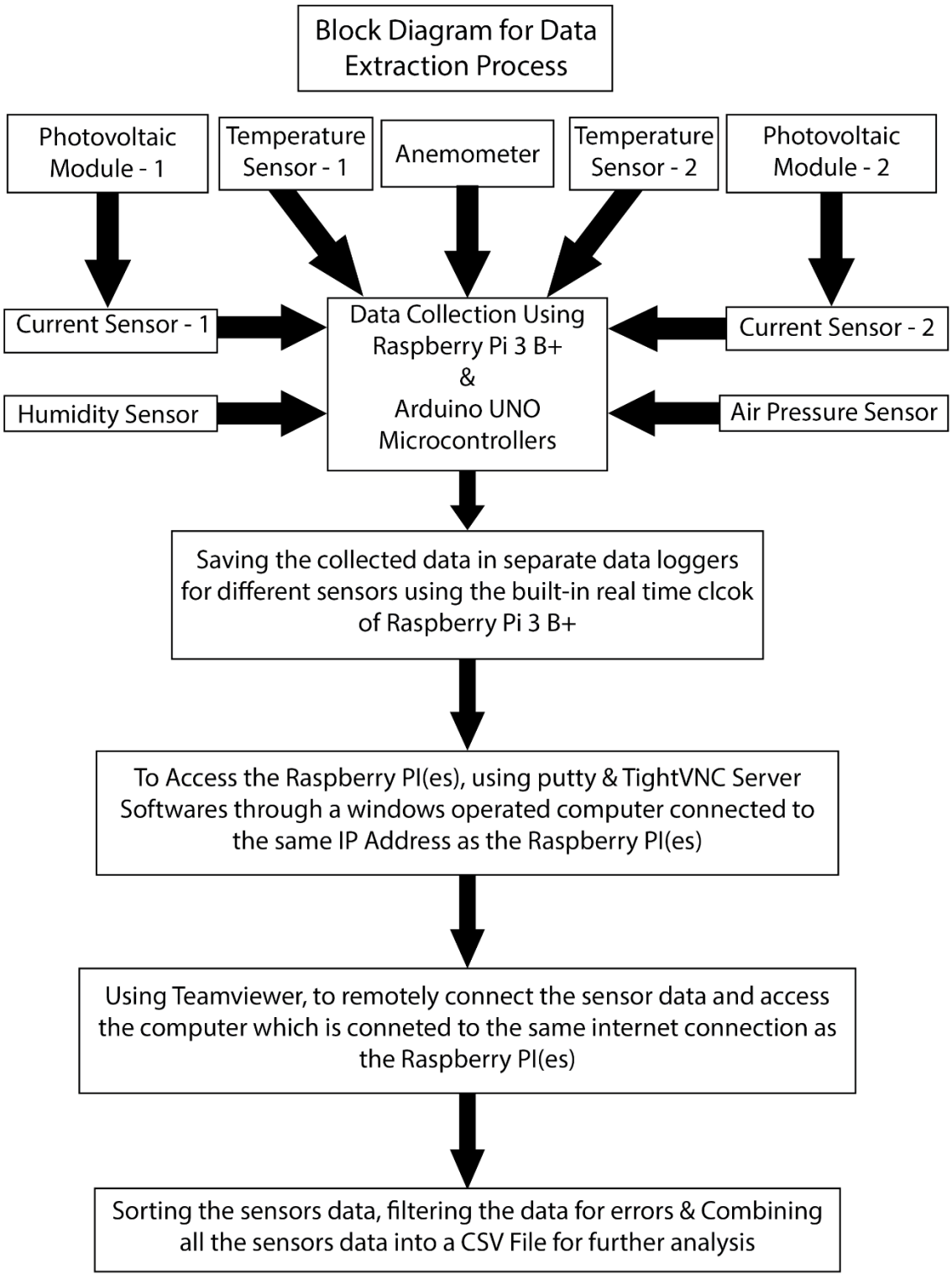

Figure 3.16: Weather Station Data Collection Process Block Diagram

The IP addresses of each Raspberry Pi 3 B+ extracted by using the Advanced IP Scanner software, are used to connect a laptop with the Raspberry Pi 3 B+ modules through Putty software. For both Raspberry Pi 3 B+ modules, the process is same.

In Figure 3.21, the Putty Configuration Console is shown. By putting the IP address of the Raspberry Pi 3 B+ in the "Host Name" box and clicking on the "Open" button generates a terminal window asking for ID and Password. The ID and Password were fixed during the installation of the Raspbian operating system on Raspberry Pi 3 B+ module. After entering the correct ID and Password, the Raspberry Pi Terminal Window (Figure 3.17) will be opened.

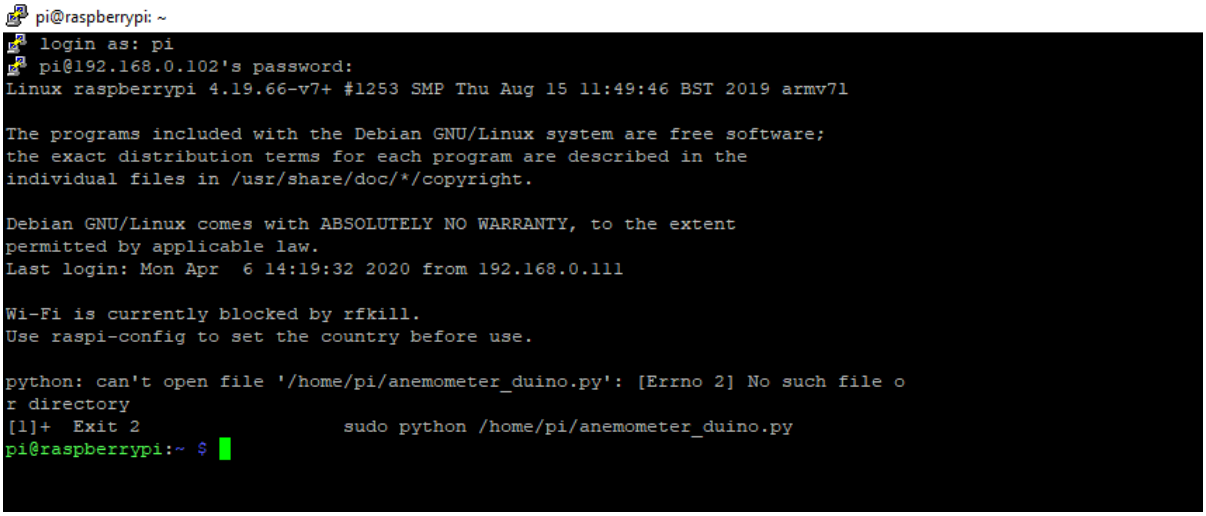

Figure 3.17: Raspberry Pi Terminal Window Through Putty

In the Terminal Window, executing "tightvncserver" command activates the Tight VNC Server.

In Figure 3.18, after executing "tightvncserver" three new lines were printed on the Terminal Window. In the first line, the raspberry pi's address is shown as "raspberrypi:1". Here, "raspberrypi" means actually the IP address of that particular raspberry pi and "1" stands for, how many laptop or computer can be connected at the same time. In the case the connectable computer number is 1. It can be increased by executing the "tightvncserver" command again.

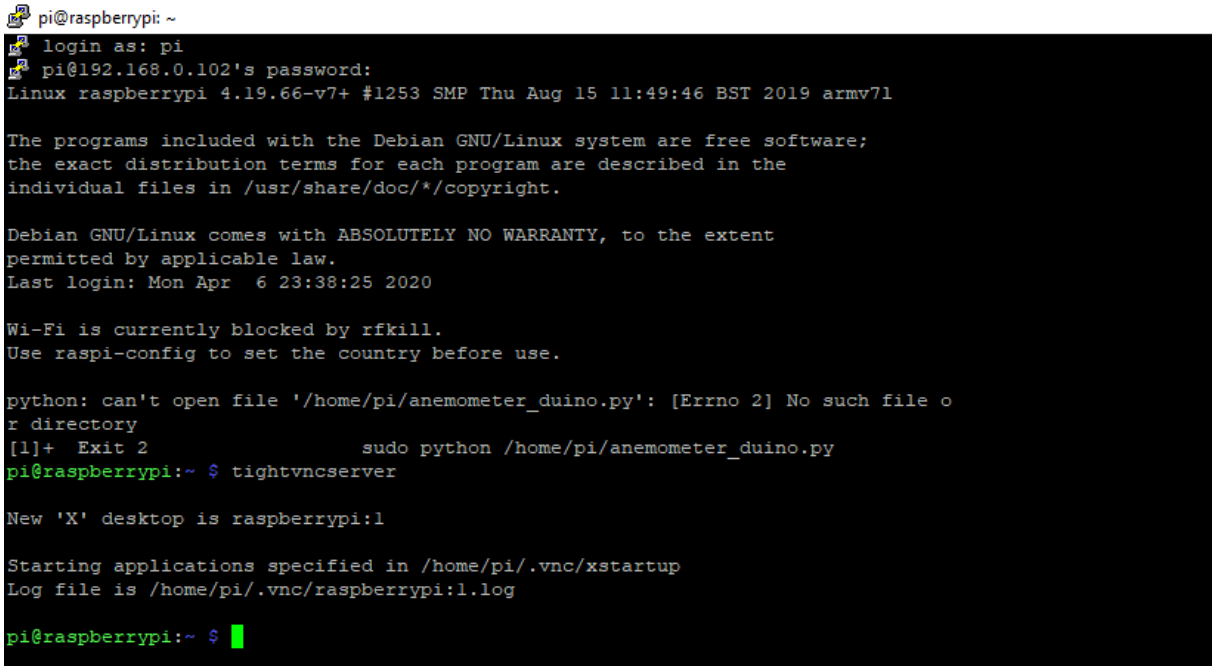

Figure 3.18: After executing the “tightvncserver” command on the Terminal Window.

Now, the TightVNC Software can be used to remotely access the Raspberry Pi connected in the same network.

In Figure 3.22, the TightVNC Configuration Console is shown. Inputting the address got by executing “tightvncserver” command, in the “Remote Host” box of the TightVNC Configuration Console and clicking on “Connect” button generates another window named “Vnc Authentication” (Figure 3.19) asking for the password.

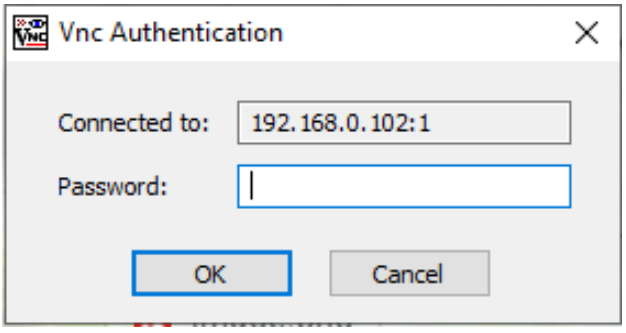

Figure 3.19: Vnc Authentication Window

The password was set when installing the “TightVNC Library” in the Raspberry Pi 3B+. Inputting the password in the “Password” box and clicking “Ok” button confirms the connection and Shows the Raspbian Operating Environment (Figure 3.20) of the Raspberry Pi 3 B+ on the laptop screen.

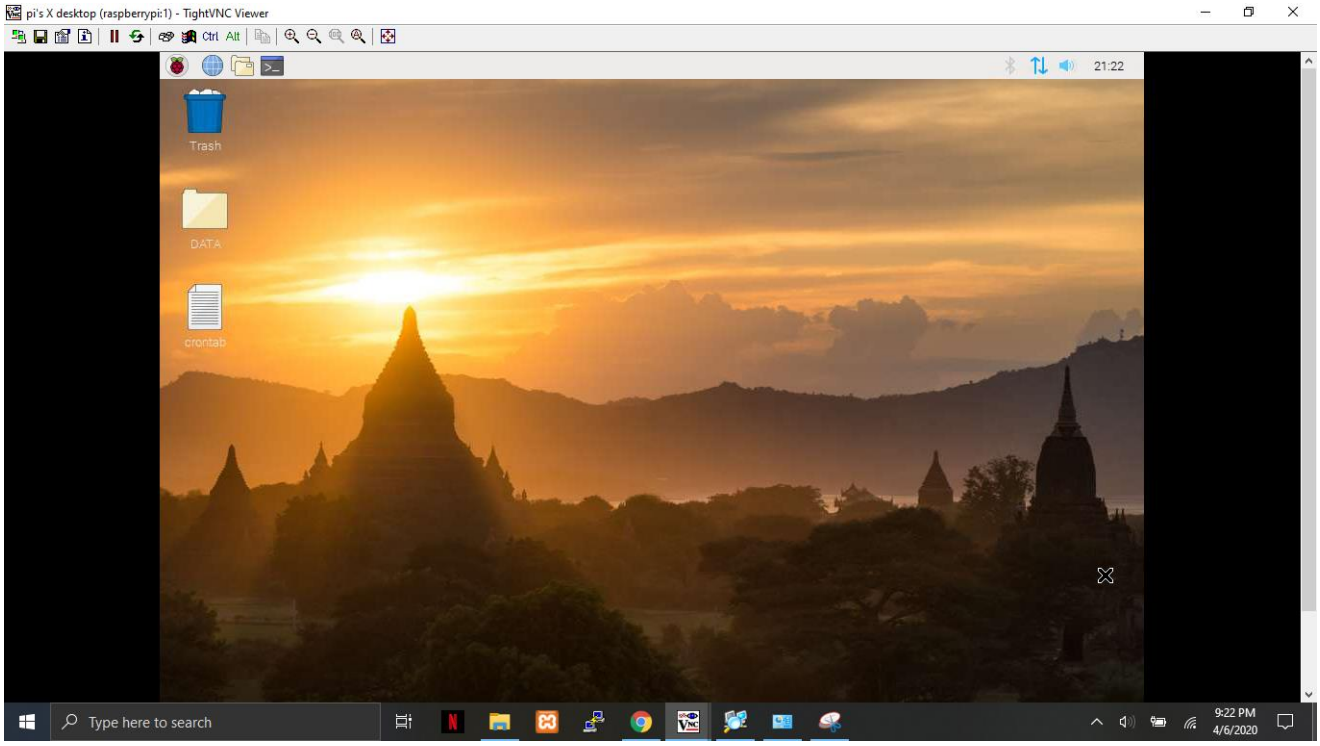

Figure 3.20: Raspbian Operating System Environment

Now, moving the “.txt” files that were saved by the Raspberry Pi to a folder named as the respective date of the collected data and uploading the folder on “Google Drive” or any other online storage using the built-in browser of the Raspbian completes the Weather Station’s Data collection process. These collected data get sorted to remove faulty data and to merge them in one “.csv” file for further analysis. Also, TeamViewer (Figure 3.23) software can be used to collect the data when the data collector is using another computer which is not connected in the same network.

3.3.2 *Software Description*

3.3.2.1 *Putty*

Putty is a free open-source terminal emulator, which helps to access the Raspberry Pi Terminal window using windows, macOS or Linux based operating system. It works through SSH Communication Protocol which is also known as Secure Shell. It is a network protocol which allows a user, a secure way to assess another computer over an unsecured network. To use Putty, the SSH Communication needs to be enabled in the Raspberry Pi Configuration settings on the Raspberry Pi. The computer that will be used to access the Raspberry Pi need to be connected into the same internet connection and same domain.

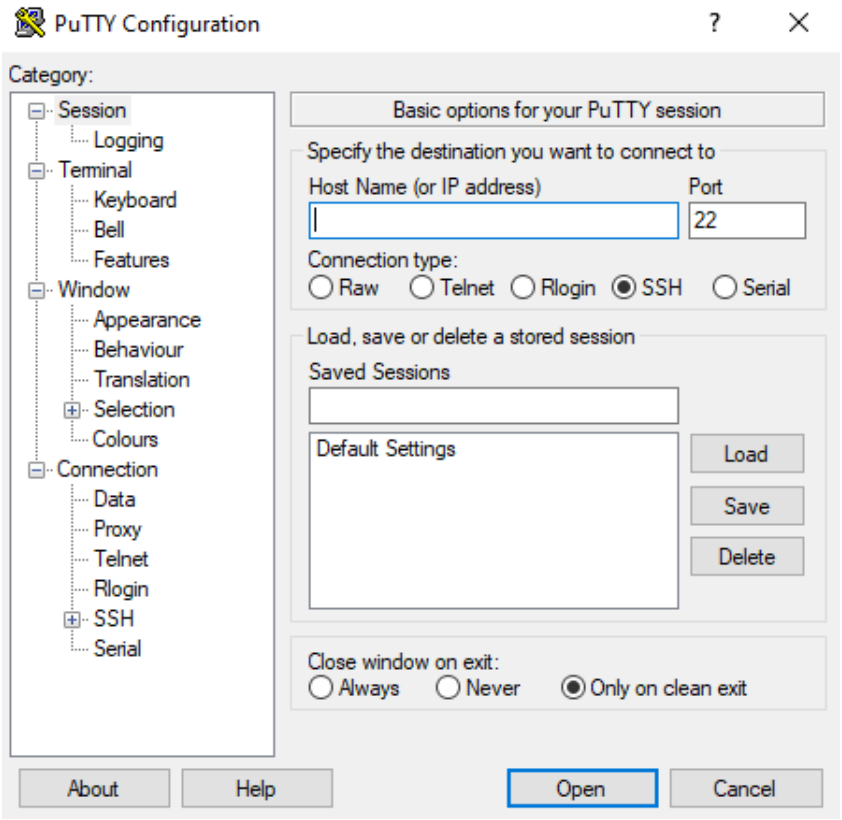

Figure 3.21: Putty Configuration Console

3.3.2.2 *Advance IP Scanner*

This software helps to track down the IP address of all the devices connected in a particular internet connection. Without this software, the alternate way to extract the IP Address of Raspberry Pi is so troublesome and time consuming.

3.3.2.3 *TightVNC*

It is a free and open-source remote desktop software application. It is developed by Constantin Kaplinsky. The RFB protocol of Virtual Network Computing (VNC) was used and extended to allow end-users to remotely control another computer's screen. This software is written in C, C++, Java. Windows and Linux operating systems can be used to run TightVNC.

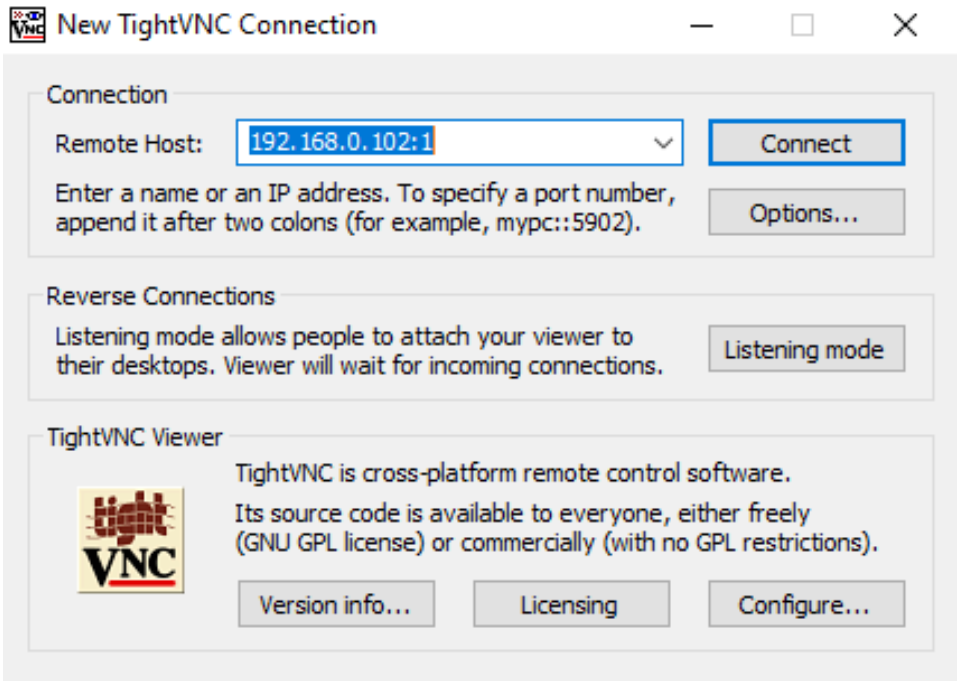

Figure 3.22: TightVNC Configuration

3.3.2.4 *TeamViewer*

TeamViewer is a software application which can be used for remotely control any other computer or laptop or mobile with TeamViewer installed in it. It also allows to share and transfer files between computers. It is available on platforms like Windows, macOS X, Linux,

iOS and Android. Best thing about this software is, it can be used from anywhere in the world with internet access.

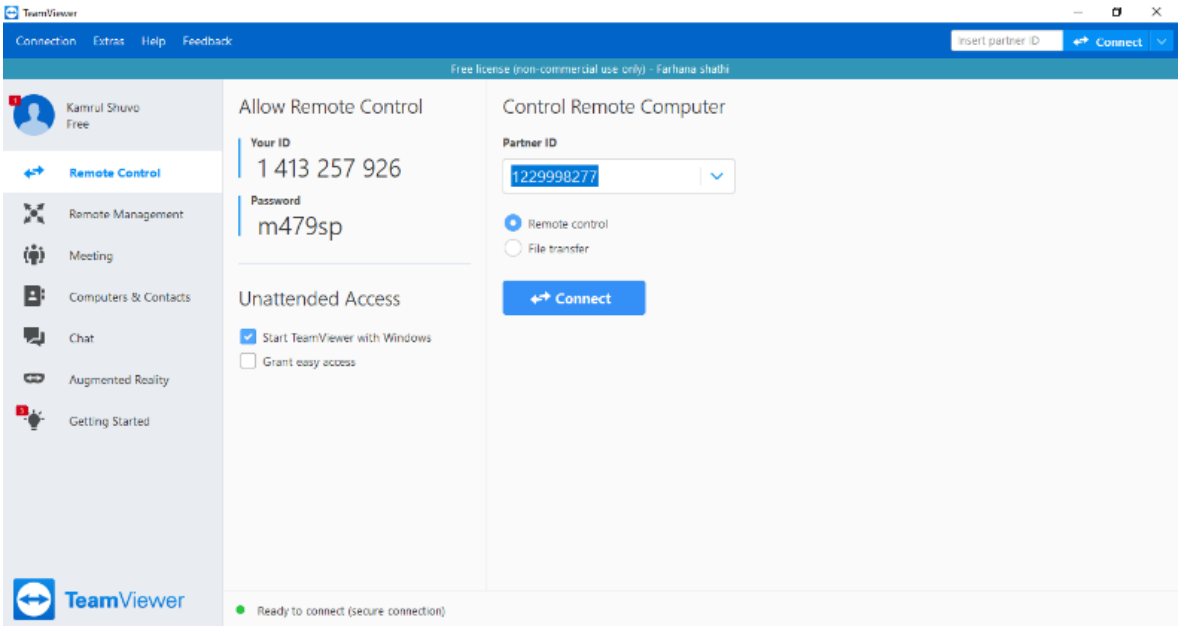

Figure 3.23: TeamViewer Connection Console

3.3.3 *Flowchart for Each Sensor Interface*

DHT11 Humidity Sensor

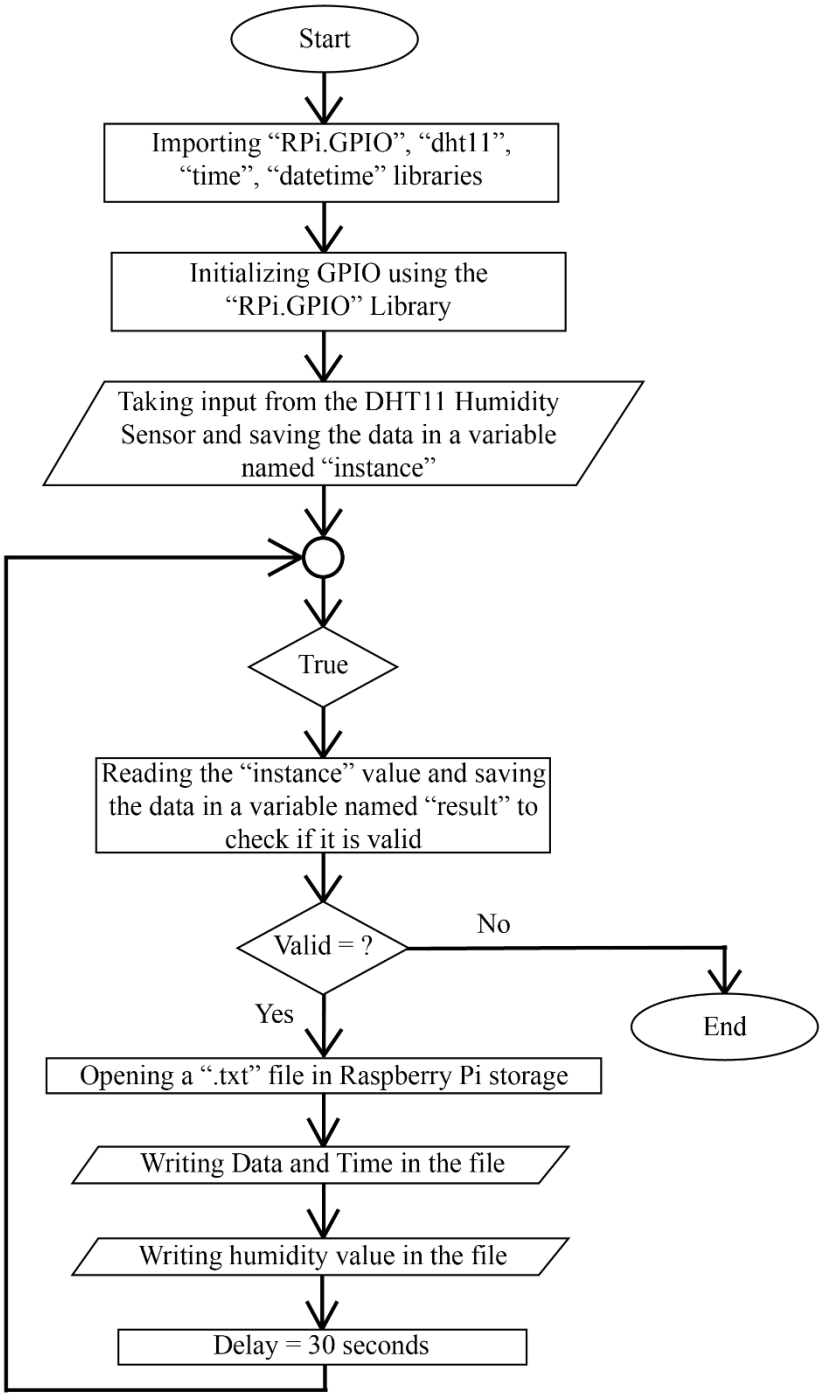

Figure 3.24: DHT11 Humidity Sensor Flowchart

Anemometer

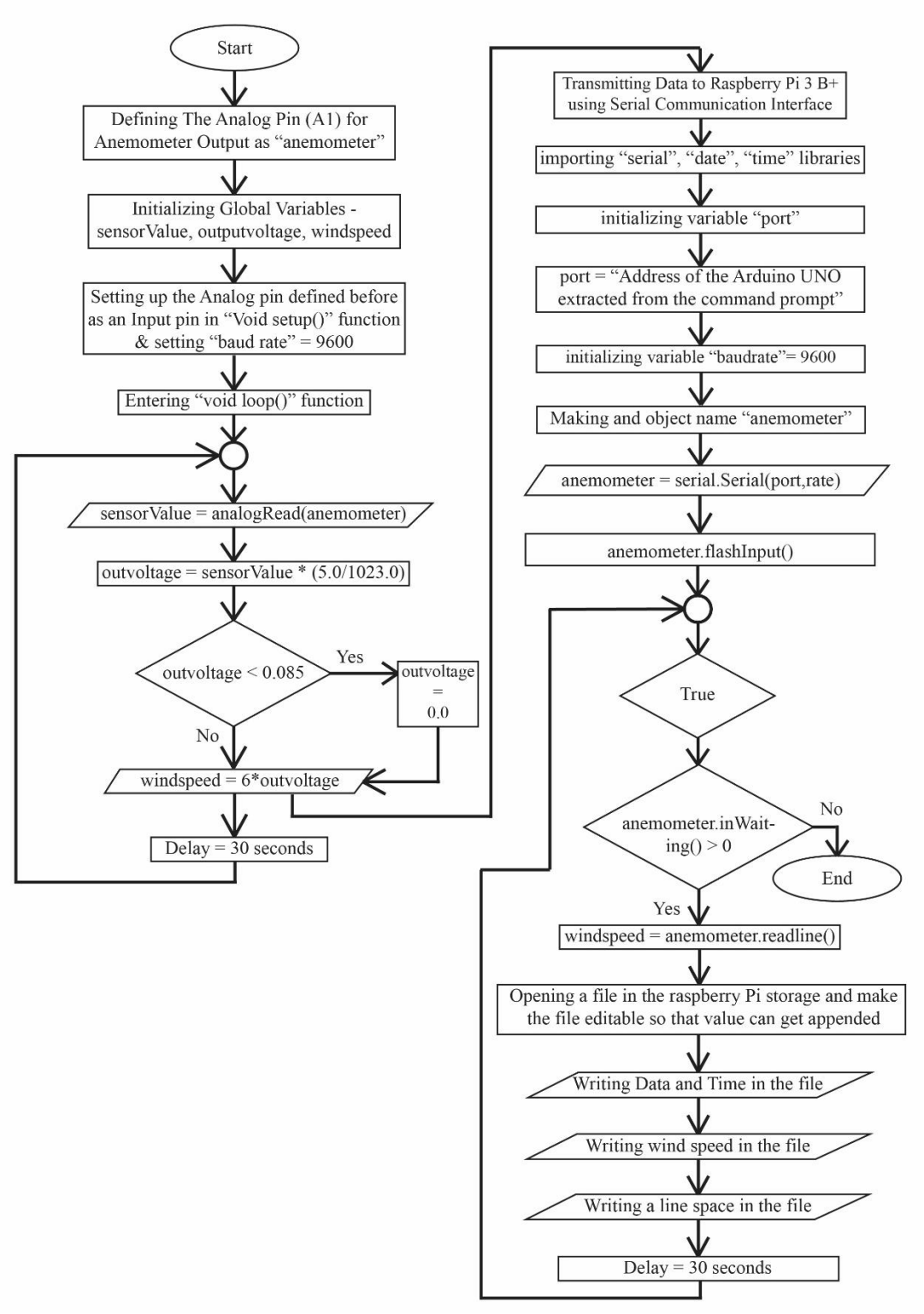

Figure 3.25: Anemometer Flowchart

INA219 Current Sensor:

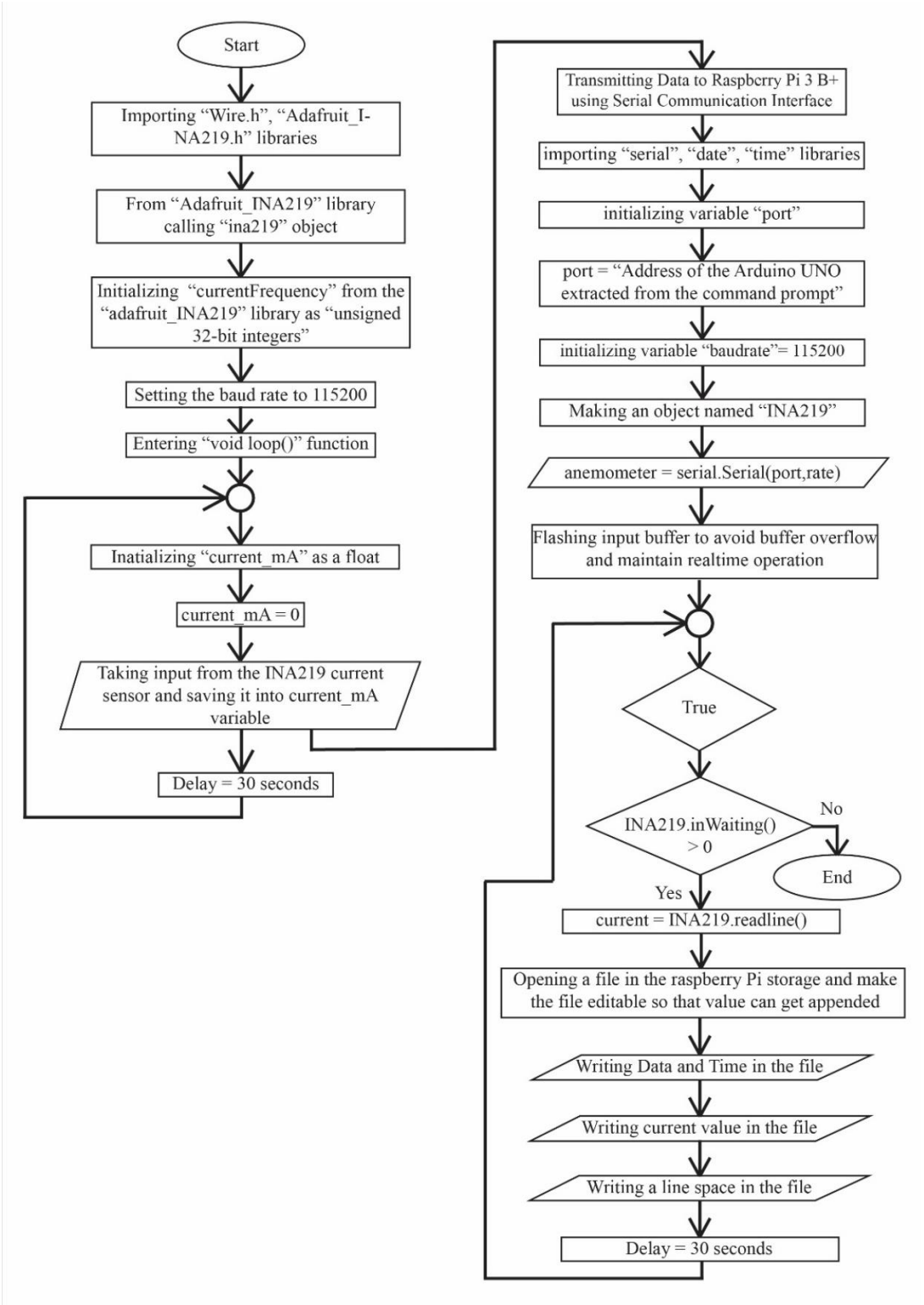

Figure 3.26: Anemometer Flowchart

DS18B20 Temperature Sensor:

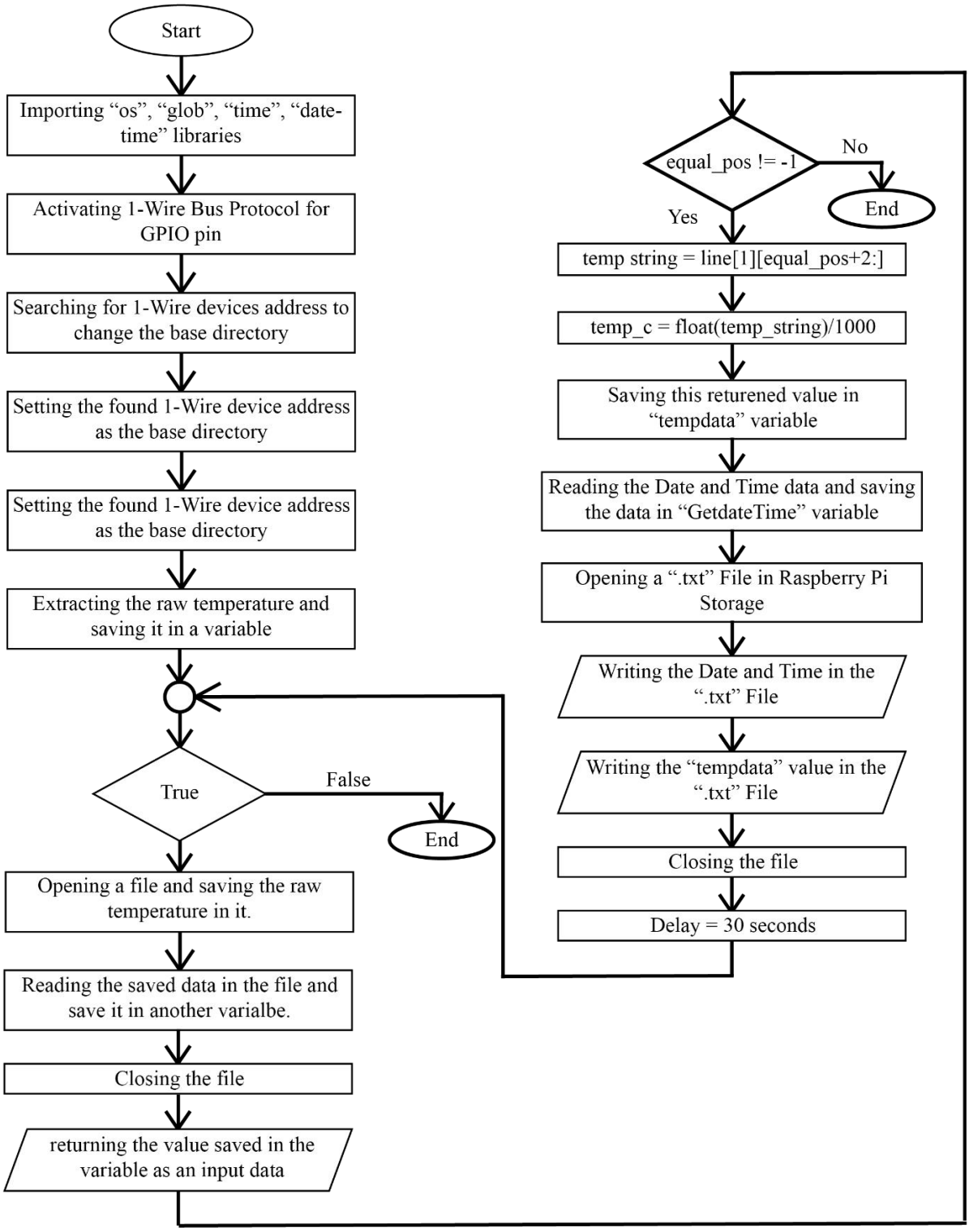

Figure 3.27: DS18B20 Temperature Sensor Flowchart

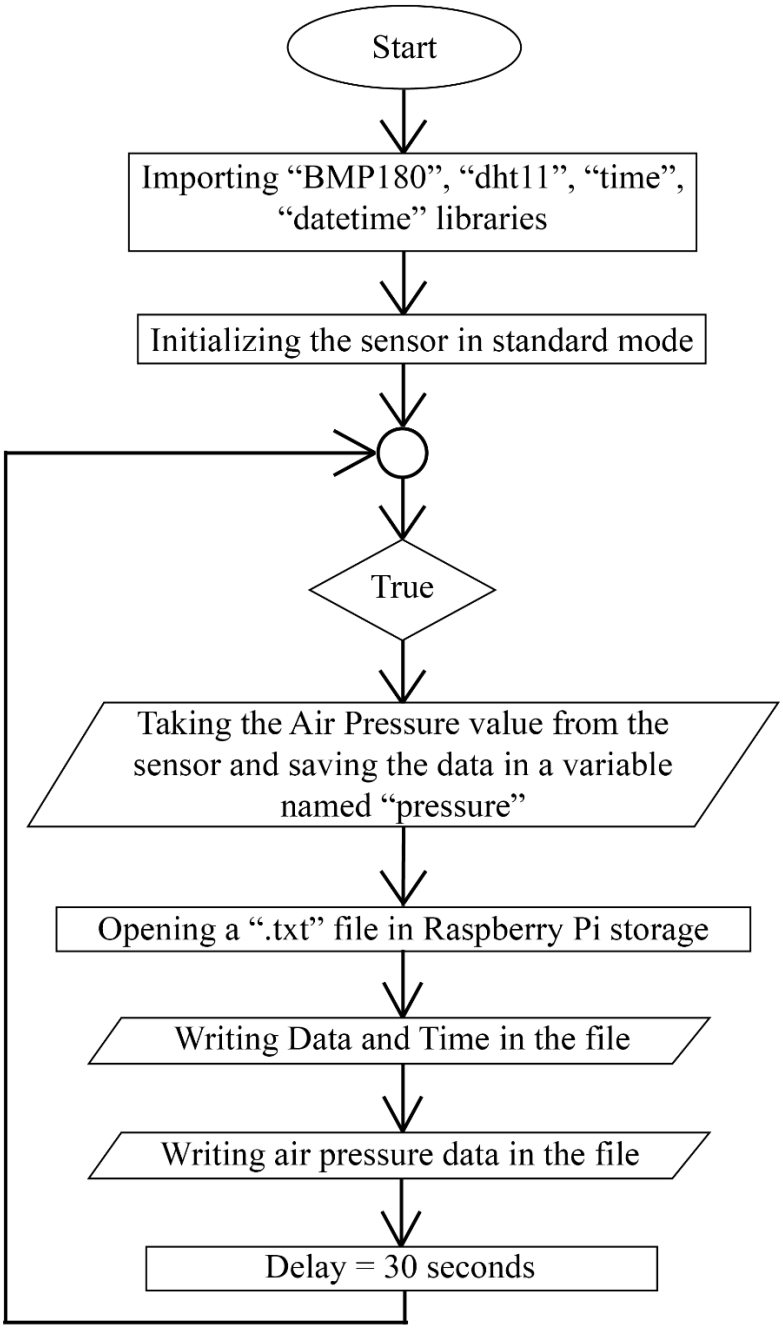

Figure 3.28: BMP180 Barometric Pressure Sensor Flowchart

3.4 Chapter Summary

So, this chapter is divided mainly into two parts, which are Hardware implementation and software implementation. In hardware implementation, it is presented that how the hardware setup was built, what electronic devices where used, how these devices are connected in the system and how the data of each sensor was collected by the raspberry pi. On the other hand, in software implementation it is presented that how the data are being extracted from the raspberry pi, what software were used and how and finally how the code of each sensor works.

Problems Faced

This hardware setup is up and running since October, 2019. Many difficulties were faced to build and maintain this hardware setup. At first in September 2019, the setup was stationed on the rooftop of BRAC University Building – 4. The difficulties that were faced there are –

i. *Internet Connectivity:* There were no internet connectivity available there, which was a big drawback for the setup. Because the built-in real-time clock of the Raspberry Pi 3 B+ need to update it's time every time it reboots or boots. As there were no internet connectivity over there, the raspberry pi could not update the time and date. As a result, the data collected by the sensors were saved with respect to wrong time and date.
ii. *Power or Electricity:* It was not possible to monitor if the hardware setup is getting power for the whole day or there were any blackout or interruption in electricity as the access to the location was not available all the time.
iii. *Remote Access:* Remotely Accessing the system was not possible then, as there was no internet connectivity.

iv. *Data Loss:* The data loss was high, as the data of each sensor from sunrise to sunset was needed and the building's electricity supply gets powered up at around 8 AM – 9 AM.

So, these were the main problems that were faced at the beginning. After moving the Weather station to the rooftop of one of the thesis group member's building, most of the problems were solved as there were available internet connectivity and 24 hours electricity supply. Though sometimes the system still losses data because of blackouts and internet connectivity problems, which are manageable as the system can be remotely monitored from anywhere needed.

Features

i. The system can collect environmental data, which are Temperature, Humidity, Wind Speed and Air Pressure.
ii. It collects data from 6 AM to 6 PM every day.
iii. Each Raspberry Pi and Arduino UNO boards connected to them requires 2.5A/5V DC Supply to work.
iv. The system is made to be water proof, as it also collects data on rainy days.
v. Low data loss.
vi. Remotely accessible and controllable.
vii. Sensors and micro-controllers are replaceable (if damaged).

Strengths and Weaknesses

Strengths:

i. It can withstand rough weather.
ii. It can be up and running for 24-hours without any break.

iii. The micro-controllers can take heavily load. The Raspberry Pi 3 B+ is basically a small computer.

iv. It can be controlled and monitored from anywhere as it is remotely accessible.

Weaknesses:

i. The circuits are built with too many connecting wires, so it is hard to detect if any of the wire gets damaged.

ii. The temperature sensors are not that durable as they should be.

iii. Without internet connectivity the system cannot be remotely accessed.

iv. The circuits are protected by a plastic box and some connecting wires get in and out of the box to connect the Anemometer, Temperature Sensors and Photovoltaic Modules with the circuit. If these wires get damaged by outside force the whole system gets damaged, as these wires are not well protected.

v. As there is no available backup power supply if there is any blackout, the system tends to lose data.

The Hardware setup is running and collecting data for almost 8 months. The target is to keep it running at least for 1 year and if possible, then more. As the developed Machine Learning Model can predict more correctly, if the training dataset gets much bigger. So, the goal is to collect as much data as possible to make the model more accurate, precise and reliable.

Chapter 4

The Theoretical Analysis for both Clean and Dusty Solar Panels over the four months datasets

4.1 Introduction

This chapter discusses the theoretical analysis of the collected data from sensors. After building the weather station that has been discussed in Chapter 3 with detail information, the data collections start at 1st November 2019 which has been running continuously for four-month, furthermore, the data collection process is ongoing with the goal of collecting one full-year data. This chapter is divided into three main sections for better understanding of Data Analysis procedure. To begin with the dataset need to be prepared for the Raw Data Analysis, the sensors give the data in the format of notepad that need to be converted into Excel format for Analysis and also Prediction purpose. In this first section, the Raw Data Analysis has been discussed for November month with relevant information and also perform analysis of the Solar Panel due to the effect of weather parameters, furthermore investigating the performance of the clean module and the dusty module due to the dust decomposition on the panel surface area. The middle section is focused on the Solar Irradiance due to lack of Pyranometer (Solar Irradiance measurement sensor), using the theoretical knowledge to calculated or measured the Solar Irradiance both for Ideal and Experimental cases. Most importantly among all the weather parameters temperature has an impact on the Solar module performance which is noticeable but besides this Solar Irradiance mostly affected the Solar module performance. The last section is the investigation of the Solar panel parameters which has been done using the I-V characteristics curve of the solar panel. The I-V characteristic curve is the performance measurement tools of the Solar panel using this simple technique panel overall behavior, and efficiency can be measured efficiently and effectively.

4.2 Raw Data Analysis

The weather station gives data of six sensors they are clean temperature, dusty temperature, clean short circuit current, dusty short circuit current, wind speed, and humidity. Moreover, the time interval is 4 data per minute and for the analysis purpose time is also one of the major factors. For a better understanding of the performance of the solar panel, weather parameters need to be in consideration moreover comparing two modules one is clean regularly and another one is clean at the first time of the installation with the passing time dust particles have been accumulated on the surface of the panel. Other than these three weather parameters (Temperature, Wind Speed and Humidity), there are more factors that affect the performance of the solar module such as cloud, sun position, location of the area etc. Using the INA219 sensor for collecting the data of module short circuit current, I_{sc}(mA) among the others parameters of the module such as open-circuit voltage, V_{oc} (V) and panel's electrical output power, P(W) the reason behind this is module short circuit current affected by the weather parameters and moreover, mostly by solar irradiance(which will be discussed in the next section) furthermore, using a simple technique such as the sensors data vs. time plot the impact of the weather parameters can be observed simply moreover, comparing between the clean panel and the dusty panel can also unclose the impact of the dust particles on the PV module on its performance. In addition, for this study November month data has been used which mainly middle of the winter season therefore others months can be understand using the similar technique, the upcoming two chapters analysis and prediction using machine learning will cover the winter season (November month). From the weather station around 1300 data per day for each sensor has been collected among these four months times period continuously, data collection procedure starts from 6 am and ends at 6:30 pm. For the purpose of understanding the effect of the factors 14th November, 2019 raw data has been plotted in one

window for the determination of raw data analysis and understanding the impact of the weather parameters along with dust and cloud effect.

The main focus will be the effect of the weather parameters along with other factors on the performance of the solar module short circuit current. At the time of the installation, both (Clean and Dusty panel) was cleaned due to this their performance was similar which means that both the panels have the same short circuit current or very close to each other, in simple word clean and dusty module short circuit current (Isc) plot overleap each other. After passing time dust particles accumulated in the surface of the dusty panel by cause of this the performance of the dusty module decrease significantly compared to the clean module performance. For the seeks of a better understanding of the degradation of the performance of the dusty module compare to the clean module performance, 14th November 2019 collected data has been plotted furthermore weather parameters impact can also be seen on this curve. The plotted dataset curve has been shown below where temperature plotting has two temperature sensors (DS18B20 Temperature sensor) for each solar panel and the temperature sensor is attached to the surface of the panel which gives the surface temperature.

The output Raw Data of 14th November 2019 is plotted below:

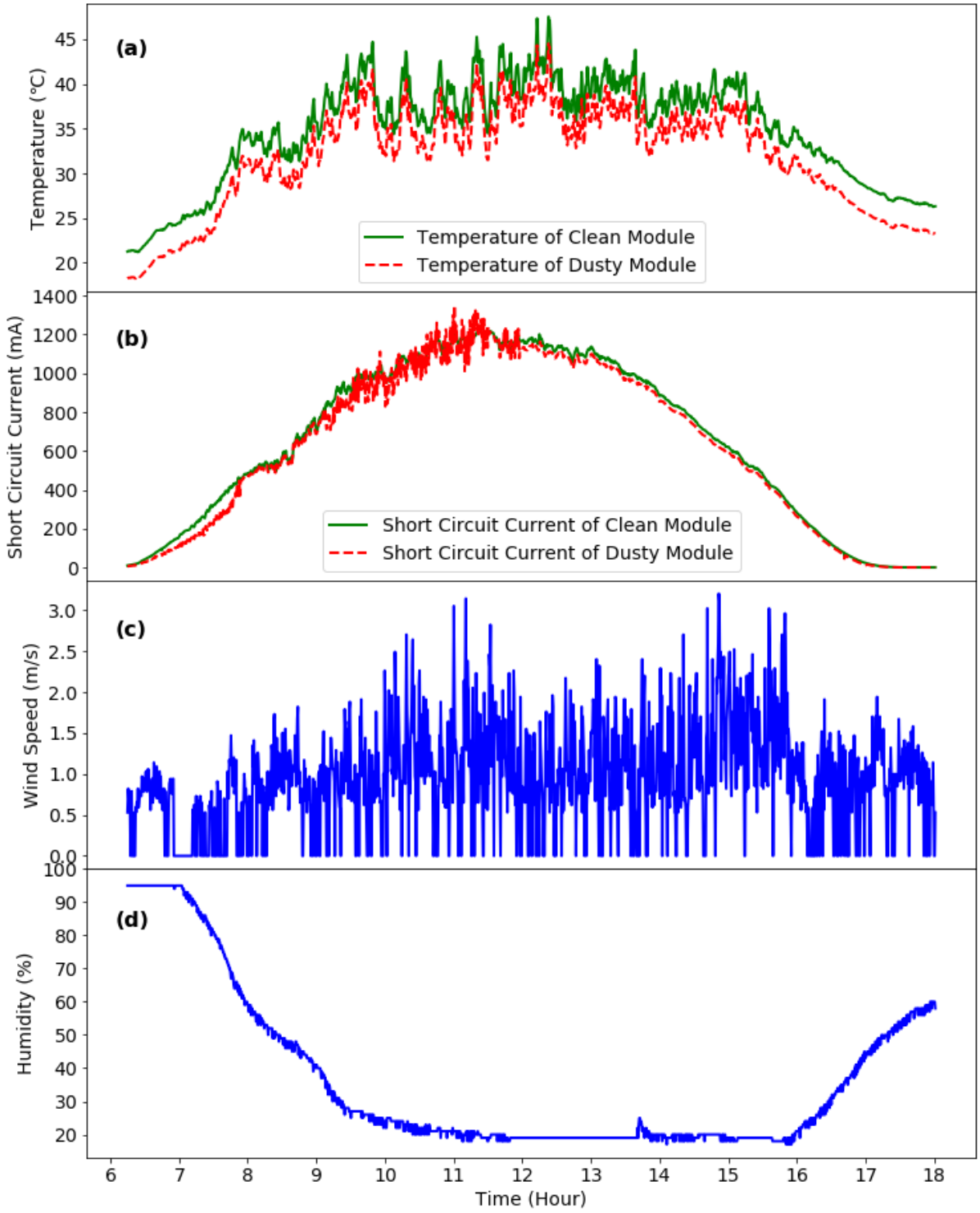

Figure 4.1: Plotting from top to bottom (a) Temperature vs. Time (b) Short Circuit Current vs. Time (c) Wind Speed vs. Time (d) Humidity vs. Time

From the above plots, the upper plot shows the two temperature sensors plotting for clean and dusty module furthermore due to the dust accumulation on the dusty module surface for 14 days after the installation procedure which affects the performance of the dusty module. Plotting of the Clean module and Dusty module Temperature vs. Time shows that the clean module temperature is slightly higher than the dusty module temperature as a result of dust decomposition on the dusty module surface area. Moving to the next plotting which shows the Clean module and Dusty module short circuit current vs. Time plotting here also clean module short circuit current is slightly higher than the dusty module short circuit current. In addition, co-relating the temperature plotting with the short circuit current plotting which shows a relationship between temperature with short circuit current. With the increasing or decreasing of temperature short circuit current is also increasing or decreasing along with it. Other weather parameters which are the humidity and the wind speed do not have a significant effect on the solar module short circuit current which can be seen clearly through the above curve, that does not mean they do not have an impact on the solar panel short circuit current but the impact is very less which can be neglect. Moreover, time is also a very important factor in the performance of solar module at the time of the sunrise module uses the sunlight to generate short circuit current and along with the passing time the short circuit current increase gradually and at the peak time (at noon) highest short circuit current can be found after that the short circuit current gradually decreases along with the passing time. In the below a picture has been captured on 20th November 2019 as attached below.

Figure 4.2: Picture of the Dusty module (20th November,2019)

The above picture gives a clear idea of the dust particles gather on the surface of the dusty module other than that there are birds shit or birds dropping along with that there are some water flowing marks due to fog as the investigation is considering the winter season. Moreover, besides the dusty module the clean module has been placed which is cleaned due to this dust, there is a performance drop on the dusty module short circuit current compare to the clean module short circuit current.

In addition, by calculating the percentage difference between the clean and the dusty module short circuit current daily over the whole month of November 2019 which will give a better understanding of the performance degradation between the clean and the dusty module. The percentage difference between the clean and the dusty module short circuit current calculation has given below:

$$\% \, Difference = \frac{Clean \, I_{sc} - Dusty \, I_{sc}}{Clean \, I_{sc}} * 100 \quad (4.1)$$

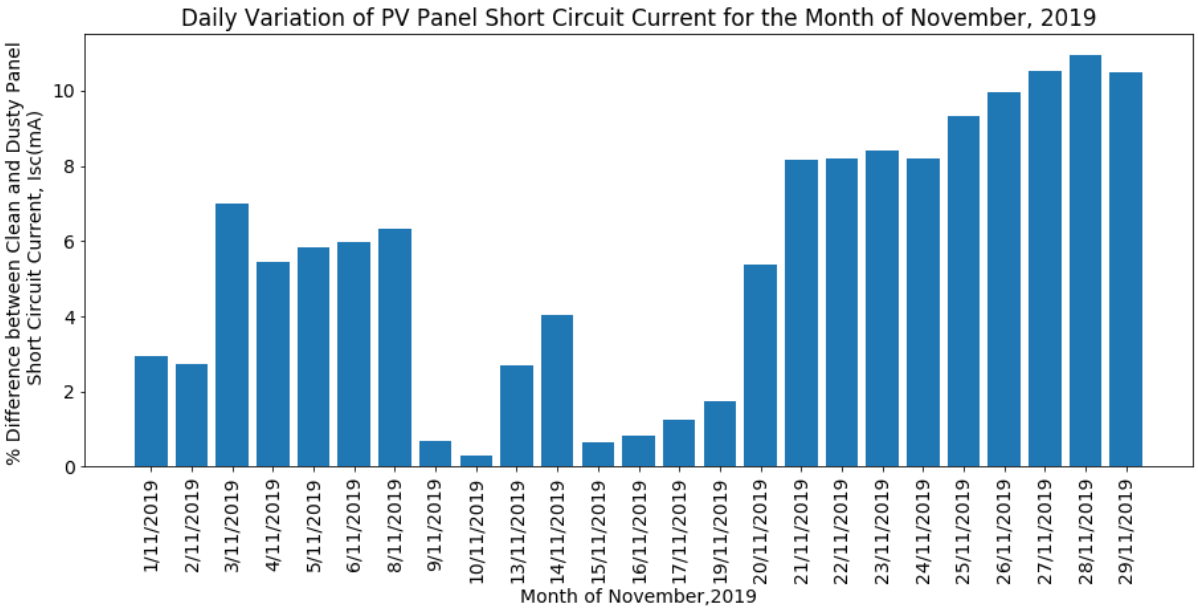

Figure 4.3: Plotting of Daily Variation of PV Module Short Circuit Current for the Month of November,2019

In the above histogram, plotting shows that at the day of 20th November 2019 the percentage difference between the clean and the dusty module is increasing due to the dust particles gather on the surface of the dusty module which affects the module short circuit current significantly. In short, the dust accumulation on the surface of the module will decrease their performance significantly. Furthermore, a monthly diagram is given below to get better knowledge about which month dust accumulation causes greatly damaged to the performance of the dusty module.

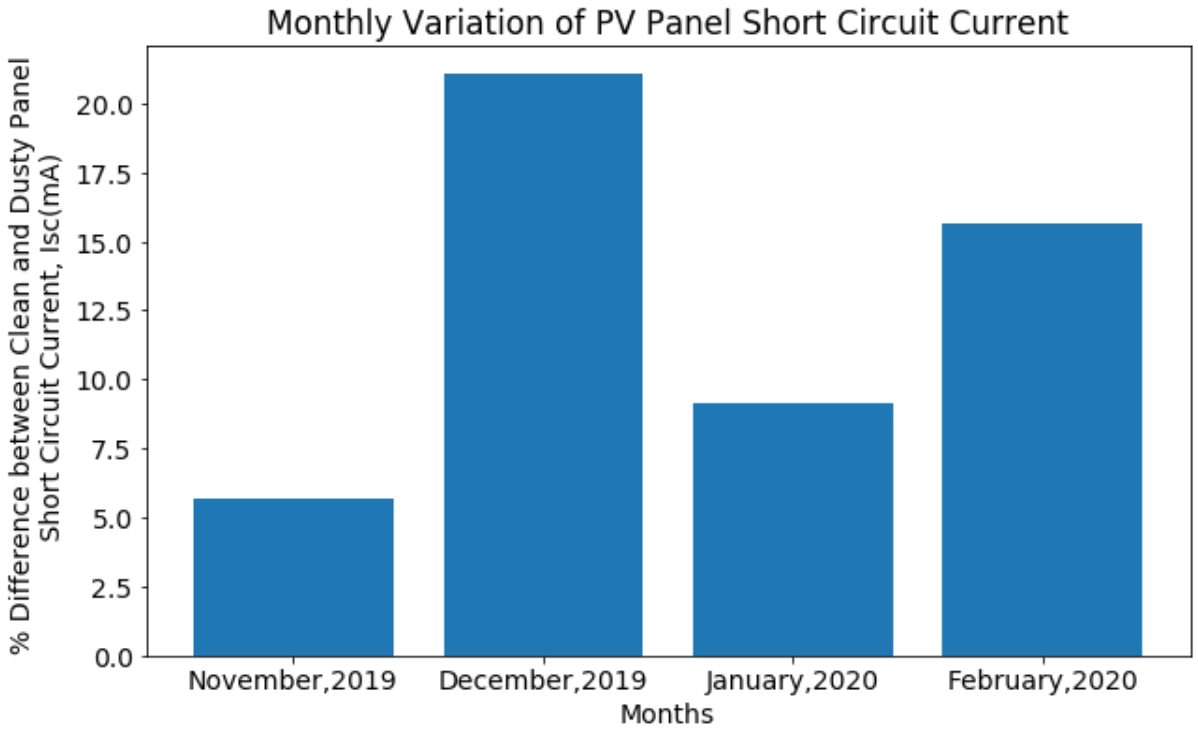

Figure 4.4: Plotting of Monthly Variation of PV Module Short Circuit Current for the Winter Season

4.3 Solar Irradiance

This section will talk about solar irradiance and the effect of solar irradiance on the performance of the solar module. In the previous section of Raw Data Analysis shows that the effect of weather parameters such as temperature, humidity, wind speed on the solar module is not much whereas temperature affect the solar module short circuit current which is not as significant as the solar irradiance which will be the discussion topic of this section. In Chapter 2 there was a discussion about the solar irradiance theory in detail, in short, solar irradiance is the sunlight energy which can be found on the earth. For solar energy sunlight is the main source, using this sunlight energy solar panel generates energy for loads. By using sensors solar irradiance can be calculated easily but lack of equipment of solar irradiance on the grounds that using the theoretical knowledge to calculate the solar irradiance.

4.3.1 *Ideal and Experimental Solar Irradiance Calculation*

In order to calculate the amount of solar irradiance from the direct sunlight that is observed by the solar module which can be done by using features such as declination angle, latitude angle, solar altitude angle, the hour angle, zenith angle and air mass. Using these features ideal solar irradiance can be measured easily whereas the experimental solar irradiance can be calculated using the ideal irradiance along with short circuit current of the solar module. For measuring the ideal solar irradiance first declination angle need to be calculated, using the below equation declination angle can be calculated:

$$\delta=23.45° \; sin\left[\frac{360(n-80)}{365}\right] \tag{4.2}$$

Here, n is the particular day of the year

The declination angle varies with the season due to the tilt of the earth on its axis of rotation and also the rotation of the earth around the sun.

Next step is to find the latitude angle and the latitude angle is the angle by which any place and location of the earth can be described. For this experiment, the latitude angle is φ=23.777176°.

Thereafter the hour angle needs to be calculated which is the measurement of the sun from the earth by an expression of time, expressed in angular measurement which is in degree from the solar noon. The equation for the hour angle is given below;

$$\omega=\omega_s-15(t-t_{sr}) \tag{4.3}$$

Here;

t is the local apparent time

t_{sr} is the sunrise time

Moving forward next feature to calculate is the solar altitude angle which is the angle between the sun's ray and a horizontal plane. This angle varies with the passing time of the day, the time of the year and also the latitude on the earth. The equation of the solar altitude angle is given below:

$$\alpha=\sin^{-1}(\sin\delta*\sin\varphi+\cos\delta*\cos\varphi*\cos\omega) \quad (4.4)$$

Here,

δ is the declination angle

φ is the latitude angle

ω is the hour angle

Proceeding to the next feature which is zenith angle, the angle between the sun and the vertical is known as zenith angle. The equation of the zenith angle is given below;

$$\theta_Z= 90°- \alpha \quad (4.5)$$

Here;

α is the solar altitude angle

The last feature is the air mass which is a large volume of air in the atmosphere that is mostly uniform in temperature and moisture. The equation of the air mass is given below;

$$AM=\frac{1}{cos\theta_z} = \csc\alpha =\sec\theta_z \quad (4.6)$$

For calculating the solar irradiance for the fixed axis solar panel, the first step is to calculate the dual-axis solar irradiance which can be calculated using the equation given below:

$$I=I_0*(0.7)^{AM^{0.078}} \quad (4.7)$$

Here,

I_0 is the solar irradiance in space outside the atmosphere which is 1376 W/m^2

AM is the air mass

For measurement of the fixed axis solar panel irradiance below equation has been used:

$$G=I*\cos\delta*\cos\theta_z \tag{4.8}$$

Here;

I is the dual-axis solar irradiance

δ is the declination angle

θ_z is the zenith angle

In addition, applying this procedure ideal solar irradiance can be calculated simply and by using the ideal solar irradiance experimental solar irradiance has been calculated using the relationship with the ideal solar irradiance with the short circuit current of the solar panel. Experimental solar irradiance equation is given below:

$$I_{irradiance} = \frac{I_{sc_{highest}} - I_{sc}}{G_{highest}} \tag{4.9}$$

Using the Python programming language the calculation has been done for each day of the data collection which makes the calculation more effective and less time-consuming.

The ideal and experimental solar irradiance plotting curve has been given below:

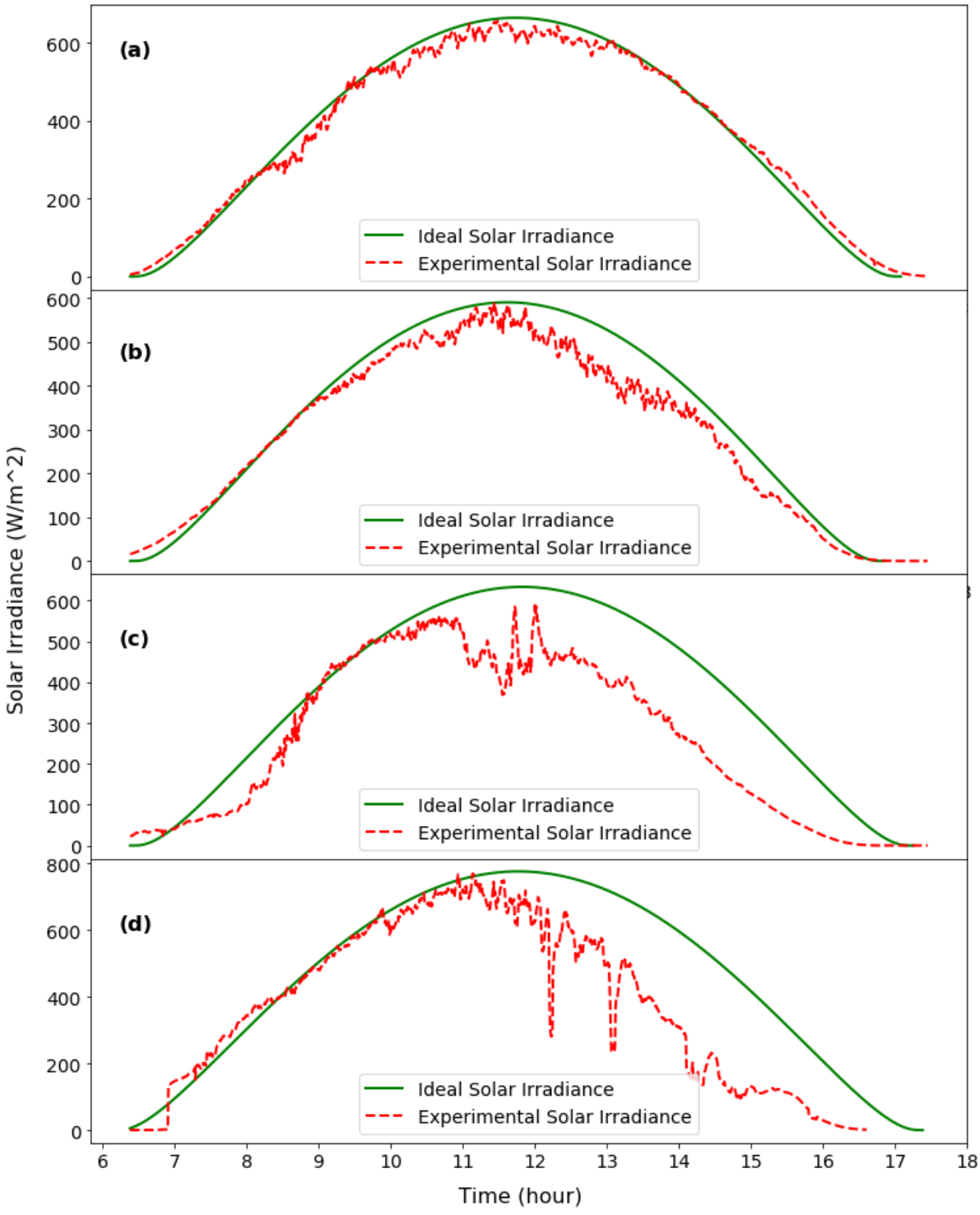

Figure 4.5: The plotting of Ideal and Experimental Solar Irradiance is shown:

(a) 14th November 2019 Ideal Solar Irradiance and Experimental Solar Irradiance

(b)15th December 2019 Ideal Solar Irradiance and Experimental Solar Irradiance

(c) 15th January 2020 Ideal Solar Irradiance and Experimental Solar Irradiance

(d) 15th February 2020 Ideal Solar Irradiance and Experimental Solar Irradiance

The above plotting shows the Ideal Solar Irradiance and the Experimental Solar Irradiance vs. Time plotting. The ideal solar irradiance is a theoretical calculation from the plotting it can be seen that it a smooth oval shape curve and which is done using the theoretical concept. On the other hand, the experimental solar irradiance is measure using the short circuit current and the ideal solar irradiance due to this the experimental solar irradiance plotting is very similar to the short circuit current plotting. Furthermore, short circuit current greatly depends on the solar irradiance since the main source of solar energy is the sunlight energy which is the solar irradiance.

Lastly, the short circuit current of the solar module increase or decrease with the solar irradiance. Due to the solar irradiance, the performance of the solar module is greatly depended on it, for example, considering the cloudy weather the performance of the solar module is very poor compared to the performance of the solar module on the sunny weather as a cause of the sunlight or solar irradiance. In short, more the solar irradiance, the performance of the solar panel will be significantly high.

4.4 I-V Characteristics of the Solar Panel

The characteristic curves generated by plotting I against V for a diode which is known as the I-V Characteristics curve of the solar module. The light has the effect of shifting the I-V curve down into the fourth quadrant where power can be extracted from the diode, in short in this fourth quadrant solar cell is generating power which is negative power. This I-V curve is most often shown reversed with the output curve in the first quadrant which is represented by;

$$I = I_L - I_0 \left[e^{\left(\frac{qV}{nkT}\right)} - 1 \right] \tag{4.10}$$

Here,

I_0 is the dark saturation current

q is the electronic charge

V is the applied voltage

n is the ideality factor

k is the Boltzmann's constant

T is the temperature

I_L is the light generated current

4.4.1 *I-V Characteristics of Clean Module and Dusty Module*

In this subsection main focused will be the current, voltage and power which gives the idea of the I-V characteristics curve and its associate parameters. Short circuit current and the open-circuit voltage are the two limiting parameters used to characterize the output of the solar cells for the given irradiance, operating temperature and area. Furthermore, the short circuit current is the maximum current of the module at zero voltage. On the other sides, open circuit voltage is the maximum voltage of the module at zero current. The product of the current and the voltage gives the power output, moreover, a solar cell can also be characterized by its maximum power point which is simply the product of $V_{mp} * I_{mp}$ at its maximum value. I-V Characteristics plotting of 1st March 2020 of the Clean and the Dusty Module is given below:

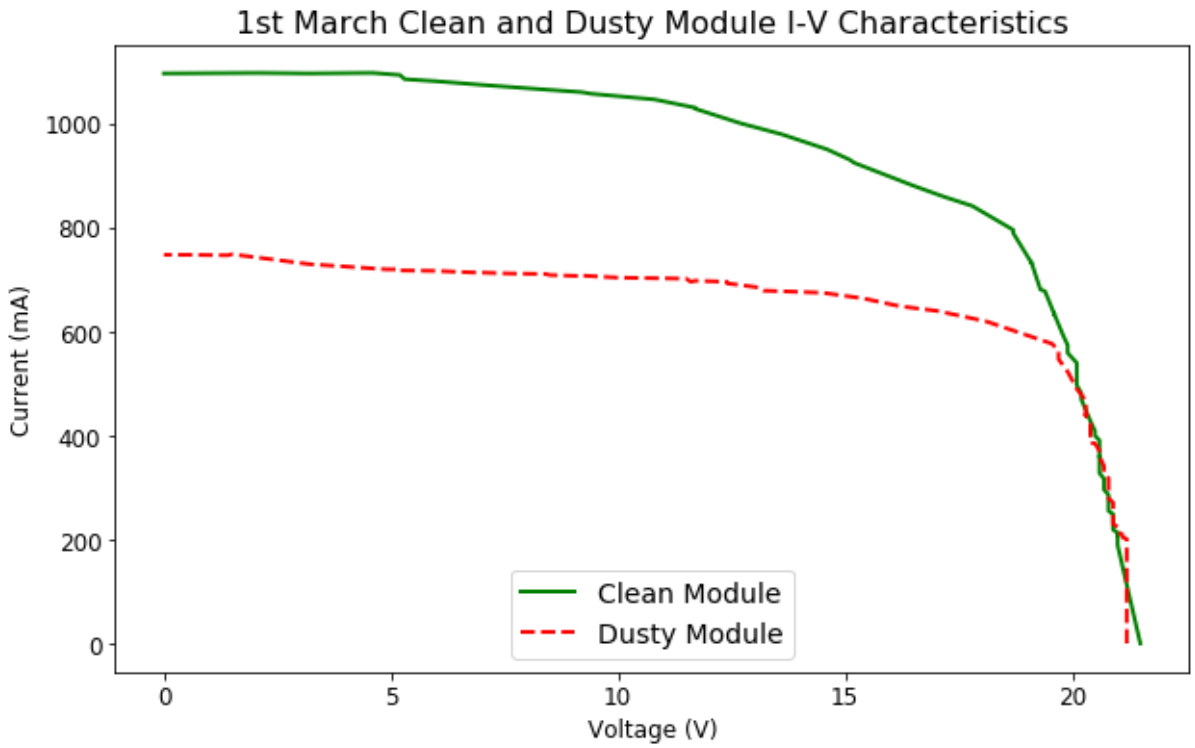

Figure 4.6: I-V Characteristics Curve of Clean and Dusty Module (1st March,2020)

From the above plotting, various parameters associated with solar cell can be calculated. For the experiment purpose, IV characteristics data were generated manually since the weather station gives only the short circuit current. Using the IV curve the maximum power of the module has been calculated moreover, by calculating the Fill Factor that measures the quality of the module and for ideal case, FF is 1 whereas in this experimental module gives FF is 0.65 but according to the module specification FF is 0.62 which is close to the experimental data.

Further discussion of the solar module parameters will be talking about in the next subsection with detail information.

4.4.2 *Various Parameters of Solar Panel*

Using two parameters of the solar panel which are the short circuit current and the open-circuit voltage along with the I-V Characteristics curve others parameters can be calculated easily. In the experiment using the weather station the short circuit current of the solar module has been

collected automatically furthermore, using Putty which is a free open source terminal emulator, which helps to control the weather station from windows, macOS or Linux based operating system. Since the weather station gives the short circuit current as an output which has been used to calculated the open-circuit voltage by using theoretical knowledge. Moreover, for calculating open circuit voltage some other parameters need to be calculated experimentally.

The ideality factor is one of the diodes I-V characteristic parameter. It is the measurement of how closely the diode follows the ideal diode equation. The equation of the ideality factor is given below;

$$n = \frac{(V_{oc1} - V_{oc2}) * q}{k * T * N_s * ln\left(\frac{I_{sc1}}{I_{sc2}}\right)} \quad (4.11)$$

Here;

q is the charge of an electron

k is the Boltzmann's constant

N_s is the number of cells connected in series in the panel

V_{oc1} & V_{oc2} is the open-circuit voltage at the same temperature with different solar irradiance

For calculating the ideality factor experimentally first step is to measure the open-circuit voltage and the short circuit current almost at the same temperature but with different solar irradiance. By using the above equation ideality factor has been calculated which in this experiment is

n=1.35 whereas ideality factor is 1 for ideal case.

Next step is to calculate the reverse saturation current of the solar module which is said to be a measure of the leakage of carriers across the p-n junction in reverse bias. The equation of the reverse saturation current is given below;

$$I_0 = \frac{I_{sc}}{e^{\left(\frac{V_{oc}*q}{n*k*T*N_S}\right)}} \tag{4.12}$$

Here;

q is the charge of an electron

k is the Boltzmann's constant

n is the ideality factor

Ns is the number of cells connected in series in the panel

T is the temperature in kelvin

I_{sc} is the short circuit current

V_{oc} is the open circuit current

For calculating the reverse saturation current an experiment has been run which take place at 12:35 pm and the I_{sc} and V_{oc} of the solar module have been measured manually furthermore, the temperature was also measured using temperature sensor which was 46°. Using the above equation experimentally the reverse saturation current has been calculated which is 1.13×10^{-7}. In addition, this experiment gathering a large number of data daily because of this manual calculation of the reverse saturation current is very difficult to do as a result new method has been applied to calculate the others reverse saturation current for each short circuit current. The equation reverse saturation current is given below:

$$I_{02}=\left(\frac{T_2}{T_1}\right)^3 * e^{\frac{Eg}{k}\left(\frac{1}{T_1}-\frac{1}{T_2}\right)} * I_0 \tag{4.13}$$

Here;

E_g is the energy bandgap of silicon

k is the Boltzmann's constant

T_1 is the temperature at I_0 calculation

I_0 is the reverse saturation current experimentally

T_2 is the temperature at I_{02} calculation

Lastly, the open-circuit voltage has been calculated and the equation of the open-circuit voltage is given below;

$$V_{oc} = \frac{n*k*T*N_s}{q} ln\left(\frac{I_{sc}}{I_{02}}\right) \quad (4.14)$$

Here,

q is the charge of an electron

k is the Boltzmann's constant

n is the ideality factor

Ns is the number of cells connected in series in the panel

T is the temperature in kelvin

I_{sc} is the short circuit current

I_{02} is the reverse saturation current

Fill factor is the ratio between the maximum power from the solar module to the product of the open-circuit voltage and short circuit current which can be calculated by using the I-V

characteristics curve. Using the experimental 1st March,2020 I-V Characteristics curve the Fill Factor of the solar module has been calculated. The equation of the fill factor is given below:

$$FF = \frac{P_{mp}}{V_{oc} * I_{sc}} \tag{4.15}$$

Using the 1st March 2020 I-V Characteristics curve the maximum power can be calculated by the large rectangle area that covers in the IV characteristic curve and the rectangle curve point cut the IV characteristic curve on that point the voltage and current is the maximum voltage (Vmp) and maximum current (I_{mp}) that the solar module can provide. The equation for maximum power is given below:

$$P_{mp} = V_{mp} * I_{mp} \tag{4.16}$$

For this experiment, the solar module fill factor is 0.65. Using this fill factor maximum power of each short circuit current and open-circuit voltage has been calculated for this experiment.

Maximum power is the product between the maximum voltage and the maximum current of the solar module. From the weather station, only the short circuit current is generating regularly because of this applying the theoretical knowledge along with a few small experiments which can generate other solar cell parameters. Due to not having the capability to generate I-V characteristic curve regularly, on the other hand, using the fill factor of the solar module for generating the maximum power of the module. The equation of the maximum power is given below:

$$P_{mp} = V_{oc} * I_{sc} * FF \tag{4.17}$$

From the above equation, the maximum power of the solar module has been calculated daily and the unit of Power is W.

In this experiment, energy calculation is done from the incident sunlight energy or the panel electrical output energy which has been calculated using the trapezoidal method of integration. Unit of the energy here is Wh.

Lastly, the efficiency of the solar module which has been calculated by the ratio of the cumulative electrical energy of the module and the cumulative incident energy of the sun. To calculated the efficiency area of the experimental solar module has been calculated which is Area=0.137 m^2 since the cumulative incident energy of the sunlight unit is Wh/m^2 per day but the experimental module area is not 1 m^2 so the area of the module needs to be multiplied with the cumulative incident energy of the sunlight. Further discussion of the solar cell parameters will be discussed along with their plotting figure which has shown below.

The Plot of Various Parameters of Solar Panel of 14th November 2019 is given below:

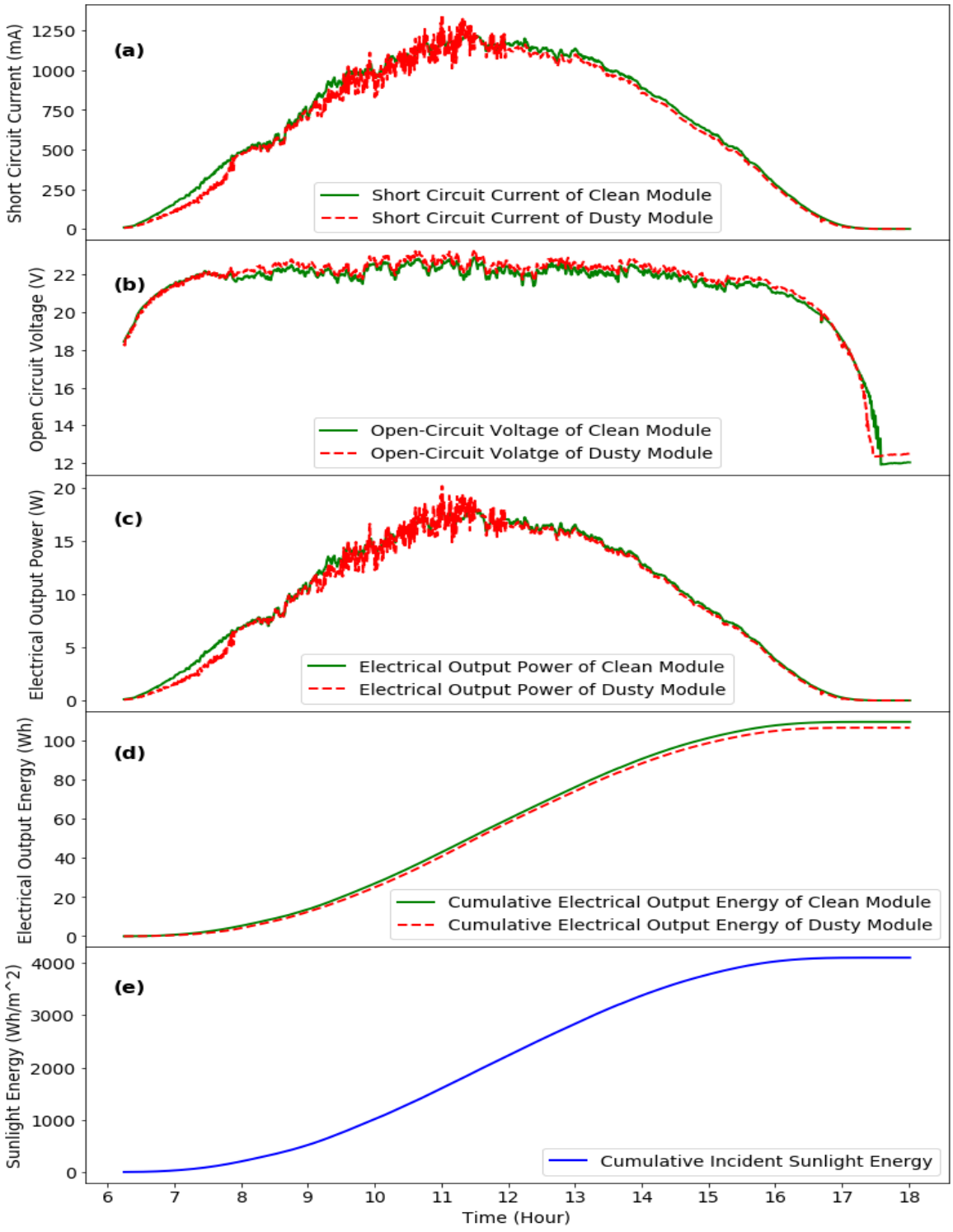

Figure 4.7: Plotting from top to bottom (a) Short Circuit Current vs. Time (b) Open Circuit Voltage vs. Time (c) Panels Electrical Output Power vs. Time (d) Panels Cumulative Electrical Output Energy vs. Time (e) Cumulative Incident Sunlight Energy vs. Time

From the above plotting figure, the upper plotting of the short circuit current vs. time plotting which has been discussed in the previous section with detail information, in short, the factors that affect the performance of the solar module short circuit current are the temperature and solar irradiance whereas solar irradiance most effect because the short circuit current is almost proportional with light intensity. With increasing temperature short circuit current increases slightly which is 0.06% per degree Celsius for a silicon solar cell.

Moving next, the open-circuit voltage of the clean and dusty module vs. time plotting which shows that V_{oc} does change with temperature because of the open-circuit voltage is the function of both solar irradiance and temperature. While open-circuit voltage increases with solar irradiance but on the other sides it decreases with temperature. Because of these two opposing factors, open circuit voltage is remaining almost constant throughout the day.

Next plotting is the electrical output power of clean and dusty module vs. time as discussed earlier in this section the electrical output power is the product of short circuit current, open-circuit voltage and the fill factor of the solar module. While a change in I_{sc} or V_{oc} will change the output of the electrical power of the module. Electrical output power increase with higher solar irradiance than 1000 W/m2 whereas the temperature exceed 25° C than solar module output power decreases. The solar module has a temperature coefficient of around -0.4% to -0.5% per degree Celsius for silicon solar cell.

Furthermore, the cumulative electrical output energy of the clean and the dusty module shows the total energy of that particular solar module has been generated using the energy from the sunlight. Due to the dust effect from the plotting, it is seen that clean module cumulative electrical output energy is higher than the dusty module cumulative electrical output energy. The cumulative electrical output energy for 14th November 2019 was for clean module

109.6825 Wh and for dusty module 106.7061. So, the dusty module has generated less energy than the clean module due to the dust accumulation on the surface of the dusty module.

Lastly, using the input as the cumulative incident energy of the sun and the output as the cumulative electrical output energy the module efficiency has been calculated for clean module efficiency is 19.52% and dusty module efficiency is 18.99%. By observing the plotting figure of November month the behavior of the solar cell parameters can be understood easily, therefore similar technique can be used for understanding the other months of the winter season.

4.5 Chapter Summary

This chapter talked about the theoretical analysis for both clean and dusty solar panels over the four months datasets. The theoretical analysis for both clean and dusty solar panels are shown with detail information with proper explanation of the factors associated with the solar cell. At first, the Raw Data Analysis has been shown based on this analysis short circuit current of the solar panel mostly effected by the temperature among the others weather parameters such as humidity, wind speed. Moreover, the dust effect on the performance of the solar panel is also discussed with dusty module picture along with Daily Variation of the Short Circuit Current of Clean and Dusty Module with detail explanation which shows that due to dust accumulation dusty module cumulative electrical output energy is less than the clean module cumulative electrical output energy. Next section shown the Solar Irradiance of both Ideal and Experimental with proper explanation of the calculation besides this effect of the solar irradiance on the performance of the solar module has been discussed in short, the solar irradiance and the solar module performance has proportional relationship. Lastly, I-V Characteristics Curve has shown which has been calculated by small experiment furthermore with the help of the I-V Characteristic curve the solar cell various parameters have been

calculated and explained with proper information. In summary, from the theoretical analysis for the both clean and dusty solar panels it can be proved that solar irradiance and the dust particles have most impact on the performance of the solar panel.

Chapter 5

Predictive Analysis with Machine Learning

5.1 Introduction

In this chapter, the application of the machine learning algorithm on the data collected and the predicted output result will be discussed. The machine learning algorithm used is an application of the Artificial Neural Networks Perceptron Model using TensorFlow Regression. Data from the seven sensors installed in the outdoor hardware setup across the two Photovoltaic Modules were collected effectively from November 2019 onwards. The data collected has to be preprocessed so that the algorithm can be trained which would act as a core foundation block in order to predict the short circuit current, Isc(mA) of both Clean Module and Dusty Module. Data preprocessing is basically the exclusion of the outliers in data due to system error because it would enforce biasness in the predicted output. Following the phase of data preprocessing, it has to be fed to the machine learning model. Afterwards, the learning algorithm is tested based on its training dataset to compare its accuracy of output prediction with the actual dataset. The predicted output short circuit current, Isc(mA) is used to calculate the Solar Irradiance (W/m^2) using empirical method and thus the Cumulative Light Energy (Wh/m^2) and compared with the Cumulative Light Energy (Wh/m^2) calculated from the experimental data of the following day.

5.2 Multivariate Artificial Neural Networks Perceptron Model

The machine learning model is used to predict the probable output short circuit current, Isc(mA) for a specific day of the year. In the learning algorithm, initially all the required libraries are called. The machine learning model requires training on similar dataset to understand the behavior of the parameters and the targeted output parameter. So, training dataset is loaded to the algorithm. The training dataset is divided into two parameters in the

algorithm, naming X_train and y_train. X_train includes the data of humidity, temperature, windspeed, air pressure sensors and time while the y_train holds the target parameter; i.e. the short circuit current, Isc(mA) from current sensors connected to the Clean Module and Dusty Module. In the following machine learning algorithm, 8 layers with 200neurons associated with each layer are used. The layers inclusively with the neurons decreases the training loss of the algorithm. The parameter epoch is set at 250, which means the algorithm passes over the training data 250times and since the whole training dataset is different from the testing dataset so the parameter batch size is equivalent to the epoch set in the machine learning algorithm. In addition to these parameters, the optimizer used is ADAMAX and it is a necessity because the optimizer is considered to be the engine of the machine learning algorithm which dominates the learning procedure of the algorithm. The activation function used in Rectified Linear Unit (ReLU) because of its ability to deal with non-linear equations with an ease. Subsequently, the training dataset is fit to the model. There is a provision of overfitting to the training dataset which biases the output. In order to refrain overfitting, early stoppage parameter is used with patience parameter set at 25.

Afterwards, the model is tested to prove its expertise when probable dataset of humidity, temperature, windspeed, air pressure and time of a specific day and obviously different from its training dataset are given as input and the algorithm is supposed to predict the output of short circuit current, Isc(mA) separately for both Clean Module and Dusty Module. The error in prediction is calculated using root mean square method comparing with the actual data from current sensor of that specific day whose Isc(mA) is predicted. The whole procedure of predicting the short circuit current, Isc(mA) using the machine learning algorithm is explained using the flowchart below:

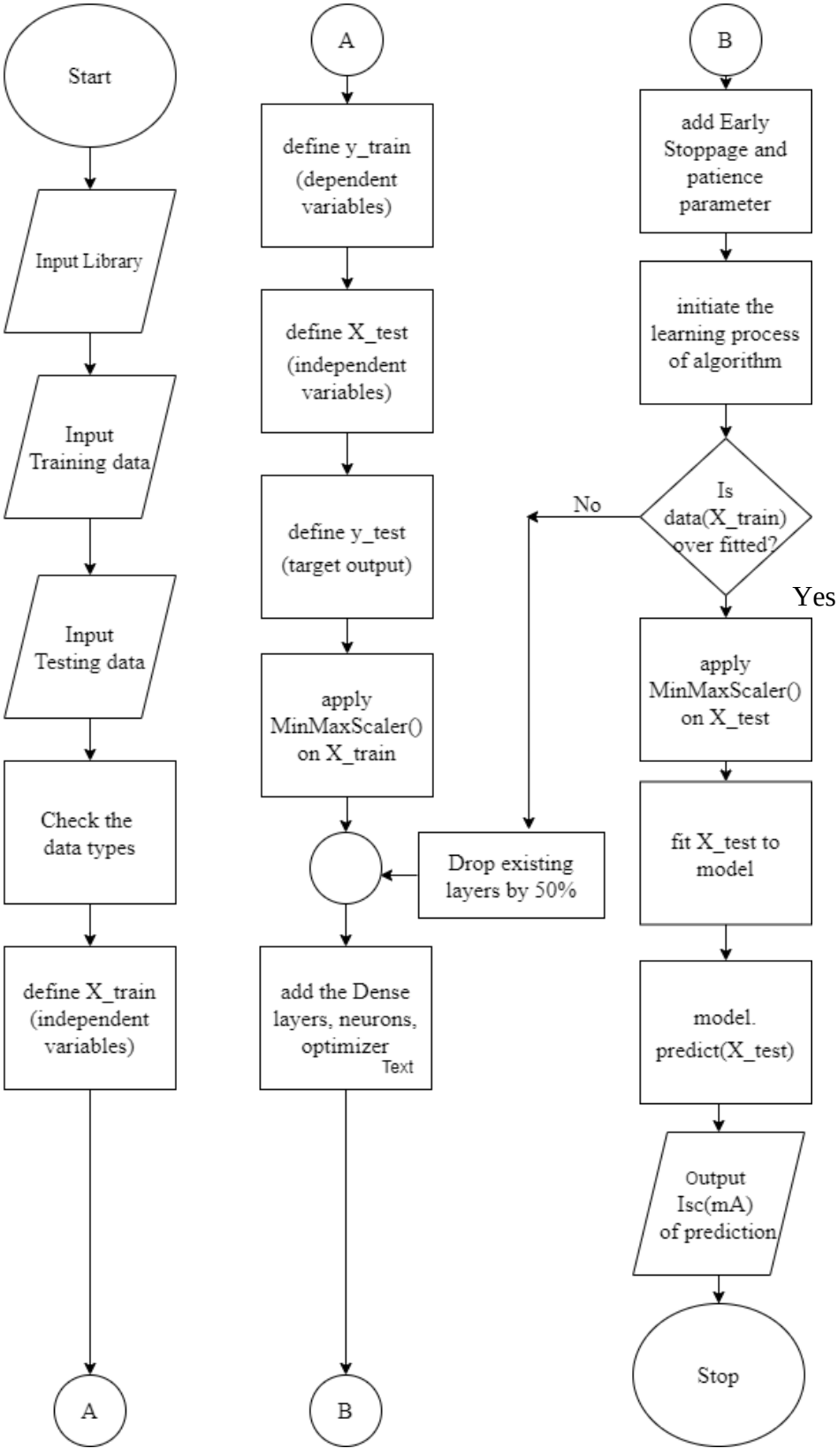

Figure 5.1: Flowchart of the working procedure of algorithm

5.2.1 *Training Set and Testing Set*

The machine learning model need to be trained on the training dataset and its learning expertise is tested based on testing dataset. There is a usual phenomenon of the learning algorithm to predict more accurately when it is trained on a dataset of a long span of time. As data from the sensors included in the hardware setup is collected effectively from November 2019 onwards. So, 4 sets of training dataset are created as follows:

- Training dataset 1: 1st November 2019 to 30th November 2019.
- Training dataset 2: 1st November 2019 to 31st December 2019.
- Training dataset 3: 1st November 2019 to 31st January 2020.
- Training dataset 4: 1st November 2019 to 27th February 2020.

The testing dataset is formed using the data of humidity, air pressure, wind speed, temperature of each Clean Module and Dusty Module and time of 28th February 2020.

5.3 Prediction Analysis with different training dataset

The four different training dataset is used to predict the short circuit current, Isc(mA) of 28th February 2020. The prediction of the short circuit current, Isc(mA) for Clean Module and Dusty Module is predicted separately and plotted against time in x-axis and Isc(mA) in y-axis.

The output for the Clean Module is plotted as follows:

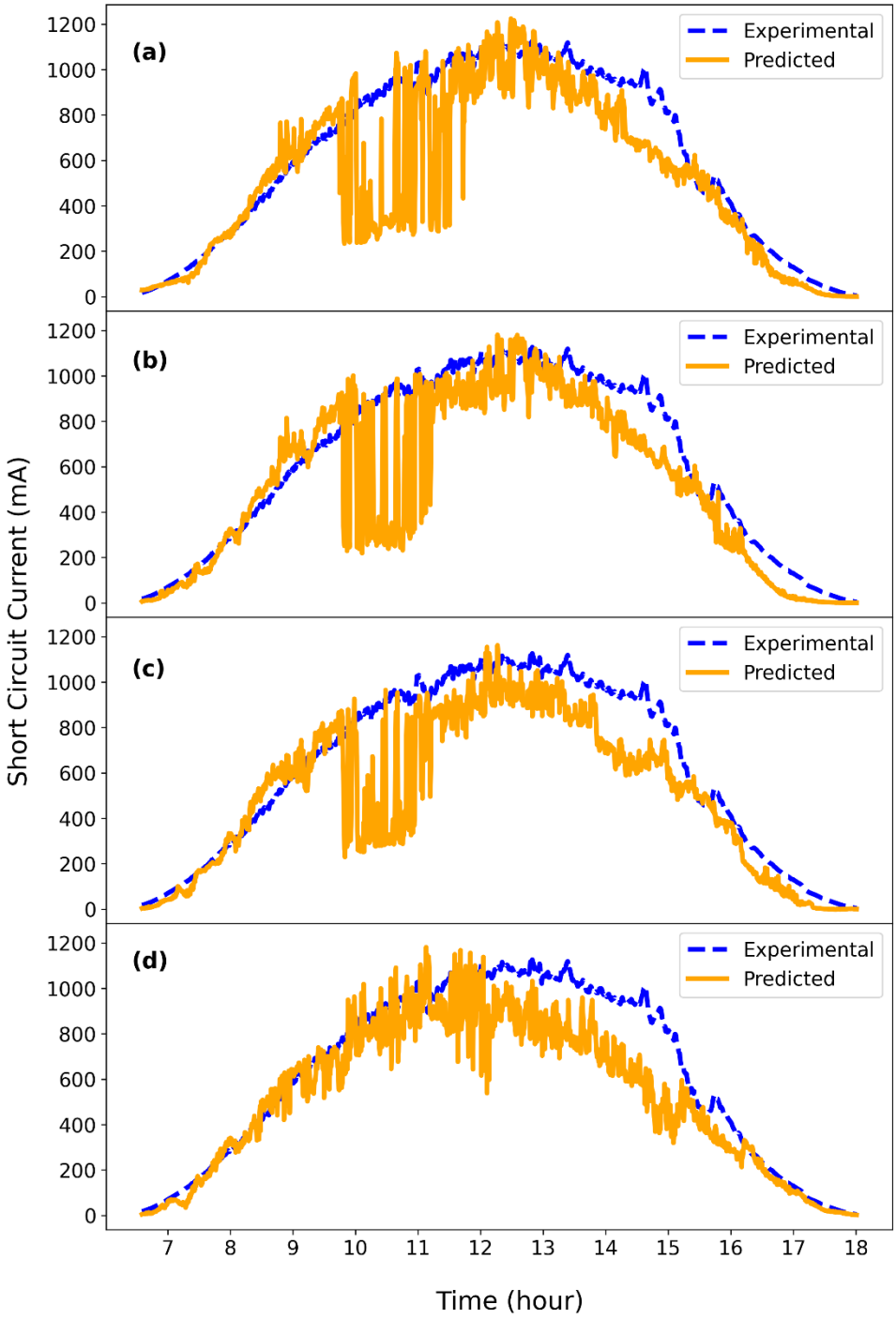

Figure 5.2: Plots of experimental and predicted short circuit current of clean module, estimated using (a) Training dataset 1, (b) Training dataset 2, (c) Training dataset 3, and (d) Training dataset 4.

The solar irradiance (W/m^2) is calculated from the experimental output short circuit current, Isc(mA) of the Clean Module using empirical method; considering the solar irradiance is same for both Clean Module and Dusty Module. Besides, it is also calculated for the predicted output short circuit current, Isc(mA) of 28th February 2020 using the aforementioned four training datasets. The experimental output of solar irradiance (W/m^2) and the predicted output of solar irradiance (W/m^2) is compared. The incident solar irradiance (W/m^2) is integrated with respect to Time (hour) in order to compute the incident cumulative light energy (Wh/m^2). The cumulative light energy (Wh/m^2) is calculated for both the experimental data and predicted data and compared to observe the difference.

The average percentage error rate of the predicted short circuit current, Isc(mA) is calculated using the formula:

$$average\ percentage\ error\ rate = \frac{((y_{true} - y_{pred})/y_{true})}{N} * 100\% \qquad (4.1)$$

where,

- y_{true} contains the value of experimental short circuit current, Isc(mA) value of 28th February 2020.
- y_{pred} contains the value of predicted short circuit current, Isc(mA) value of 28th February 2020.
- N is the total number of data in a Training dataset.

5.4 Effect of Weather Parameters

The sensors in the hardware setup which includes humidity, air pressure, wind speed and temperature sensors for each Clean Module and Dusty Module are somewhat weather parameters. Previously, in the section 5.3 of this book, the machine learning algorithm is trained and tested based on the datasets consisting these weather parameters. So, to understand

and analyze the effect of each of these four weather parameters on the output short circuit current, Isc(mA) of Clean Module and Dusty Module a correlation heatmap is produced. In the heatmap, the magnitude or effect of each parameter on the other is measured on a scale of 1 with corresponding variation of color intensities.

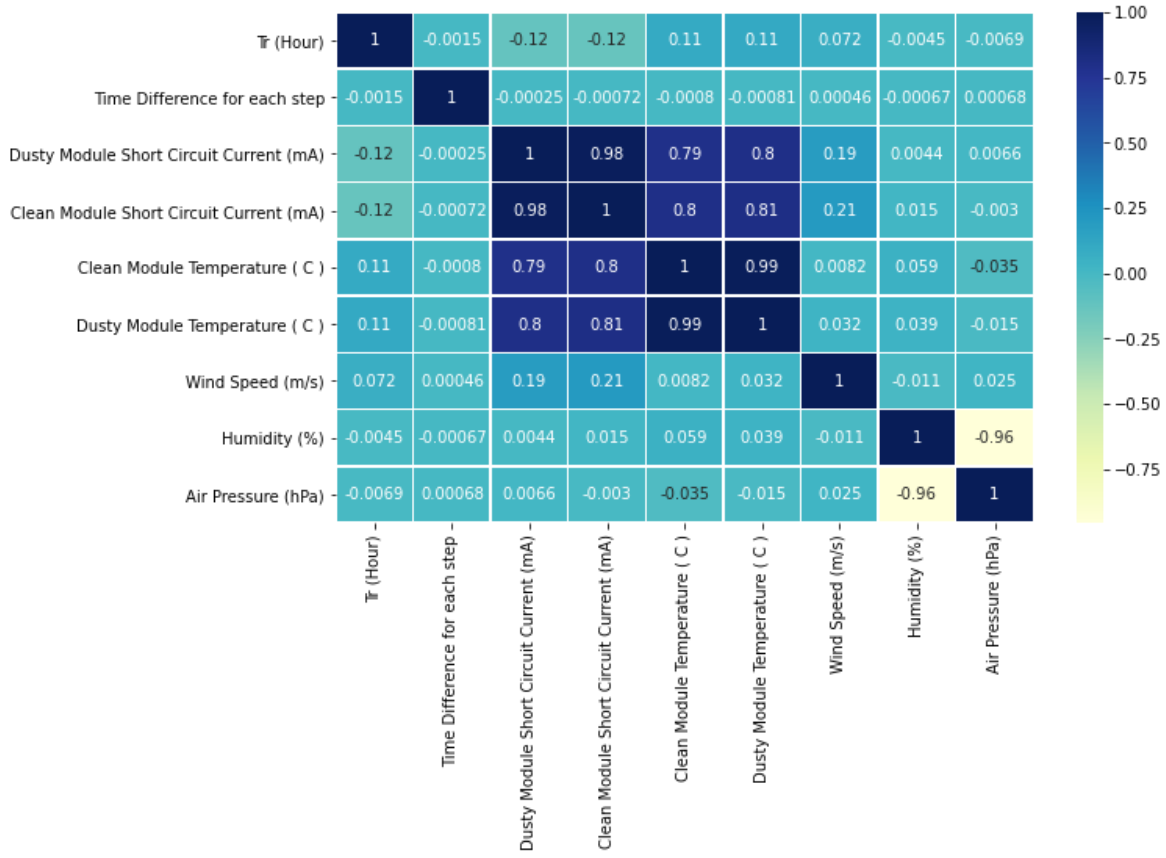

Figure 5.3: Correlation Graph

Heatmaps are graphical presentation where values are depicted by color intensity. The heatmap is created using the training dataset from 1st November 2019 to 27th February 2020. Since the Figure 5.3 illustrates the effect of every single parameter included in the dataset on the other, it can be used to understand the correlation between the short circuit current, Isc(mA) and the weather parameters; humidity, air pressure, windspeed and temperature. It is evident from the value assigned to humidity and air pressure relative to the short circuit current, Isc(mA) of both modules that these parameters affect the least. On the other hand, the weather parameter

temperature is assigned a value of 0.8 when measured on a scale of 1. It means temperature has the highest effect on the output short circuit current, Isc(mA) of both modules.

5.4.1 *Analysis of the Heatmap*

The heatmap in the section 5.4 shows the effect of the four weather parameters on both Clean Module and Dusty Module. So, to observe the effect of each of the individual weather parameters in the prediction results of short circuit current, Isc(mA) the parameters are excluded each time from both the training dataset and testing dataset. Then the machine learning algorithm is trained and tested to observe the variation in the prediction output. The results are compared with the prediction outcome of section 5.3 where all weather parameters are included and experimental short circuit current, Isc(mA) of 28th February 2019.

The output for the Clean Module is plotted as follows:

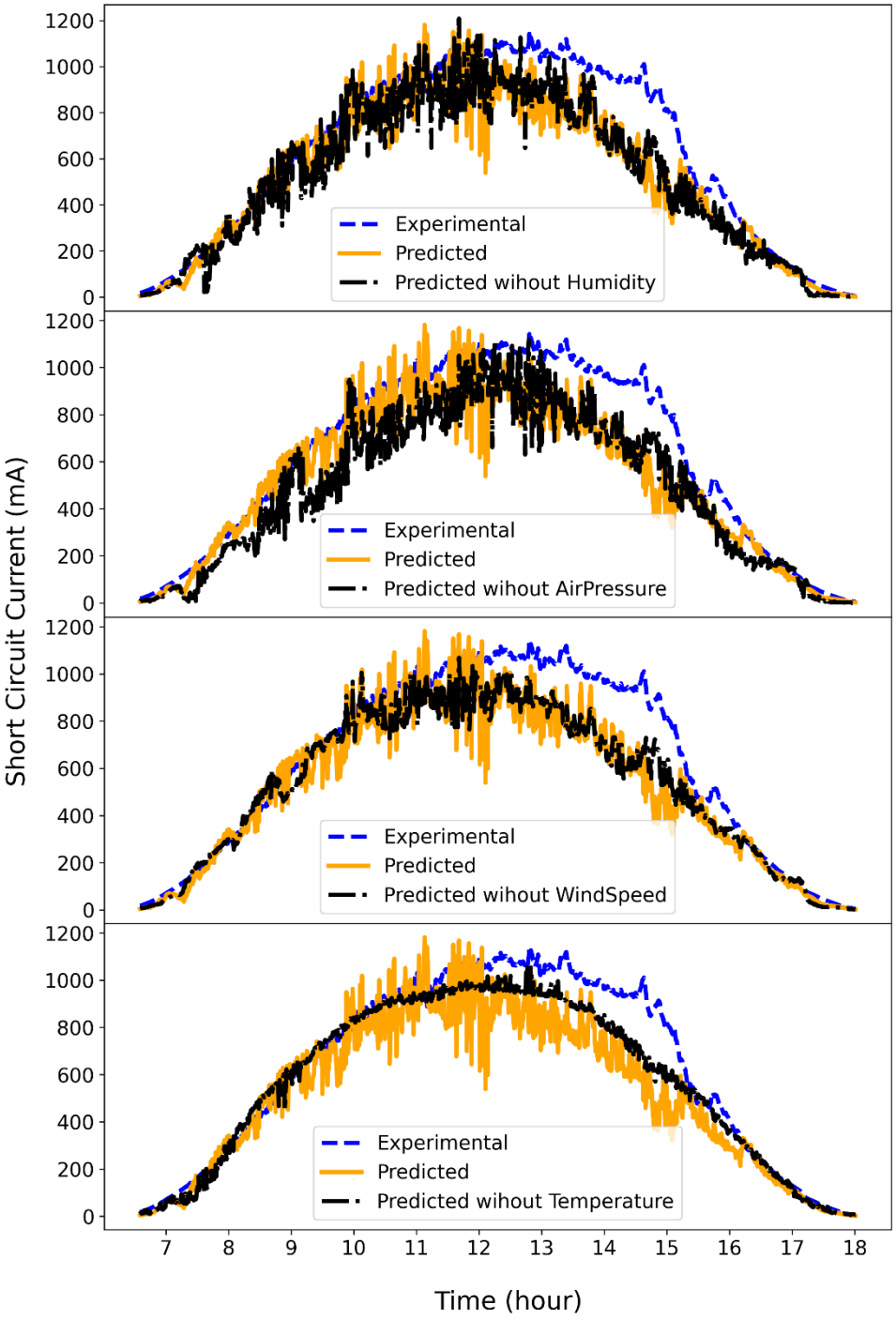

Figure 5.4: Effect of weather parameters on the predicted Isc(mA) of clean module using Training dataset 4.

The output for the Dusty Module is plotted as follows:

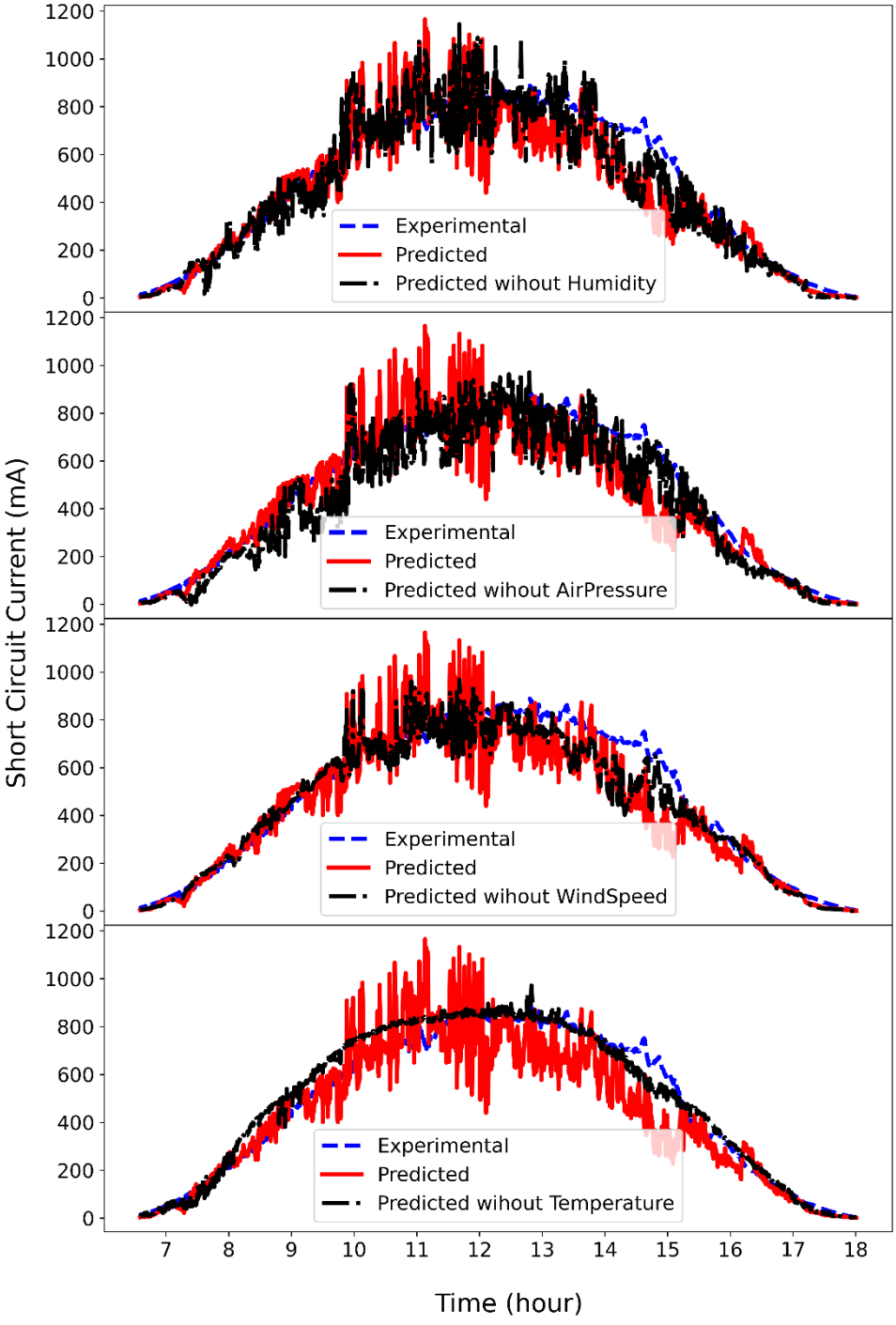

Figure 5.5: Effect of weather parameters on the predicted Isc(mA) of dusty module using Training dataset 4.

The curves in Figure 5.4 and Figure 5.5 interprets that the prediction of short circuit current, Isc(mA) without considering weather parameters Humidity (%), Air Pressure (hPa) the output is similar to some extent to the predicted output when all weather parameters were included in the training dataset and testing dataset. The prediction result of short circuit current, Isc(mA) when WindSpeed (m/s) is excluded shows a moderate variation with the curve of the predicted output when all weather parameters are included. However, when the parameter Temperature (°C) is excluded from the datasets and the machine learning algorithm is trained and tested, the shape of the output graph is similar to an ideal curve of short circuit current, Isc(mA). In short, the parameter Humidity (%) and Air Pressure (hPa) are least effective in terms of prediction of Isc(mA) whereas Windspeed (m/s) has a moderate effect on the prediction and Temperature (°C) is the most effective parameter in terms of predicting output short circuit current, Isc(mA) of Photovoltaic Modules.

5.4.2 *Prediction of short circuit current, Isc (mA) considering Temperature (°**C**) only*

It is observed, previously the prediction of short circuit current, Isc(mA) is predicted using all of the four weather parameters which includes, humidity, air pressure, windspeed and temperature of both Clean Module and Dusty Module. Afterwards, in section 5.4 a correlation graph was made to analyze the effect of weather parameters on the output short circuit current, Isc(mA) of both the Clean Module and Dusty Module. As a result, it is found that only the parameter Temperature (°C) for both the modules has the highest correlation of 0.8 on a scale of 1 among the four weather parameters relative to the output short circuit current, Isc(mA) from both Clean Module and Dusty Module. So, the short circuit current, Isc(mA) of 28th February 2020 is predicted using Temperature (°C) only using the following training datasets:

- Training dataset 1: 1st November 2019 to 30th November 2019.

- Training dataset 2: 1st November 2019 to 31st December 2019.
- Training dataset 3: 1st November 2019 to 31st January 2020.
- Training dataset 4: 1st November 2019 to 27th February 2020.

All of the training datasets only contain the Clean Module Temperature (℃) and the Dusty Module Temperature (℃) for the period of days mentioned for each training dataset. The machine learning algorithm was trained with these training datasets and tested using the Clean Module Temperature (℃) and the Dusty Module Temperature (℃) of 28th February 2020. The results of the calculated cumulative light energy (Wh/m^2) from the predicted short circuit current, Isc(mA) considering Temperature (℃) of Clean Module and Dusty Module only is compared with the cumulative light energy (Wh/m^2) calculated from the prediction of short circuit current, Isc(mA) in the section 5.3 where all the weather parameters such as humidity, air pressure, windspeed and temperature of Clean Module and Dusty Module are included.

5.5 Chapter Summary

This chapter covers the result and analysis part of machine learning model application of this thesis work. The machine learning model is applied to predict the short circuit current, Isc(mA) for a specific day. The learning algorithm was trained with four different datasets consisting data of different time span to predict the Isc(mA) for a specific day; 28th February 2020. The results of the predicted Isc(mA) shown in the Figure 5.2 provides a clear concept about the length of training dataset on which the learning algorithm is trained. It is observed, the algorithm provides better results when it is trained on a dataset of a longer period of time. As a result, average percentage error rate calculated compared to the experimental short circuit current, Isc(mA) of 28th February 2020 decreases. In addition to this, the effect of each of the four weather parameters are analyzed using a heatmap. The results of the heatmap illustrates that Temperature (℃) has the highest effect on the output short circuit current, Isc(mA) of

Photovoltaic Module. Subsequently, short circuit current, Isc(mA) of 28th February 2020 is predicted using the weather parameter Temperature (°C) only. The cumulative light energy (Wh/m^2) calculated from the short circuit current, Isc(mA) predicted using Temperature (°C) only is compared with the cumulative light energy (Wh/m^2) calculated from the short circuit current, Isc(mA) predicted using all weather parameters. The results of the following comparison show that the percentage difference between the two calculated cumulative light energy (Wh/m^2) varies about 0.76% on an average. So, it can be concluded that prediction of short circuit current, Isc(mA) for a specific day can be done using the weather parameter Temperature (°C) and the output short circuit current, Isc(mA) of the Photovoltaic Module.

Chapter 6

An Effective Prediction Analysis Using Multi-Layer Perceptron (MLP) of Artificial Neural Network

6.1 Introduction

In this chapter, the application of Multi-Layer Perceptron of Artificial Neural Network on collected data and an effective prediction on Solar Panel Short Circuit Current, Isc(mA) will be discussed. From the earlier theory and data analysis, it is proven that not all the weather parameters have a relevant correlation to predict the solar panel short circuit current, Isc(mA). Among the four collected weather parameters (wind speed, air pressure, humidity, temperature), the only temperature has a correlation with the short circuit current. Another parameter is solar irradiance which has a great impact and correlation with the solar panel short circuit current. Due to the lack of Pyranometer, the accurate surface irradiance couldn't be collected, rather using a theoretical method Solar Panel Surface Irradiance collected based on solar panel short circuit current, Isc(mA). The effective prediction will be seen using temperature and solar panel surface irradiance parameters. The Multi-Layer Perceptron algorithm of Artificial Neural Network is to predict the solar panel short circuit current, Isc(mA) based on collected data. In this chapter, there will also discussion regarding the comparison on solar panel experimental energy (Wh/day) and predictive energy (Wh/day). This comparison will show how accurately our algorithm predicted the solar panel energy (Wh/day).

6.2 Artificial Neural Network and Multi-Layer Perceptron Algorithm

Artificial Neural Network (ANN) or connectionist systems are computing systems that inspired by biological neural network that represent animal brains. This kind of system learn to perform

certain task based on previous experience or examples. This learning process is not programmed with any task specific rules. But this tool is very useful to find the patterns which are too complex or numerous for a human programmer to extract and to program it. Artificial Neural Network consist of input layer, hidden layer (single or multiple) and output layer. Every Node in one layer is connected to every other node in the next layer except the output layer. Thus, one can make the network deeper increasing the number of hidden layers.

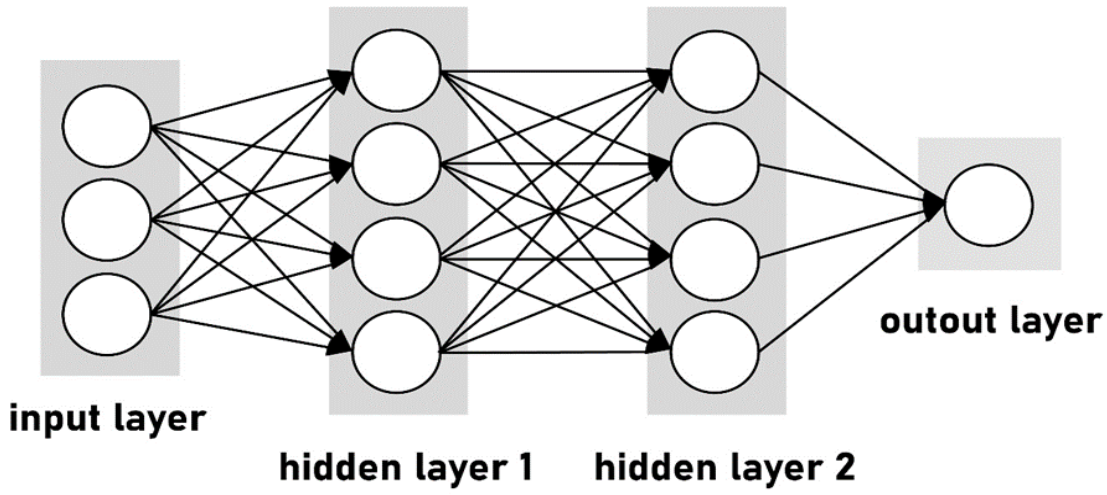

Fig 6.1: Artificial Neural Network Architecture

There are many types of neural network, each of this come with its own specific use cases and level of complexity. Multilayer Perceptron is used for solar panel short circuit current prediction. A Multi-Layer Perceptron (MLP) is a class of feed forward Artificial Neural Network. Multi-Layer Perceptron (MLP) consists of at least three layers on nodes: an input layer, a hidden layer, an output layer. Except for the input nodes, each node is a neuron that uses a nonlinear activation function. MLP utilizes a supervised learning technique called

backpropagation for training. Its multiple layers and non-linear activation distinguish MLP from a linear perceptron which can distinguish data that is not linearly separable.

Keras API(Application Programming Interface) is used to build the algorithm. Keras is a high-level neural networks API, written in Python and it used TensorFlow 2.0 in backend [31]. Jupyter Notebook environment is used to run the Keras API. At first, a notebook is created in Jupyter and then import all the necessary libraries from Keras to use those libraries while creating the MLP algorithm.

In this MLP algorithm, there is one input layer, 5 hidden layers with different nodes at different layers and one predicted output which is short circuit current, Isc(mA). Relu activation function is used for this model. An activation function is a crucial component of artificial neural network which determine the output of the model, its' accuracy and computational efficiency of training a model. Batch normalization is used which is a technique designed to automatically standardize the inputs to a layer in this neural network. Another important function is loss function or cost function which is a function that maps an event onto a real number intuitively representing some cost associated with the event. The loss function is used for this model is 'mean_absolute_error' (MAE) and to get the expected prediction a minimum error is use as a base, which varies in between 60 to 100 for different cases.

At first, all the necessary libraries are imported to the Jupyter notebook and then the training and testing dataset are also imported. After importing the training and testing datasets data framing part comes. In this data framing, x_tarin and y_train data frames are created from training dataset. x_train contains all the input(independent) variables (like time, temperature and solar panel surface irradiance) and y_train contain the corresponding solar panel short circuit current, Isc(mA). And x_test is created from the testing dataset which contains all the input(independent) variables. Then the Multi-Layer Perceptron model is created and the model

is trained based on x_train and y_train datasets. The loss function which is mean_absolute_error (MAE) in this case is the indicator whether the model trained effectively or not. If the MAE is in between 60 to 100, then the model is trained perfectly. After training the model, solar panel short circuit current, Isc(mA) is predicted for the next day based on x_test. A flowchart of working procedure of the model is shown in the next page.

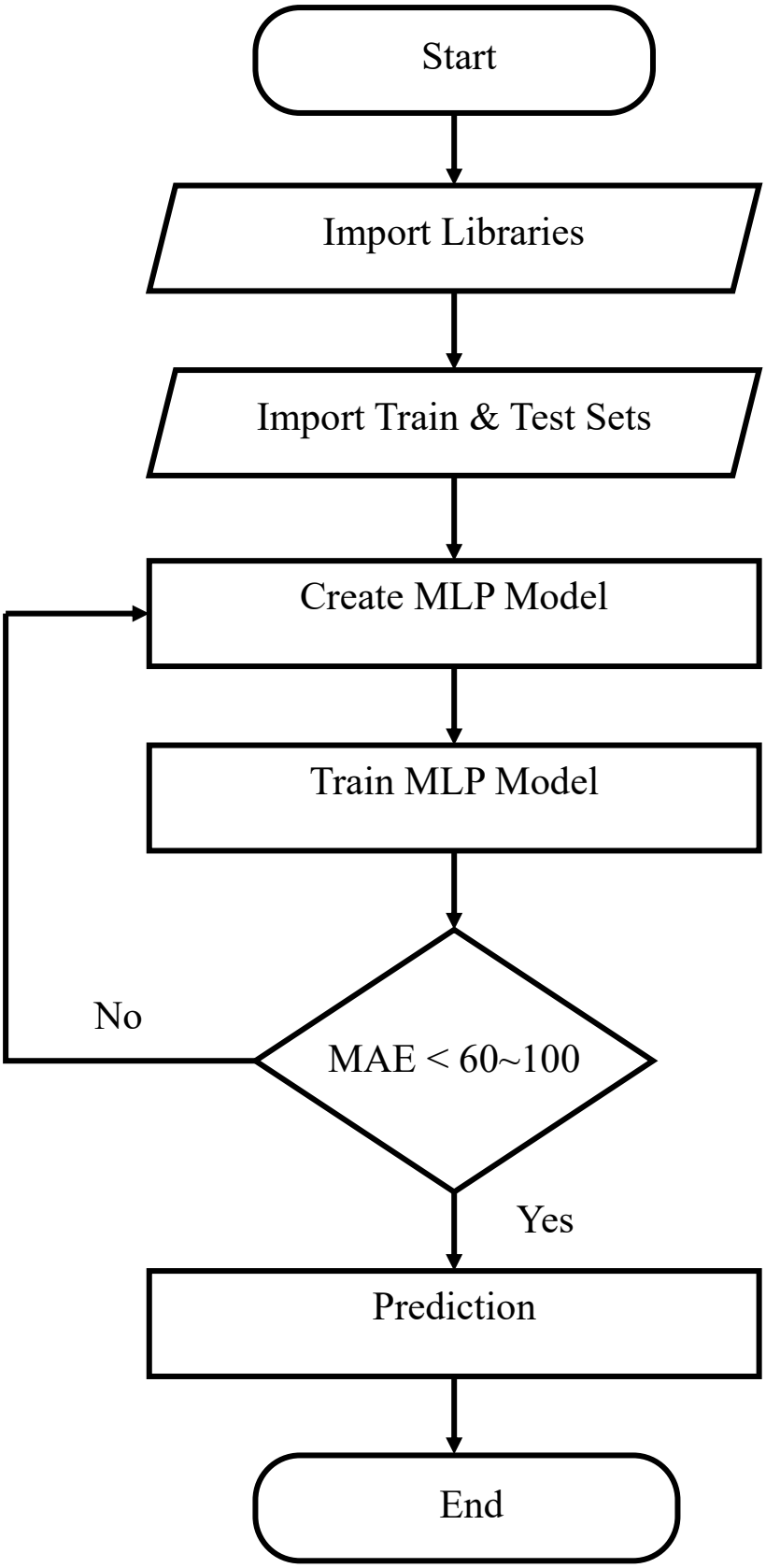

Figure 6.2: Flowchart of the working procedure of MLP model

6.3 Prediction Analysis

Prediction for both clean solar panel and dusty solar panel short will be performed based on dataset from first two weeks data of each months to predict the next day short circuit current, Isc(mA). Parameters will be used in this segment is Time, Temperature and Solar Panel Surface Irradiance.

The comparison between the experimental and predicted solar panel energy (Wh/day) for both clean and dusty panel will also be discussed with their plots.

6.3.1 *Prediction Based on Dataset of First Two Weeks of Each Months*

In this segment, four different training datasets is used to predict the next day short circuit current, Isc(mA). In these training datasets, the input(independent) variables are time, temperature and solar panel surface irradiance. The output(dependent) variable is short circuit current, Isc(mA).

- Training dataset 1: 1st November 2019 to 14th November 2019.
- Training dataset 2: 1st December 2019 to 14th December 2019.
- Training dataset 3: 1st January 2020 to 14th January 2020.
- Training dataset 4: 1st February 2020 to 14th February 2020.

Four testing datasets are formed using data of input(independent) variables which are time, temperature and solar panel surface irradiance.

a. Testing dataset 1: 15th November 2019.
b. Testing dataset 2: 15th December 2019.
c. Testing dataset 3: 17th January 2020.
d. Testing dataset 4: 15th February 2020.

The experimental and predicted short circuit current, Isc(mA) for Clean Solar Panel and Dusty solar panels are plotted against time in x-axis and Isc(mA) in y-axis.

The output Shot Circuit Current for the Clean Solar Panel is plotted as below:

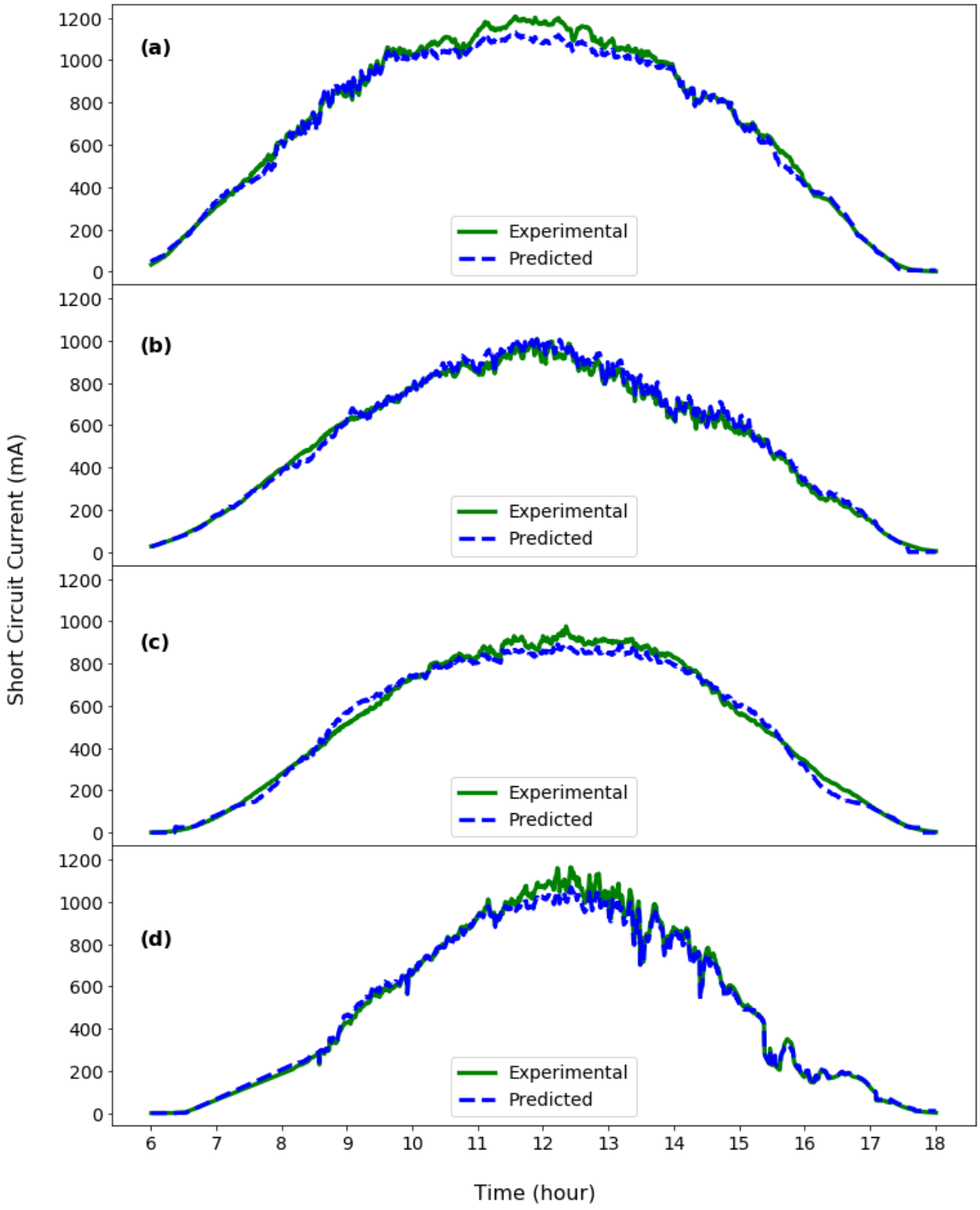

Figure 6.3: Plots of experimental and predicted short circuit current, Isc(mA) of Clean Solar Panel is shown: (a) 15th November 2019, (b) 15th December 2019, (c) 17th January 2020, and (d) 15th February 2020.

The Shot Circuit Current output for the Dusty Solar Panel is plotted as below:

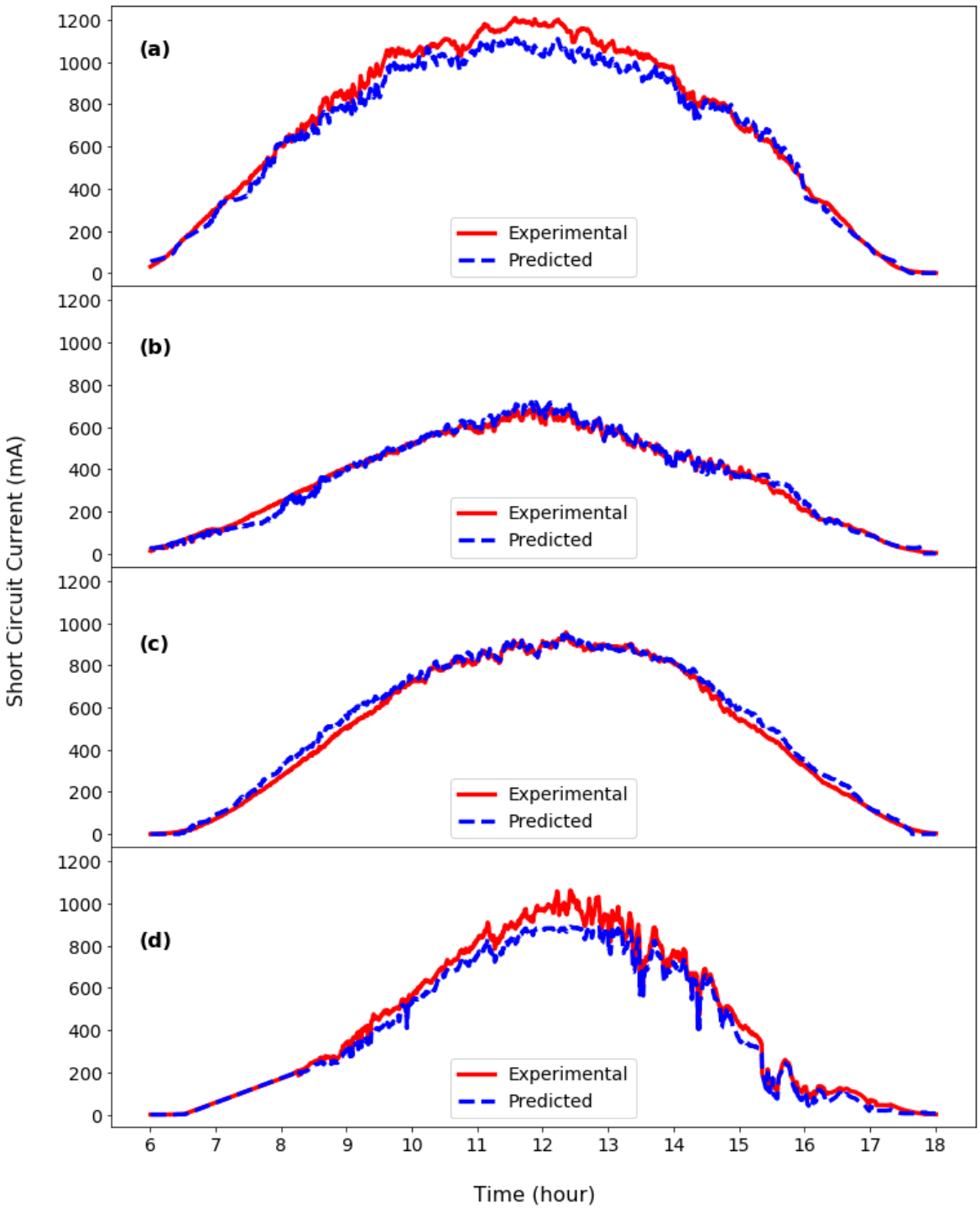

Figure 6.4: Plots of experimental and predicted short circuit current, Isc(mA) of Dusty Solar Panel is shown: (a) 15th November 2019, (b) 15th December 2019, (c) 17th January 2020, and (d) 15th February 2020.

Table 6.1: Comparison of the results between the Experimental and Prediction Short Circuit Current Isc(mA) for Clean Solar Panel and Dusty Panel:

Training Period	Clean Panel		Dusty Panel	
	Average Percentage Difference (%)	Root Mean Square Error (RMSE)	Average Percentage Difference (%)	Root Mean Square Error (RMSE)
1st November 2019 to 14th November 2019	2.21%	37.96	3.87%	61.22
1st December 2019 to 14th December 2019	-1.92%	23.96	0.44%	22.11
1st January 2020 to 14th January 2020	1.58%	34.85	-7.32%	30.03
1st February 2020 to 14th February 2020	0.07%	30.06	13.35%	57.23

$$\text{Average Percentage Difference (\%)} = \frac{1}{n}\sum_{i=1}^{n}\frac{I_{true}-I_{pred}}{I_{true}} * 100\% \quad (6.1)$$

$$Root\ Mean\ Square\ Error\ (RMSE) = \sqrt{\frac{1}{n}\sum_{i=1}^{n}\left(I_{true}-I_{pred}\right)^2} \quad (6.2)$$

Where,

- I_{true} contains the value of experimental short circuit current, Isc(mA).
- I_{pred} contains the value of predicted short circuit current, Isc(mA).
- n is number of predicted observations in the estimation period.

Here, negative sign (-ve) indicates that the predicted short circuit current is greater than experimental short circuit current. On the other hand, positive sign (+ve) indicates that the experimental short circuit current is greater than the predicted short circuit current.

From the above plots and error tables, it can be seen that the prediction over the first two weeks datasets of each months is quite close.

The average percentage difference for the clean solar panel is in between -1.92 % to 2.21 % and the Root Mean Square Error (RMSE) for the clean solar panel is in between 23.96 to 37.96.

On the other hand, the average percentage difference for the dusty solar panel is in between -7.32 % to 13.35 % and the Root Mean Square Error (RMSE) for the dusty solar panel is in between 22.11 to 61.22.

The experimental and predicted solar Panel output energy for Clean Solar Panel and Dusty Solar Panel are plotted against time in x-axis and Panel energy (Wh) in y-axis.

The output energy for the Clean Solar Panel is plotted as below:

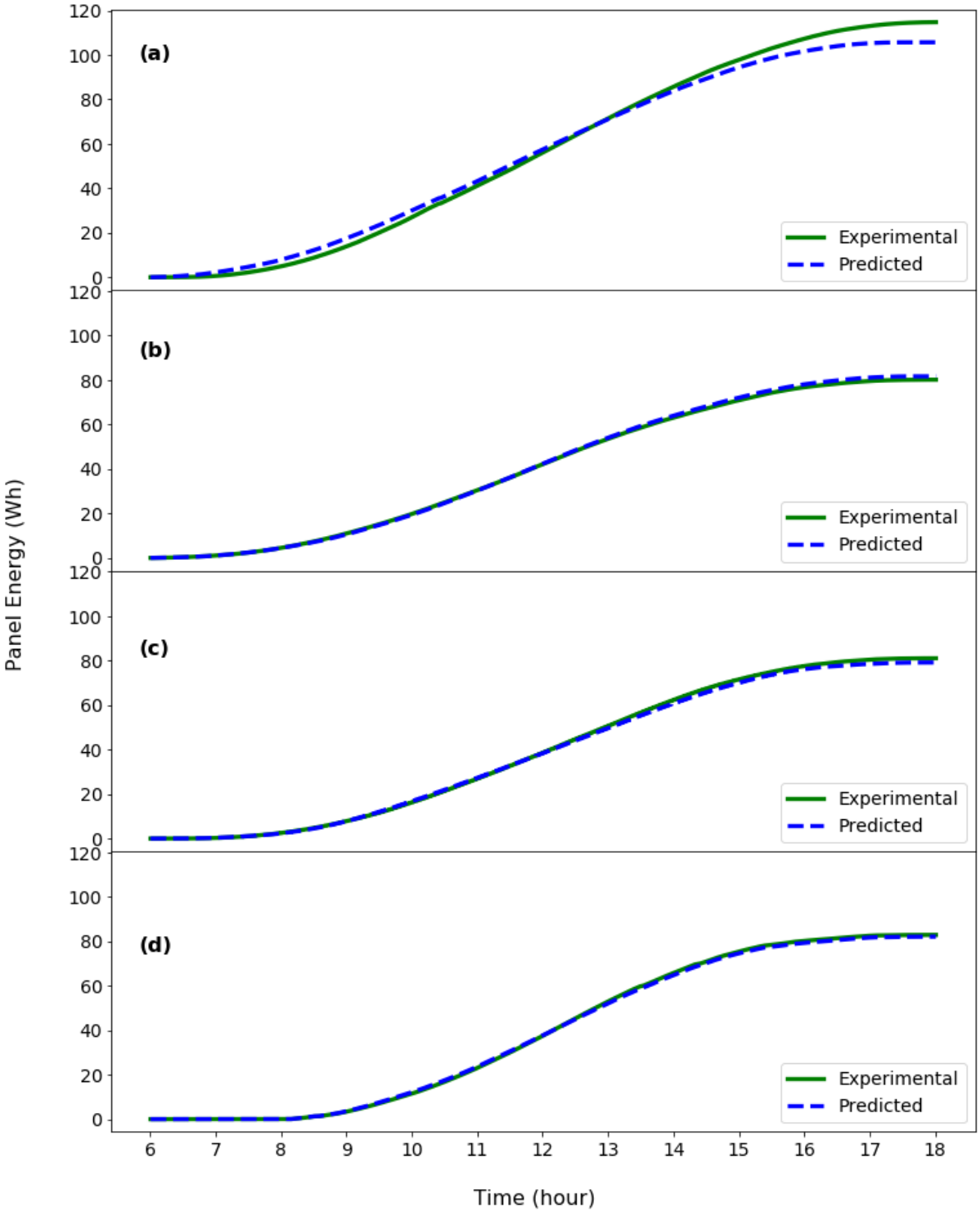

Figure 6.5: Plots of experimental and predicted Clean Solar Panel Energy (Wh) is shown:

(a) 15th November 2019, (b) 15th December 2019, (c) 17th January 2020, and (d) 15th February 2020.

The output energy for the Dusty Solar Panel is plotted as below:

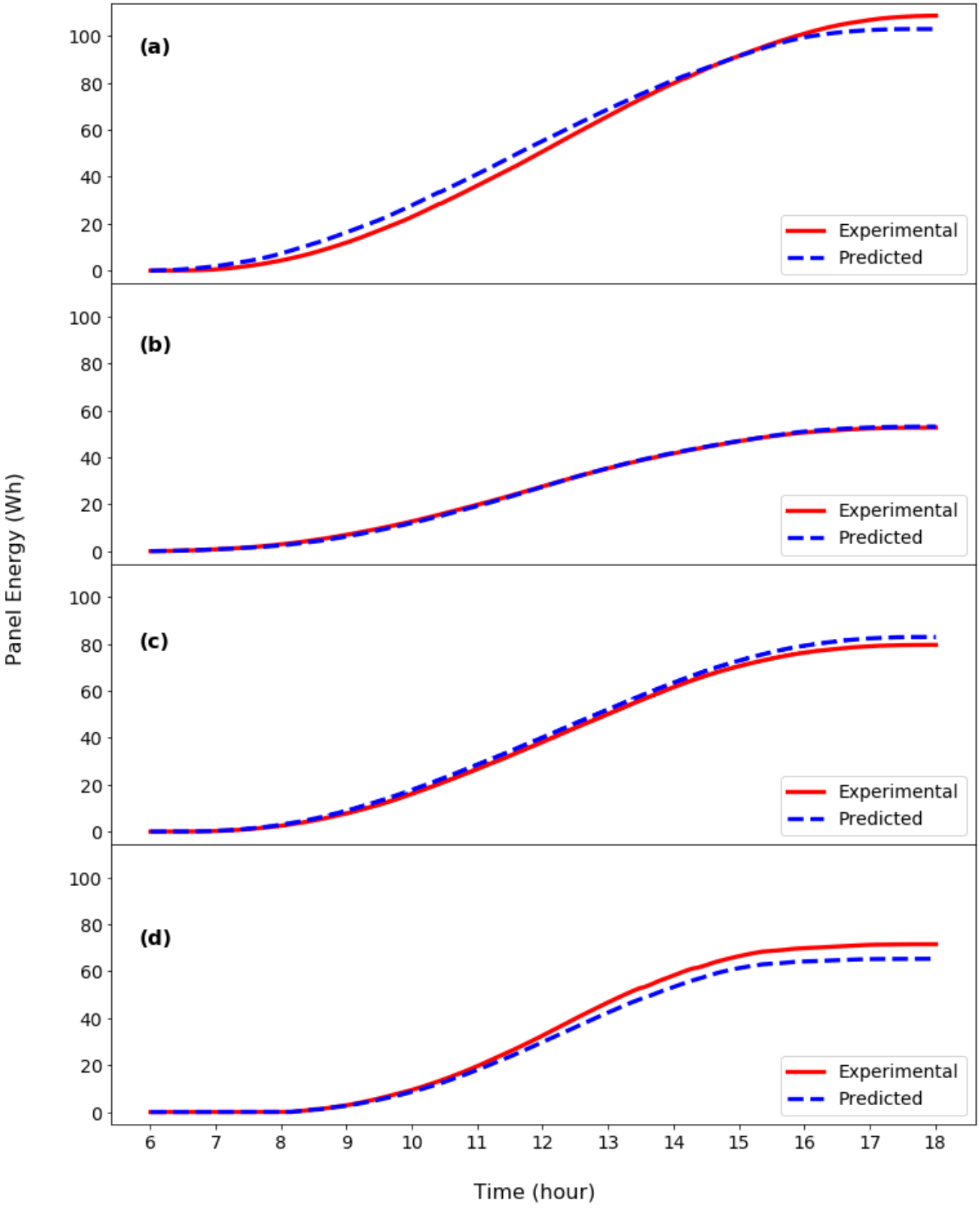

Figure 6.6: Plots of experimental and predicted Dusty Solar Panel Energy (Wh) is shown: (a) 15th November 2019, (b) 15th December 2019, (c) 17th January 2020, and (d) 15th February 2020.

Table 6.2: Comparison of the results between the Experimental and Prediction Solar Panel Energy (Wh/day) for Clean Solar Panel and Dusty Panel:

Training Period	Clean Panel			Dusty Panel		
	Experimental Energy (Wh/day)	Predicted Energy (Wh/day)	Percentage Difference (%)	Experimental Energy (Wh/day)	Predicted Energy (Wh/day)	Percentage Difference (%)
1st November 2019 to 14th November 2019	114.77	105.70	7.9 %	108.67	102.97	5.25 %
1st December 2019 to 14th December 2019	80.17	81.67	-1.87 %	52.63	53.08	-0.86 %
1st January 2020 to 14th January 2020	81.09	79.20	2.33 %	79.58	82.93	-4.21 %
1st February 2020 to 14th February 2020	82.90	82.13	0.93 %	71.52	65.32	8.67 %

$$\text{Percentage Difference (\%)} = \frac{E_{true} - E_{pred}}{E_{true}} * 100\% \quad (6.3)$$

Here, negative sign (-ve) indicates that the predicted panel energy (Wh/day) is greater than experimental panel energy (Wh/day). In contrast, positive sign (+ve) indicates that the experimental panel energy (Wh/day) is greater than the predicted panel energy (Wh/day).

The percentage difference for clean panel energy (Wh/day) prediction varies from -1.87 % to 7.9 %, and the percentage difference for dusty panel energy (Wh/day) prediction varies from -4.21 % to 8.67 %.

6.4 Chapter Summary

This chapter discussed the effective prediction using the Multi-Layer Perceptron algorithm of Artificial Neural Network. The prediction analysis for both clean solar panel and dusty solar panel is shown in terms of their short circuit current, Isc(mA) and solar panel energy (Wh/day). The prediction analysis is shown based on only first two weeks dataset of each months to predict the next day short circuit current, Isc(mA) for both clean and dusty solar panel and their prediction errors very low. In this segment, the highest percentage difference of solar panel energy (Wh/day) prediction for both clean panel and dusty panel are consecutively 7.9 % and 8.67%. In summary, from the comparison between the solar panel experimental energy (Wh/day) and predictive energy (Wh/day), it can be proved that this prediction model can approximately predict the solar panel energy (Wh/day) of any day of the year within 10 % percentage difference error, if there is enough collection of datasets.

Chapter 7

Summary

This thesis work is done based on the data collected from November 2019 to February 2020 of two PV panels and environmental parameters. Data are extracted with a combine implementation of hardware and software which is presented in Chapter 3. The analysis works are discussed into two main parts, one is a performance analysis and the other one is prediction analysis of PV panels. Initially, this study investigates the performance analysis of both Clean and Dusty panels in environmental conditions based on the experimental and theoretical analysis in chapter 4. It concludes that weather parameters such as humidity and wind speed have an ignorable impact on PV panels output. The output short circuit current of PV panels increases slightly with temperature and the temperature dependence of the short circuit current for a silicon solar cell is 0.06% per$°C$. However, the short circuit current is mostly correlated with the solar irradiance among all the weather parameters. The short circuit current and the solar irradiance is mostly proportional as with increasing sunlight more energy can be generated. Besides this dust has a very important role in the performance of the solar module, in chapter 4 dust impact on the performance of solar panel has been described in a various way which can be concluded that due to dust accumulation on the surface of the dusty panel, the performance of the dusty panel compared to the clean module is degraded. Finally, in Chapter 5 and 6, prediction analysis is discussed using Multi-Layer Perceptron (MLP) models. These two chapters establish that the prediction for a specific day PV panels short circuit current is improved and stabled with longer training datasets, in addition, choosing correct weather parameters can improve the performance of prediction. Cumulative light energy and cumulative panels electrical energy output are also determined using theoretical methods which are also shown in chapter 4. In chapter 5, it is observed that the average percentage error of the four distinct training datasets between the prediction results considering all weather

parameters and experimental incident cumulative light energy is 16.71%. Moreover, the average percentage error of four training datasets is 17.38% when the prediction is done only considering temperature as the weather parameter relative to the experimental results. In addition, the average percentage error between the results of the two distinct prediction analysis is 0.76%. So, analyzing the results of chapter 5, it can be stated that only considering temperature as the weather parameter, it is possible to predict the incident cumulative energy with similar precision comparing to the results when the weather parameters (Humidity, Air pressure, Wind speed, Temperature) are considered. In chapter 6, the MLP model is created with different hyperparameters to improve the prediction errors. The prediction results training with temperature and solar panel surface irradiance have even lower prediction errors in short circuit current and panels output energy as solar irradiance has a greater correlation with panel short circuit current. For the clean panel, the average percentage difference and RMSE for short circuit current are on absolute average 1.45% and 31.71 respectively, and the percentage difference in solar energy output is on absolute average 3.26%. On the other hand, for the dusty panel, the average percentage difference and RMSE for short circuit current are on absolute average 6.25% and 42.65 respectively, and the percentage difference in solar energy output is on absolute average 4.75%.

For future work, a longer period dataset can assist the analysis of dust on both panels over the year. MLP model needs the independent variables like temperature and solar panel surface irradiance for prediction of short circuit current on a specific day. Hence, in future, a longer period datasets collection will be a great assist for this MLP model to predict the short circuit current and panel energy output for any day of the year with high accuracy.

References

1. S. Ahmed, A. H. Zenan, N. Tasneem and M. Rahman, "Design of a solar powered LED street light: Effect of panel's mounting angle and traffic sensing," 2013 IEEE Conference on Sustainable Utilization and Development in Engineering and Technology (CSUDET), Selangor, 2013, pp. 74-79, doi: 10.1109/CSUDET.2013.6670990.
2. P. G. Kale, K. K. Singh and C. Seth, "Modeling Effect of Dust Particles on Performance Parameters of the Solar PV Module," 2019 Fifth International Conference on Electrical Energy Systems (ICEES), Chennai, India, 2019, pp. 1-5, doi: 10.1109/ICEES.2019.8719298.
3. R. Bhol, R. Dash, A. Pradhan and S. M. Ali, "Environmental effect assessment on performance of solar PV panel," 2015 International Conference on Circuits, Power and Computing Technologies [ICCPCT-2015], Nagercoil, 2015, pp. 1-5, doi: 10.1109/ICCPCT.2015.7159521.
4. R. Zhang, M. Feng, W. Zhang, S. Lu and F. Wang, "Forecast of Solar Energy Production - A Deep Learning Approach," 2018 IEEE International Conference on Big Knowledge (ICBK), Singapore, 2018, pp. 73-82, doi: 10.1109/ICBK.2018.00018.
5. HM Fahad, Aporajita Islam, Md. Fahim Hasan, Wasima Fariha, "The Performance Analysis of Single and Dual Axis Sun Tracking System: A Comparative Study," dspace.bracu.ac.bd, 2017. Available: http://dspace.bracu.ac.bd/xmlui/bitstream/handle/10361/8643/13121064,%2013121137,13121049,13121050_EEE.pdf?sequence=1. [Accessed January 10, 2020]
6. PVEducation, [Online]. Available: https://www.pveducation.org/. [Accessed January 15, 2020]

7. Bangladesh Power Development Board, [Online]. Available: https://www.bpdb.gov.bd/bpdb_new/index.php/site/page/5a3f-2fdb-e75f-3cab-e66b-f70d-5408-cbc9-f489-c31c. [Accessed April 24, 2020]
8. Ferdaus Ara Begum, "Rooftop solar power -- a sustainable option for Bangladesh ," The Financial Express, November 08, 2019. [Online]. Available: https://thefinancialexpress.com.bd/views/rooftop-solar-power-a-sustainable-option-for-bangladesh-1573226883. [Accessed April 26, 2020]
9. QS Study, [Online]. Available: https://www.qsstudy.com/physics/define-conductor-insulator-and-semiconductor. [Accessed March 28, 2020]
10. RENEWABLES IN AFRICA, [Online]. Available: https://www.renewablesinafrica.com/how-does-a-solar-panel-work/. [Accessed March 28, 2020]
11. PVPerformance, [Online]. Available: https://pvpmc.sandia.gov/modeling-steps/2-dc-module-iv/diode-equivalent-circuit-models/. [Accessed March 28, 2020]
12. Ossila, [Online]. Available: https://www.ossila.com/pages/iv-curves-measurement. [Accessed March 28, 2020]
13. ScienceDirect, [Online]. Available: https://www.sciencedirect.com/topics/engineering/solar-altitude-angle. [Accessed March 28, 2020]
14. BRITANNICA, [Online]. Available: https://www.britannica.com/science/latitude. [Accessed March 28, 2020]
15. Trifun Savić, Milutin Radonjić, “One approach to weather station design based on Raspberry platform,” IEEE Xplore, January 11, 2016. [Online]. Available: https://ieeexplore.ieee.org/document/7377544. [Accessed March 24, 2020].

16. Palak Kapoor, Ferdous Ahmed Barbhuiya, “Cloud Based Weather Station using IoT Devices,” IEEE Xplore, December 12, 2019. [Online]. Available: https://ieeexplore.ieee.org/document/8929528. [Accessed March 26, 2020].
17. Hakan Üçgün, Zeynep Kübra Kaplan, “Cloud Based Weather Station using IoT Devices,” IEEE Xplore, November 02, 2017. [Online]. Available: https://ieeexplore.ieee.org/document/8093397. [Accessed March 26, 2020].
18. DALLAS SEMICONDUCTOR, “DS18B20 Programmable Resolution 1-Wire Digital Thermometer,” DALLAS SEMICONDUCTOR. [Online]. Available: https://image.dfrobot.com/image/data/DFR0198/DS18B20.pdf. [Accessed March 29, 2020].
19. ebay, “Anemometer wind speed Sensor Output 0~5VDC range 0~30m/s Arduino Weather Station,” ebay. [Online]. Available: https://www.ebay.com/itm/Anemometer-wind-speed-Sensor-Output-0-5VDC-range-0-30m-s-Arduino-Weather-Station-/254119722017. [Accessed March 29, 2020].
20. BOSCH Sensortec, “DS18B20 Programmable Resolution 1-Wire Digital Thermometer,” BOSCH Global. [Online]. Available: https://cdn.datasheetspdf.com/pdf-down/B/M/P/BMP180_Bosch.pdf. [Accessed March 29, 2020].
21. lady ada, “Adafruit INA219 Current Sensor Breakout,” adafruit, October 26, 2012. [Online]. Available: https://learn.adafruit.com/adafruit-ina219-current-sensor-breakout. [Accessed March 30, 2020].
22. ePro Labs, “DS18B20 Temperature Sensor,” ePro Labs, July 12, 2016. [Online]. Available: https://wiki.eprolabs.com/index.php?title=DS18B20_Temperature_Sensor#:~:text=W

orking%20Principle%20of%20DS18B20%20Temperature%20Sensor,and%200.0625%C2%B0C%2C%20respectively. [Accessed April 1, 2020].

23. lady ada, “DHT11, DHT22 and AM2302 Sensors,” adafruit, January 12, 2019. [Online]. Available: https://cdn-learn.adafruit.com/downloads/pdf/dht.pdf?timestamp=1591351304. [Accessed April 1, 2020].
24. Dejan, “DHT11 & DHT22 Sensors Temperature and Humidity Tutorial using Arduino,” How to Mechatronics, January 13, 2016. [Online]. Available: https://howtomechatronics.com/tutorials/arduino/dht11-dht22-sensors-temperature-and-humidity-tutorial-using-arduino/. [Accessed April 1, 2020].
25. The Editors of Encyclopaedia Britannica, “Anemometer,” Encyclopaedia Britannica, July 20, 1998. [Online]. Available: https://www.britannica.com/technology/anemometer. [Accessed April 2, 2020]
26. Raspberry Pi, “Raspberry Pi 3 Model B,” Raspberry Pi. [Online]. Available: https://www.raspberrypi.org/products/raspberry-pi-3-model-b. [Accessed April 2, 2020].
27. Raspberry Pi, “Raspberry Pi 3 Model B+,” Raspberry Pi. [Online]. Available: https://static.raspberrypi.org/files/product-briefs/Raspberry-Pi-Model-Bplus-Product-Brief.pdf. [Accessed April 2, 2020].
28. Component 101, “Arduino Uno,” Component 101, February 28, 2018. [Online]. Available: https://components101.com/microcontrollers/arduino-uno. [Accessed April 4, 2020].
29. Putty, [Online]. Available: https://www.putty.org. [Accessed September 14, 2019].
30. TightVNC Software, [Online]. Available: https://www.tightvnc.com. [Accessed September 17, 2019].

31. Keras, [Online]. Available: https://keras.io/. [Accessed January 5, 2020].

Appendix A.

Experimental Setup

Anemometer

Working Principle:

The Anemometer or the wind speed sensing sensor has a total of three cups attached to its horizontal arms and these are attached to a vertical rod. When the cups of the sensor rotate because of the air flow, they make the rod spin. The rod spins faster when the flow of the wind rises. The anemometer counts the number of rotations and gives an analog value, which is later used to calculate the output voltage. This output voltage is used to find wind speed with the help of an equation that was given in the sensor datasheet.

Table 3.1: Technical Index of the Anemometer

Output	4mA ~ 20mA
Working Voltage	12V ~ 30V (DC)
Testing Range	0.5 m/s ~ 50 m/s
Start Wind Speed	≤0.5 m/s
Operating Environment	-20ºC ~ +85ºC
Accuracy	±0.5 m/s
Material	All Aluminum Alloy

The sensor gives two types of outputs -

iii. Voltage Output

iv. Current Output

It depends on the pinouts' combination used by the user. The pin details are given in the pinout Table 3.2. In our case, we considered the voltage output.

Table 3.2: Anemometer Pinouts and Combination for output signal

Direct Outlet	Wires	Output Signal	Wiring Method	
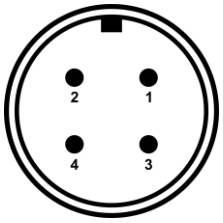	3 - Wire	Voltage Type	1	Positive Pole
			2	Negative Pole
			3	Voltage Signal
	3 - Wire	Current Type	1	Positive Pole
			2	Negative Pole
			4	Current Signal

INA219 Current Sensor

Working Principle:

The module works equivalent to a conventional ammeter such that it is in series with the circuit. At the point when the module is connected in series, the similar current will course through the module and the remainder of the circuit. This current will produce a voltage drop on the already mentioned shunt resistor, proportional to the current, which compares to Ohm's law. This analog voltage is then converted by analog-to-digital converter to digital data so that we can easily transmit it through the I2C communication interface. The specification of the INA219 Current sensor is given in the Table 3.3.

Table 3.3: INA219 Current Sensor Technical Index

Power Supply Voltage	3V ~ 5.5V
Maximum Measured Voltage	26V
Maximum Measured Current	3.2A
ADC's Precision	12-bit
Communication Interface	I2C
Shunt Resistor	0.1 Ω
Dimensions	18 mm * 20 mm
Operating Environment	-40ºC ~ 125ºC

DHT11 Humidity Sensor

Working Principle:

The sensor consists of a capacitive humidity sensing component, an IC on the back side of the sensor and an NTC temperature sensor. DHT11 or Digital temperature and humidity sensor contains digital calibrated signal output. It uses a dedicated storage system which increases its reliability. The humidity sensing capacitor has two electrodes with moisture holding substrate as a dielectric between them. The change in the capacitance value takes place, when there is a change in humidity levels. When the temperature varies about 0.5ºC the conductivity of the sensor changes or the resistance changes. This change in resistance is measured and processed by the IC which converts the analog signal into digital signal, which is easily readable from the sensing component using a microcontroller.

The humidity range of this sensor is from 20% to 80% with 5% accuracy, where the sampling rate of the sensor is 1Hz. It means, the sensor gives one reading each second. DHT11 is small in size and its operating voltage is from 3V to 5V.

DHT11 sensor has four pins (Figure 3.10), which are VCC, Ground, Data Pin and Not Connected (NC) pin. A pull-up resistor of 5kΩ to 10kΩ is used between VVC & output for communication between sensor and micro-controller. The specification of the DHT11 Current sensor is given in the Table 3.4.

Table 3.4: DHT11 Humidity Sensor Technical Index

Power Supply Voltage	3V ~ 5V
Range of working capacity	20% ~ 95%
DHT11's Precision	5%
Maximum Current Usage: 2.5mA	2.5mA
Communication Interface	I2C
Sampling Rate	1Hz
Dimensions	15.5mm x 12mm x 5.5mm

DS18B20 Temperature Sensor

Working Principle:

DS18B20 Temperature sensor's works on the principle of direct conversion of temperature into a digital value. The core functionality of the DS18B20 is to change its bit numbers according to the change in temperature. A bit gets changed into 9,10,11,12 bits as temperature changes in values 0.5ºC, 0.25ºC, 0.125ºC and 0.0625ºC respectively. The default resolution is 12-bit at power-up. In a low power idle state, the DS18B20 powers up. Convert T [44h] command must be issued to start a temperature measurement and analog-to-digital conversion of data. During the conversion of analog data to digital data, in the 2-byte temperature register in the scratchpad memory the resulting thermal data gets stored, while the DS18B20 returns to its idle state. After the Convert T command "Read Time Slots" command can be issued, if the sensor is powered by an external power supply. The DS18B20 will respond by transmitting 0 while the temperature conversion is in progress and 1 when the conversion is done. The Functional commands are explained in the Table 3.5.

Read Time Slots

The DS18B20 temperature sensor can only transmit data to the master when the master issues "Read Time Slots". Therefore, after issuing a Read Scratchpad [BEh] or Read Power Supply [B4h] command, the master must generate read time slots immediately, so that the sensor can provide the requested data. In addition, the master can generate "Read Time Slots" after issuing Convert T [44h] command.

Table 3.5: DS18B20 Temperature Sensor Function Commands & 1-Wire Activity.

Command	Description	Protocol	1-Wire Activity After A Command is Issued
Convert T	Initiates Temperature Conversion.	44h	DS18B20 transmits conversion status to the master.
Read Scratchpad	Reads the entire scratchpad including the CRC byte.	BEh	DS18B20 transmits up to 9 data bytes to master
Read Power Supply	Signals DS18B20 power supply mode to the master	B4h	DS18B20 transmits supply status to master

Table 3.6: DS18B20 Technical Index

Power Supply Voltage	3V ~ 5.5V
Temperature Measurement Range	-55°C ~ +125°C
Accuracy	±0.5°C from -10°C ~ +85°C
Communication Interface	1-Wire
Modes	Normal Mode, Parasitic Mode
Temperature Conversion Time	93.75ms
Output Resolution	9-bit ~ 12-bit

BMP180 Barometric Pressure Sensor

Working Principle:

The BMP180 connects to a microcontroller by the I2C bus. The sensor has a piezo-resistive sensor, an analog-to-digital converter and a control unit with E2PROM and a serial I2C interface. The uncompensated value of pressure and temperature gets delivered by the sensor. To compensate offset, temperature dependence and other parameters of the sensor, the E2PROM stores 176-bit of individual calibration data.

UP = Pressure Data (16-bit ~ 19-bit)

UT = Temperature Data (16-bit)

Before starting a pressure or a temperature measurement, the microcontroller sends a start sequence. After the conversion time, the result value (UP and UT, respectively) can be read by the I2C interface. The calibration data has to be used for calculating the pressure in hPa and temperature in ºC. At the software initialization, theses constants can be read out from the BMP180 E2PROM by the I2C interface. For dynamic measurement, the sampling rate can be increased up to 128 samples per second (standard mode). In this case, it is sufficient to measure the temperature only once per second and to use this value later for all pressure measurements during the same period.

Hardware Pressure Sampling Accuracy Modes:

By using different modes, the optimum compromise between power consumption, speed and resolution can be selected. Details are given in the Table 3.7.

Table 3.7: BMP180 Hardware Pressure Sampling Accuracy Modes

Mode	**Parameter Over Sampling Setting**	**Internal number of samples**	**Conversion Time Pressure max. [ms]**	**Average Current at 1 sample/s typ. [uA]**	**RMS Noise typ. [hPa]**	**RMS Noise typ. [m]**
Ultra-Low Power	0	1	4.5	3	0.06	0.5
Standard	2	2	7.5	5	0.05	0.4
High Resolution	3	4	13.5	7	0.04	0.3
Ultra-High Resolution	4	8	25.5	12	0.03	0.25

Table 3.8: Technical Index of BMP180 Barometric Pressure Sensor

Supply Voltage	1.8V ~ 3.6V
Power Consumption	Low (0.5uA at 1Hz)
Interface	I2C
Speed	Max I2C Speed is 3.5MHz
Noise	0.06hPa (0.5m) in Ultra Low Power Mode 0.02hPa (0.17m) advanced resolution mode
Measurement Range	300hPa ~ 1100hPa (+9000m ~ -500m)

Raspberry Pi 3 B+

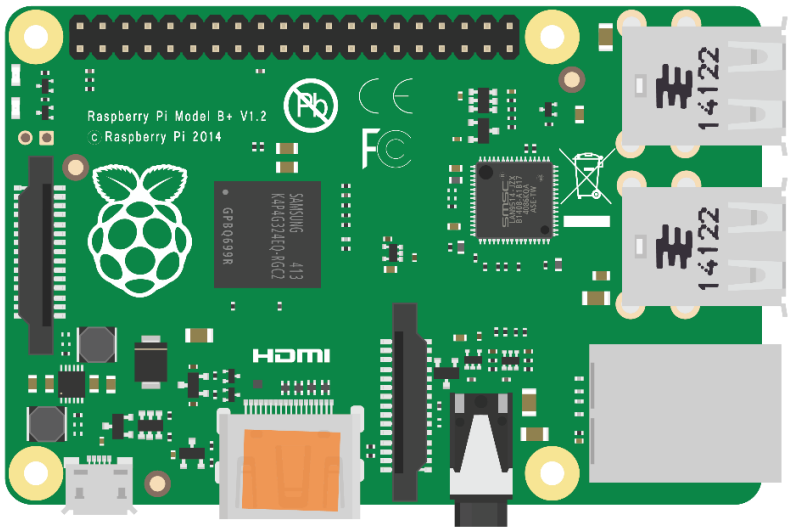

Figure 3.29: Raspberry Pi 3 B+

The Raspberry Pi 3 B+ (Figure 3.18) is the most upgraded version of the Raspberry Pi 3 range. This little computer is made of a 64-bit quad-core processor running at 1.4GHz, dual-band 2.4GHz and 5GHz wireless LAN, Bluetooth 4.3/BLE, faster Ethernet and PoE capability by a separate PoE HAT. The specification of the Raspberry Pi 3 B+ is given in Table 3.9.

Hardware:

- Low Cost
- Low Power
- High Availability
- High Reliability
- User Friendly

Software:

- ARMv8 Instruction Set
- Mature and stable Linux Software Stack

Raspberry Pi 3 B+ can be used like a desktop computer, where it the CPU. By connecting mouse, keyboard, Ethernet connection, Speaker and a 5V/2A power supply, it can be made whole. A cemera module can be connected also, if needed.

Table 3.9: Raspberry Pi 3 B+ Specifications

Processor	Broadcom BCM2837B0, Cortex-A53 64-bit SoC at 1.4GHz
Memory	1GB LPDDR2 SDRAM
Connectivity	• 2.4GHz & 5GHz IEEE 802.11.b/g/n/ac wireless LAN, Bluetooth 4.2, BLE • Gigabit Ethernet over USB 2.0 (Maximum throughout 300Mbps • 4×USB 2.0 ports
Access	Extended 40-Pin GPIO Header
Video & Sound	• 1×HDMI • MIPI DSI Display Port • MIPI CSI Camera Port • 4 Pole Stereo output & Composite Video Port
Multimedia	H.264, MPEG-4 decode (1080p30); H.264 Encode(1080p30); OpenGL ES 1.1,2.0 Graphics

SD Card Support	Micro SD Format for Loading Operating System & Data Storage
Input Power	• 5V/2.5A DC Via micro USB Connector • 5V DC via GPIO Header • Power Over Ethernet (PoE)- Enabled (requires separate PoE HAT)

Raspberry Pi 3 B+ Pinouts:

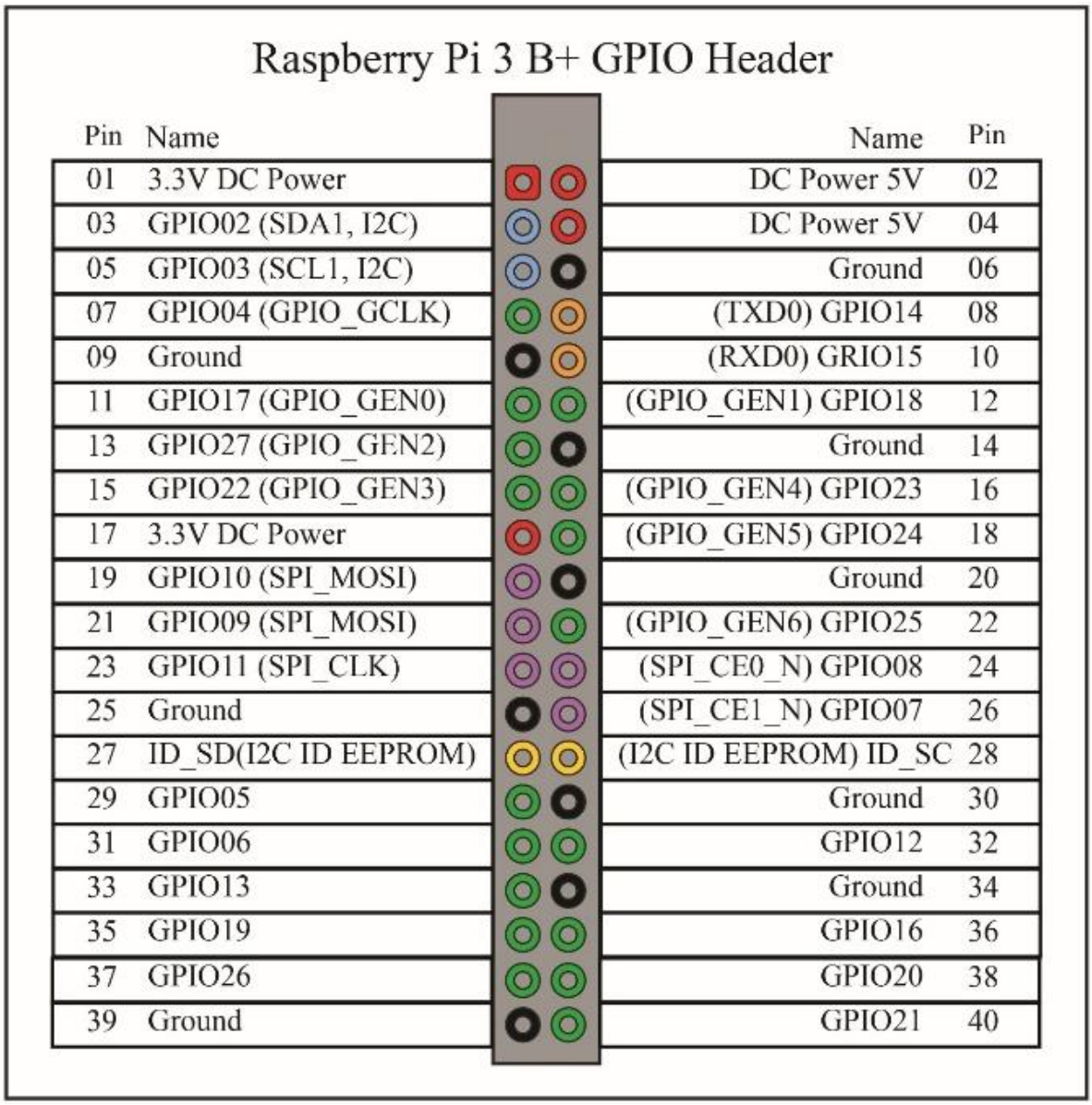

Figure 3.30: Raspberry Pi 3 B+ Pinouts Diagram

Voltages:

There are two 5V pins, two 3.3V pins and eight ground pins on the board. The remaining pins are all general-purpose 3.3V pins, which means outputs are set to 3.3V and inputs are 3.3V tolerant.

Outputs:

GPIO pins can be designated as output pins. They can be set to High (3.3V) or Low (0V) as per the user the needs. GPIO pins start from GPIO00 ~ GPIO27. A total of 28 GPIO pins exists on the board.

Inputs:

A GPIO pin designated as an input pin can be read as high or low. This is made easier with the use of internal pull-up or pull-down resistor. The GPIO02 and GPIO03 pins have fixed pull-up resistors. For other GPIO pins, a pull-up or pull-down resistor can be configured in software.

More:

Besides, acting as an input or output pin, GPIO pins can be used with a variety of alternative functions.

i. PWM (Pulse-Width Modulation):

- Software PWM available on all pins
- Hardware PWN avaialbe on only GPIO12, GPIO13, GPIO18, GPIO19.

ii. SPI (Serial Peripheral Interface):

- SPI0: MOSI (GPIO10); MISO (GPIO09); SCLK (GPIO11); CE0 (GPIO08); CE1 (GPIO07)
- SPI1: MOSI (GPIO20); MISO (GPIO19); SCLK (GPIO21); CE0 (GPIO18); CE1 (GPIO17); CE2 (GPIO16)

iii. I2C:

1. Data: (GPIO02); Clock (GPIO03)
2. EEPROM Data: (GPIO00); EEPROM Clock (GPIO01)

iv. Serial:

- TX (GPIO14)
- RX (GPIO15)

Software & Programming:

Raspbian is the official operating system for all models of the Raspberry Pi. Raspbian comes preloaded with Python, which is the offical programming language of the Raspberry Pi and Python IDLE 3. So, Raspberry Pi is a Python integrated Development Environment.

Arduino UNO

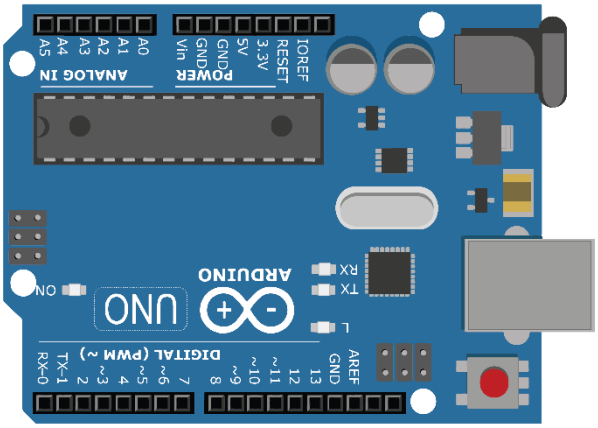

Figure 3.31: Arduino UNO

The Arduino UNO (Figure 3.20) is a microcontroller board based on the ATmega328. It has fourteen digital input or output pins (of which 6 pins can be used as PWM outputs), six analog pins, SDA & SCL pins that are near the AREF pin, a 16MHz Ceramic Resonator, a USB connection, a power jack, an ICSP header and a reset button. It can be powered up by

connecting to a computer with a USB cable or by connecting an AC-to-DC adapter or a battery. The chip model is ATmega 16U2. The specification of the Arduino UNO is given in the Table 3.11.

Table 3.10: Specifications of Arduino UNO

Microcontroller	ATmega328
Operating Voltage	5V
Input Voltage (Recommended)	7V ~ 12V
Input Voltage (Limits)	6V ~ 20V
Digital I/O Pins	14 (6 PWM Pins)
Analog Input Pins	6
DC Current per I/O Pin	40 mA
DC Current for 3.3V Pin	50 mA
Flash Memory	32 KB (ATmega328) of which 0.5 KB used by bootloader
SRAM	2 KB (ATmega328)
EEPROM	1 KB (ATmega328)
Clock Speed	16 MHz

Power:

USB connection or external power supply can be used to power up the Arduino UNO. The external (non-USB) power can come either from an AC-to-DC adapter or a battery. The adapter can be connected by a 2.1mm center-positive plug into to board's power jack.

- **VIN Pin:**

  This pin is used to pass the input voltage to the Arduino board when an external power supply is being used. This is an alternative way to connect an external source.

- **5V Pin:**

  This pin outputs a regulated 5V from the regulator on the board.

- **3.3V Pin:**

  This pin supplies 3.3V, which is generated by on board regulator. Maximum current draw is 50mA.

- **Ground Pin:**

  There are 3 Ground pins available on the board. Two are on the side of Analog Input Pins and one is on the side of the digital I/O pins.

Input and Output Pins:

- **Serial Communication:**

  Digital Pin 0 and 1 are respectively RX and TX Pins. They are used to receive (RX) and transmit (TX) TTL serial data. These pins are connected to the corresponding pins of the ATmega8U2 USB-to-TTL Serial chip.

- **External Interrupts:**

  Digital Pin 2 & 3. These pins can be configured to trigger an interrupt on a low value, a rising or falling edge, or a change in value.

- **PWM (Pulse-Width Modulation):**

  Digital Pin 3,5,6,9,10 & 11 are PWM output pins which provide 8-bit PWM outputs.

- **SPI Communication:**

  Digital Pin 10 (SS), 11 (MOSI), 12 (MISO), 13 (SCK). These pins support SPI communication using the SPI Library.

- **LED:**

  Digital pin 13 is connected to a built-in LED. When the pin is HIGH (1) the LED is on, when the pin is LOW (0) the LED is off.

- The Arduino UNO has 6 analog input pins, labeled as a0 through A5. Each of them provides 10-bits of resolution. By default, they measure from ground to 5V, though it is possible to change the upper end of their range using the AREF pin.

- **TWI (Two-Wire Interface/ I2C):**

  - On the Digital Pin side after the AREF pin there are two unnamed pins on the board, which are respectively SDA & SCL pins.
  - On the Analog pin side Pin A4 and A5 are respectively SDA & SCL pins.

  These two combinations of pins can be used to build TWI communication with another device which also supports TWI communication.

AREF Pin:

Reference voltage for the analog inputs.

Reset Pin:

To reset the microcontroller, this pin needs to be set to Low (0). It is used to activate a reset button automatically through coding.

Software & Programming:

The Arduino UNO can be programmed with the software named “Arduino IDE”. The user gets preloaded library for different communication system and wiring projects but new libraries for different projects can be added by the user. The Arduino IDE supports the languages C and C++ using special rules of code structuring.